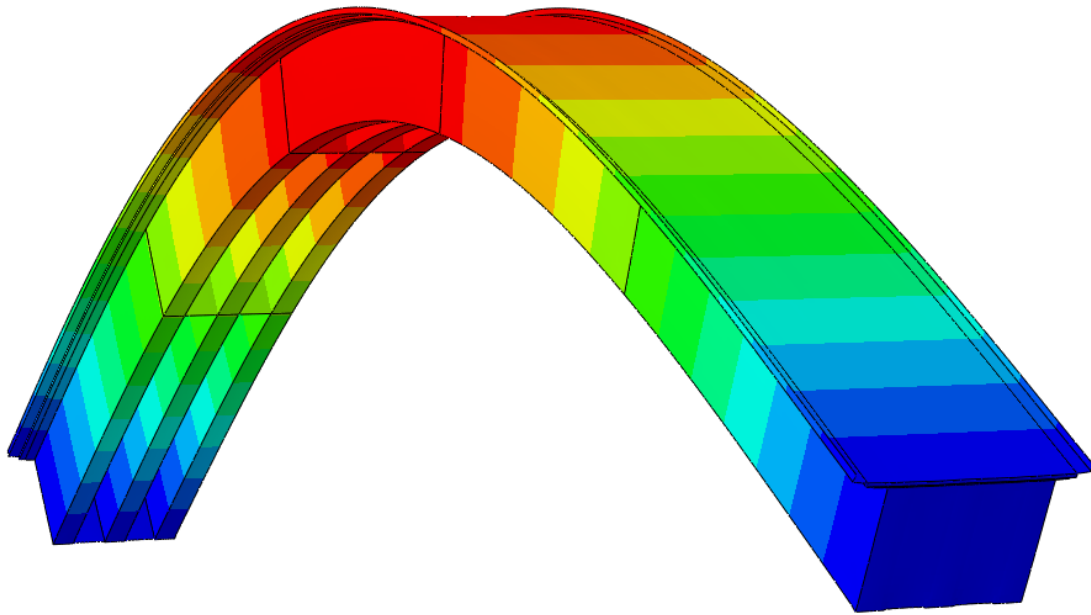




**CHALMERS**  
UNIVERSITY OF TECHNOLOGY

---



# Dynamic and Economic Aspects of Carbon Fiber Reinforced Polymer Footbridges

Master's Thesis in the Master's Programme Structural Engineering and Building Technology

JONAS BOND  
VICTOR HJELMGREN

---

Department of Architecture and Civil Engineering  
*Division of Structural Engineering*  
*Steel and Timber Structures*  
CHALMERS UNIVERSITY OF TECHNOLOGY  
Master's Thesis ACES30-18-28  
Gothenburg, Sweden 2018





MASTER'S THESIS ASEX30-18-28

# Dynamic and Economic Aspects of Carbon Fiber Reinforced Polymer Footbridges

*Master's Thesis in the Master's Programme Structural Engineering  
and Building Technology*

JONAS BOND  
VICTOR HJELMGREN

Department of Architecture and Civil Engineering  
*Division of Structural Engineering*  
*Steel and Timber Structures*  
CHALMERS UNIVERSITY OF TECHNOLOGY  
Gothenburg, Sweden 2018

Dynamic and Economic Aspects of Carbon Fiber Reinforced Polymer Footbridges

*Master's Thesis in the Master's Programme Structural Engineering and Building Technology*

JONAS BOND

VICTOR HJELMGREN

© JONAS BOND VICTOR HJELMGREN, 2018

Supervisors: Hanna Jansson and Thomas Darholm, Cowi AB

Examiner: Reza Haghani Dogaheh, Department of Architecture and Civil Engineering

Examensarbete ACEx30-18-28

Institutionen för arkitektur och samhällsbyggnadsteknik

Chalmers tekniska högskola, 2018

Department of Architecture and Civil Engineering

Division of Structural Engineering

Steel and Timber Structures

Chalmers University of Technology

SE-412 96 Göteborg

Sweden

Telephone: +46 (0)31-772 1000

Cover: First vertical eigenmode of the slender footbridge design, with an additional mass from a pedestrian density of  $0.5 \text{ pedestrians}/\text{m}^2$ , see Section 9.2.1.

Department of Architecture and Civil Engineering

Göteborg, Sweden 2018

Dynamic and Economic Aspects of Carbon Fiber Reinforced Polymer Footbridges  
*Master's Thesis in the Master's Programme Structural Engineering and Building Technology*

JONAS BOND

VICTOR HJELMGREN

Department of Architecture and Civil Engineering  
Division of Structural Engineering  
Steel and Timber Structures  
Chalmers University of Technology

## Abstract

There is a growing interest for carbon fiber reinforced polymers (CFRP) on the construction market. The material is very lightweight but also very expensive. This master's thesis looks into whether CFRP is an economically favorable alternative for footbridges. An economic comparison is made between two slightly different CFRP designs – one slender and one bulky – and a conventional steel truss solution. The CFRP footbridge designs are made by the master's thesis group in cooperation with experienced structural engineers from Cowi and Aston Harald. The economic comparison accounts for the major costs that the considered bridge projects are associated with. Within the limitations of this master's thesis, it cannot be concluded that using CFRP is a reasonable choice before a steel truss solution. However, further development of the concept might pay off in the future.

A dynamic study was carried out, in which the slender and the bulky bridge design were evaluated using FE software Brigade/Plus and the design guide Sétra. The influence by mass additions from pedestrians were taken into account and the results indicated that only the slender bridge design can be seen as dynamically approved. It was concluded that, for the lightweight bridges studied, the eigenfrequency is the most important aspect for the dynamic behavior. It should be designed to be close to, or above, 5.0 Hz. If lower, the risk for unacceptable accelerations is significant, and the damping contribution from the added crowd masses is not likely to help.

Keywords: CFRP, carbon fiber, footbridge, lightweight, economy, dynamics, eigenfrequency, accelerations, Sétra.

Dynamiska och ekonomiska aspekter av gångbroar i kolfiberarmerade polymerer  
*Examensarbete inom masterprogrammet Konstruktionsteknik och Byggnadsteknologi*

JONAS BOND

VICTOR HJELMGREN

Institutionen för Arkitektur och Civil Ingenjörskonst  
Avdelningen för Konstruktionsteknik  
Stål- och Träbyggnad  
Chalmers Tekniska Högskola

## Sammanfattning

Det finns ett ökande intresse för kolfiberarmerade polymerer (CFRP) inom byggbranschen. Materialet är väldigt lätt men också mycket dyrt. Detta examensarbete gör en ansats till att undersöka huruvida en gångbro i CFRP kan vara gångbar även ekonomiskt. Kriterier för ett lämpligt tillämpningsområde för kolfiberbroar ringades in och därefter jämfördes två tämligen lika CFRP-designer – en slank och en någorlunda bulkig – ur ekonomisk synvinkel med en konventionell stålfackverksbro. Kolfiberbroarna designades av examensarbetarna i samarbete med erfarna ingenjörer från Cowi och Aston Harald. Den ekonomiska jämförelsen beaktar de huvudsakliga kostnaderna som kopplas till respektive broalternativ. Utifrån detta examensarbete, med gällande avgränsningar, kan någon ekonomisk fördel med kolfiber inte påvisas. Däremot är det rimligt att tro att en utveckling av konceptet kan visa sig lönsam i framtiden.

I en dynamisk studie utvärderades den slanka och den bulkiga brodesignen med hjälp av FEM-programmet Brigade/Plus och designkoden Sétra. Masspåslaget från fotgängarna togs i beaktning och resultaten pekar på att bara den slanka designen kan anses vara dynamiskt godkänd. Det fastslogs, för de lättviktiga broarna i fråga, att egenfrekvensen är den klart viktigaste aspekten när det kommer till dynamiskt beteende. En lättviktig bro i storleksklassen som studerats bör designas på ett sådant sätt att egenfrekvensen ligger nära eller – ännu hellre – över 5 Hz. Är egenfrekvensen lägre är risken för oacceptabelt stora accelerationer överhängande. Dämpningsbidraget från det masspåslag som fotgängarna står för väntas inte hjälpa.

Nyckelord: CFRP, kolfiber, gångbro, lättviktig, ekonomi, dynamik, egenfrekvens, accelerationer, Sétra.

# Contents

<b>1</b>	<b>Introduction</b>	<b>1</b>
1.1	Background . . . . .	1
1.2	Purpose . . . . .	2
1.3	Method . . . . .	2
1.4	Limitations . . . . .	3
<b>2</b>	<b>Carbon Fiber Reinforced Polymers (CFRP)</b>	<b>5</b>
2.1	Introduction . . . . .	5
2.2	Components of the Composite . . . . .	6
2.3	Fiber Reinforcement . . . . .	6
2.3.1	Carbon Fibers . . . . .	8
2.4	Matrix . . . . .	9
2.4.1	Resin . . . . .	10
2.4.1.1	Thermosoftening Polymers . . . . .	10
2.4.1.2	Thermosetting Resins . . . . .	10
2.4.2	Fillers . . . . .	11
2.4.3	Additives . . . . .	12
2.5	Composite . . . . .	12
2.5.1	Rule of Mixture . . . . .	12
2.6	Sandwich Structures . . . . .	13
2.7	Manufacturing Techniques . . . . .	15
2.7.1	Hand Lay-up . . . . .	15
2.7.2	Spray Lay-up . . . . .	16
2.7.3	Pultrusion . . . . .	17
2.7.4	Resin Transfer Molding (RTM) . . . . .	17
2.7.5	Pre-impregnated Laminates (Prepreg) . . . . .	18
2.8	Regulations . . . . .	21
2.8.1	Prospect for New Guidance in the Design of FRP Structures . . . . .	21
<b>3</b>	<b>CFRP in Civil Applications</b>	<b>23</b>
3.1	Introduction . . . . .	23
3.2	FRP Strengthening of Existing Structures . . . . .	23
3.3	Examples of Existing Structures . . . . .	24
3.3.1	Gangbroa, Fredrikstad, Norway . . . . .	24
3.3.2	Bridge 254, Malmö, Sweden . . . . .	24

<b>4</b>	<b>Dynamics of Footbridges</b>	<b>27</b>
4.1	Introduction . . . . .	27
4.2	Basics of Structural Dynamics . . . . .	27
4.3	Vibrations in Footbridges Imposed by Pedestrians . . . . .	29
4.3.1	Load Frequencies in Vertical, Longitudinal, and Lateral Directions . . . . .	29
4.3.1.1	Lateral Lock-in . . . . .	31
4.4	Damping . . . . .	31
4.4.1	Aspects that Influence the Damping Behavior of Footbridges . . . . .	33
4.4.1.1	Structural Damping . . . . .	33
4.4.1.2	Mechanical Dampers . . . . .	34
4.4.1.3	Material Damping . . . . .	34
4.5	Human–Structure Interaction (HSI) . . . . .	35
4.5.1	Experiments that Support the HSI Effect . . . . .	35
4.5.2	New Calculation Models Accounting for HSI . . . . .	36
4.6	Regulations in Footbridges . . . . .	37
4.6.1	Eurocode . . . . .	37
4.6.2	Sétra . . . . .	38
4.6.2.1	Resonance Risk by Frequency Range . . . . .	39
4.6.2.2	Comfort Levels . . . . .	40
<b>5</b>	<b>Suitable Applications for CFRP Footbridges</b>	<b>45</b>
5.1	Manufacturing . . . . .	45
5.2	Supports . . . . .	45
5.3	Transportation . . . . .	46
5.4	Installation . . . . .	47
5.4.1	Crane . . . . .	47
5.4.2	Traffic Disruptions . . . . .	47
5.5	Maintenance . . . . .	48
5.6	Summarized Criteria for Suitable Applications of CFRP Footbridges . . . . .	49
<b>6</b>	<b>Economic Comparison Between Existing Steel Truss Bridge and CFRP Alternatives</b>	<b>51</b>
6.1	Introduction . . . . .	51
6.2	Bridge 581-909-1 . . . . .	52
6.3	Comparison . . . . .	53
6.3.1	Manufacturing . . . . .	53
6.3.2	Supports . . . . .	54
6.3.3	Transportation . . . . .	55
6.3.4	Installation . . . . .	55
6.4	Maintenance . . . . .	56
6.5	Cost Adjustments . . . . .	57
<b>7</b>	<b>Bridge Design</b>	<b>59</b>
7.1	Fiber Orientation . . . . .	59
7.2	Manufacturing . . . . .	60
7.3	Sizing . . . . .	60

7.4	Two Final Designs . . . . .	61
7.4.1	Deck . . . . .	62
7.4.2	Girders . . . . .	63
7.5	Materials . . . . .	64
7.5.1	Deck . . . . .	65
7.5.2	Webs and Diaphragms . . . . .	65
7.5.3	Flanges . . . . .	66
7.6	Static Loads . . . . .	66
7.7	Requirements . . . . .	68
7.7.1	Moment and Shear Force Resistance in the ULS . . . . .	69
7.7.2	Deflection in the SLS . . . . .	69
7.8	Checks . . . . .	69
<b>8</b>	<b>Finite Element Modeling of the Bridge Alternatives</b>	<b>73</b>
8.1	Brigade Plus . . . . .	73
8.2	Model Design . . . . .	73
8.2.1	Boundary Conditions . . . . .	74
8.2.2	Material Input . . . . .	75
8.2.3	Material Lay-up . . . . .	76
8.2.4	Steps . . . . .	77
8.2.4.1	Static Analysis . . . . .	77
8.2.4.2	Frequency Analysis . . . . .	77
8.2.4.3	Modal Dynamic Analysis . . . . .	78
8.2.5	Interaction . . . . .	78
8.2.6	Loads . . . . .	79
8.2.6.1	Static Loads . . . . .	79
8.2.6.2	Mass Additions and Dynamic Loads . . . . .	79
8.2.7	Mesh . . . . .	81
8.3	Convergence Study . . . . .	81
8.3.1	Mesh Sizing . . . . .	81
8.3.2	Time Step . . . . .	82
8.4	Verification of the FE model . . . . .	84
8.4.1	Verification by Assigning Steel Properties . . . . .	84
8.4.2	Verification of FE Model Using Nastran . . . . .	85
8.5	Checks . . . . .	86
8.5.1	Bending Stress . . . . .	86
8.5.2	Shear Stress . . . . .	87
8.5.3	Deflection . . . . .	87
<b>9</b>	<b>Results</b>	<b>89</b>
9.1	Economic Comparison Between Existing Steel Truss Bridge and CFRP Alternatives . . . . .	89
9.2	Dynamic Response . . . . .	89
9.2.1	CFRP1 . . . . .	89
9.2.1.1	CFRP1 <sub>0</sub> , Crowd Class III . . . . .	90
9.2.1.2	CFRP1 <sub>0</sub> , Crowd Class II . . . . .	90
9.2.1.3	CFRP1 <sub>0.5</sub> , Crowd Class III . . . . .	91

9.2.1.4	CFRP <sub>10.8</sub> , Crowd Class II . . . . .	91
9.2.2	CFRP <sub>2</sub> . . . . .	92
9.2.2.1	CFRP <sub>20</sub> , Crowd Class III . . . . .	93
9.2.2.2	CFRP <sub>20</sub> , Crowd Class II . . . . .	94
9.2.2.3	CFRP <sub>20.5</sub> , Crowd Class III . . . . .	94
9.2.2.4	CFRP <sub>20.8</sub> , Crowd Class II . . . . .	95
9.2.3	Summary of Maximum Accelerations . . . . .	96
<b>10</b>	<b>Discussion</b>	<b>97</b>
10.1	The Suitability of CFRP Bridges . . . . .	97
10.2	Bridge Design . . . . .	99
10.3	Dynamic Response . . . . .	100
10.4	Buckling . . . . .	102
<b>11</b>	<b>Conclusion</b>	<b>103</b>
<b>12</b>	<b>Further Studies</b>	<b>105</b>
<b>13</b>	<b>References</b>	<b>107</b>
<b>A</b>	<b>Appendix: Bridge 581-909-1 Drawings</b>	<b>A:1</b>



## Acknowledgements

Finally, our time at Chalmers University of Technology is through and those have been unforgettable years. We didn't choose to become civil engineers because it is easy; but thanks to great help and inspiration from the amazing people we've had around us, we made it. Friends, personnel, our families, and a generous federal financial support have not only made it possible, but also enjoyable.

This master's thesis is a bonanza of personal communication, or "pers. comm.", as we call it. A lot of skilled and experienced professionals have spent their valuable time helping us out with this thesis. Not least, we should mention our supervisors at Cowi AB; Hanna Jansson and Thomas Darholm, along with Thomas Hallgren who has given us tonnes of time and support. We also had a good cooperation with our supervisor and examiner at Chalmers University of Technology – the always very positive Reza Haghani.

We hope that you, as a reader, will have a good time reading this report. Our wish is to teach you something useful about bridge dynamics and CFRP. If you have any questions or thoughts about the report, about engineering, or about life in general, feel free to contact either one of us in any way preferred.

Two handwritten signatures in black ink. The first signature on the left is 'Jonas Bond' and the second signature on the right is 'Victor Hjelmgren'.

Jonas Bond and Victor Hjelmgren  
Gothenburg, Sweden, June 2018



## Abbreviations

2DOF	Two-Degree-of-Freedom
AFRP	Aramid Fiber Reinforced Polymers
CFRP	Carbon Fiber Reinforced Polymers
CFRP1	Slender CFRP footbridge design
CFRP2	Bulky CFRP footbridge design
CFRP <sub>10</sub>	CFRP1 with no mass addition
CFRP <sub>10.5</sub>	CFRP1 with mass addition from 0.5 <i>pedestrians/m<sup>2</sup></i>
CFRP <sub>10.8</sub>	CFRP1 with mass addition from 0.8 <i>pedestrians/m<sup>2</sup></i>
CFRP <sub>20</sub>	CFRP2 with no mass addition
CFRP <sub>20.5</sub>	CFRP2 with mass addition from 0.5 <i>pedestrians/m<sup>2</sup></i>
CFRP <sub>20.8</sub>	CFRP2 with mass addition from 0.8 <i>pedestrians/m<sup>2</sup></i>
FE	Finite Element
FEM	Finite Element Method
FRF	Frequency Response Function
FRP	Fiber Reinforced Polymers
GFRP	Glass Fiber Reinforced Polymers
HSI	Human–Structure Interaction
JRC	Joint Research Center
MDOF	Multi-Degree-of-Freedom
MSD	Mass–Spring–Damper
PAN	Polyacrylonitrile
PET	Polyethylene Terephthalate
PVC	Polyvinyl Chloride
RC	Reinforced Concrete
RoM	Rule of Mixture
RTM	Resin Transfer Molding
SAN	Styrene Acrylonitrile
SDOF	Single-Degree-of-Freedom
SEK	Swedish Crowns
SLS	Serviceability Limit State
UD	Unidirectional
ULS	Ultimate Limit State
UV	Ultraviolet
VARMT	Vacuum-Assisted Resin Molding
VARI	Vacuum-Assisted Resin Injection

# Notations

## Roman Upper Case Letters

<b>C</b>	Structural damping matrix
$E$	Young's modulus [ $Pa$ ]
$E'$	Storage modulus [ $Pa$ ]
$E''$	Loss modulus [ $Pa$ ]
$E_1$	Young's modulus parallel to fiber [ $Pa$ ]
$E_2$	Young's modulus perpendicular to fiber [ $Pa$ ]
$E_f$	Young's modulus of fiber [ $Pa$ ]
$E_m$	Young's modulus of matrix [ $Pa$ ]
$F_0$	Amplitude of a harmonic force [ $N$ ]
$F(t)$	External, dynamic force [ $N$ ]
$\mathbf{F}(t)$	External, dynamic force vector
$I$	Moment of inertia [ $m^4$ ]
<b>K</b>	Structural stiffness matrix
$L$	Span length [ $m$ ]
<b>M</b>	Structural mass matrix
$N_{eq}$	Equivalent amount of pedestrians [ <i>pedestrians</i> ]
$P_c$	Property of composite [ ]
$P_f$	Property of fiber [ ]
$P_m$	Property of matrix [ ]
$Q$	Static design load [ $N/m$ ]
$Rd$	Response Factor [ ]
$S$	Loaded area [ $m^2$ ]
$T_g$	Glass transition temperature [ $^{\circ}C$ ]
$V_f$	Volume of fraction fiber [ ]
$V_m$	Volume of fraction matrix [ ]
$X_d$	Design strength [ $Pa$ ]
$X_k$	Characteristic strength [ $Pa$ ]
$X_{Ed}$	Effect of applied loads
$X_{Rd}$	Resistance

## Roman Lower Case Letters

$c$	Damping coefficient [ $Ns/m$ ]
$c_c$	Critical damping coefficient [ $Ns/m$ ]
$d$	Crowd density [ $pedestrians/m^2$ ]
$f_0$	Eigenfrequency [ $Hz$ ]
$f_{step}$	Step frequency [ $Hz$ ]
$k$	Stiffness [ $N/m$ ]
$i$	Order of eigenmode
$m$	Modal mass [ $kg$ ]
$m_{tot}$	Total mass [ $kg$ ]
$t$	Time [ $s$ ]
$\tan\delta$	Loss tangent [ ]
$u(t)$	Displacement [ $m$ ]
$\mathbf{u}(t)$	Displacement vector
$\dot{u}(t)$	Velocity [ $m/s$ ]
$\dot{\mathbf{u}}(t)$	Velocity vector
$\ddot{u}(t)$	Acceleration [ $m/s^2$ ]
$\ddot{\mathbf{u}}(t)$	Acceleration vector

### Greek Upper Case Letter

$\Delta t$	Time increment [ $s$ ]
------------	------------------------

### Greek Lower Case Letters

$\beta$	Frequency ratio [ ]
$\gamma_G$	Partial coefficient for permanent load [ ]
$\gamma_M$	Partial factor [ ]
$\gamma_Q$	Partial coefficient for variable load [ ]
$\varepsilon$	Ultimate tensile strain [%]
$\eta$	Conversion factor [ ]
$\xi$	Damping Ratio [ ]
$\rho$	Density [ $kg/m^3$ ]
$\sigma$	Tensile strength [ $Pa$ ]
$\psi$	Reduction factor based on eigenfrequency [ ]
$\psi_{0snow}$	Reduction factor for secondary load [ ]
$\omega_0$	Angular eigenfrequency [ $rad/s$ ]



# 1

## Introduction

### 1.1 Background

The use of carbon fiber reinforced polymers (CFRP) is a common method to strengthen existing structures such as bridges and exhibition halls. The use of CFRP as a main structural material is limited as of today, although it has become more common in recent years. CFRP is a lightweight material that is normally cast in factories. In case of civil engineering applications, the structures are transported on trucks and installed at the site (Mara, 2014).

In modern day urban planning, pedestrians and cyclists are getting a higher priority than they used to. At many places in the world, pure walking and cycling streets are being planned and built. With the environment in mind, there is a desire to provide pedestrians and cyclists with smooth ways to get around. That may include bridges to cross rivers, highways, railways, and other barriers within the built environment. Even a construction site tends to be a big distraction in a neighborhood, forcing roads to close and people to take detours. This is associated with high so-called social costs, hence a desire even to minimize this effect of construction work (Jarkiewicz, 2012).

The characteristics of CFRP and the growing demands for smooth interactions in the built environment are reasons to develop the use of CFRP as a structural material, both in terms of volume and of the range of applications. Being a lightweight material, CFRP is relatively easy to transport and lift, allowing a big rate of prefabrication. That, in turn, can limit the in-situ construction time, hence little distraction of traffic et cetera. Furthermore, CFRP has a high stiffness-to-weight ratio and strength-to-weight ratio (Gurit, 2018b). Therefore, a high potential is seen in the application of CFRP in footbridges, according to Darholm (2017, pers. comm., July 10<sup>th</sup>). However, CFRP is rather expensive compared to conventional construction materials, although there are predictions of a price decrease over time (Svahn, 2018, pers. comm., April 10<sup>th</sup>).

Considering the material cost, it is important to find applications where CFRP can be used in an cost- and effort-efficient way. That is, the biggest possible advantage has to be taken from its beneficial characteristics.

Worldwide, CFRP is sparsely used in civil structures compared to conventional construction materials like steel, timber, and concrete. There are a couple of bridges made of CFRP and, more commonly, glass fiber reinforced polymers (GFRP); although in very moderate spans. In Sweden, there is only one carbon fiber bridge as of 2018. In fact, there are several structural challenges that are still to be faced.

One challenge in designing a lightweight structure as a CFRP footbridge respond to the variable loads in a good way. In design of lightweight footbridges, vibrations induced by footsteps is an important issue. Lightweight bridges have a higher eigenfrequency than heavy bridges; however, the acceleration response of such bridges is greater, in the case that resonance is obtained. The perception when walking on a bridge is a considerable matter; the bridge has to fulfill the comfort requirements given in the Eurocode (SIS, 1990). Even several recommendations are available, with different approaches to match comfort criteria regarding vibrations. This master's thesis will use the Eurocode and a guide called Sétra (2006), described in Section 4.6.

## 1.2 Purpose

One aim of this master thesis is to investigate whether a CFRP solution is a good option in footbridge construction, with the economic aspect in mind. This shall include both the application in which a CFRP bridge suits best and, in general terms, how such a bridge can be designed to get the best possible use of its favorable characteristics.

This thesis also has a dynamic focus. Two CFRP footbridge designs, one slender and one bulky, have their dynamic behavior evaluated, to determine which one is the most suitable. The master's thesis investigates how the design affects the dynamic behavior and assess what parameters have the biggest influence on the maximum accelerations. From that, conclusions are made on how the design of a CFRP footbridge should be approached.

Economics and dynamics are the two primary objectives in assessing the concept of CFRP footbridges that are gone through in this master's thesis.

## 1.3 Method

The first part of the master's thesis is a literature study aiming to increase the knowledge within CFRP as a material and obtain a deepened awareness of the dynamic behavior of footbridges. Further research was carried out in order to highlight the advantages of using a lightweight material such as CFRP instead of conventional, heavier construction materials. Criteria for suitable applications for CFRP footbridges were distinguished. Aspects taken into consideration were manufacturing, foundation, transportation, installation, and maintenance.



Subsequently, a 32-meter footbridge was preliminarily designed in cooperation with experienced structural engineers and specialists within bridge design and CFRP design. The preliminary design was developed into two different versions, namely a slender version and a bulky version, the latter being significantly heavier than the former. Chapter 7 describes the bridge designs.

With the worked out footbridge design at hand, a brief case study was carried out. A steel truss footbridge in Åby, Sweden, was studied. A hypothetical scenario, in which a CFRP bridge was built instead of the particular truss bridge, was considered. Associated costs were estimated and finally, numbers indicating the priceworthiness of a CFRP solution, compared to the actual truss solution, were obtained.

For the dynamic analysis, Brigade/Plus was used for the finite element (FE) modeling, using hand calculations and Nastran to verify the models. The two different bridge designs were modeled as described in Chapter 8. The dynamic assessment is made using requirements from the Eurocode (SIS, 1990) and a load model according to Sétra (2006). The results, in terms of eigenfrequencies and maximum accelerations, were analyzed and conclusions were made.

## 1.4 Limitations

Since the proposed bridges are planned to be manufactured in factories – manufactured basically in one piece – transportation implies a limitation in the size that the structures can obtain. More about the design-wise limitations in section 5.

For reasons mentioned in Section 6.3.4, costs for closing roads and railways are not included in any calculations.

This study focuses on carbon fiber reinforced polymers. That is, aramid fibers and glass fibers will only be mentioned briefly. As a consequence, epoxy will be the only resin investigated, since that is the most common resin in combination with carbon fiber (Allroth, 2018, pers. comm., February 27<sup>th</sup>; Armstrong, 2018, pers. comm., February 27<sup>th</sup>). Pre-impregnated laminates will be the manufacturing method considered. It is assumed that the outer layers of the CFRP members have a matrix that protects them against ultraviolet (UV) radiation, that is, no gel coating is needed. The glued connections of a CFRP structure are usually not checked, since these are usually not an issue (Allroth, 2018, pers. comm., March 26<sup>th</sup>).

The dynamic loads considered are those from walking people. Wind loads make aerodynamic aspects interesting for the bridge concept. However, the interaction between dynamic pedestrian and wind loading is not accounted for. Neither is the influence of long-term load, temperature changes, and humidity are not accounted for. Local buckling is considered, but not designed for. Instead, solutions to the buckling problems are suggested in Section 10.4.



# 2

## Carbon Fiber Reinforced Polymers (CFRP)

Throughout this master's thesis, the material in question will mainly be referred to as CFRP or carbon fibers. In some cases, the information provided will apply to all kinds of fiber reinforced polymers (FRP), while in some cases, it will apply to CFRP specifically.

### 2.1 Introduction

Allegedly, commercial carbon fibers were invented by Thomas Edison, more commonly known as the man who invented the light bulb. Trying to find a proper material for the filament, he baked strains of bamboo and cotton at high temperatures. Bamboo and cotton are made up of natural polymers, which were carbonized by the heat, forming carbon fibers. Eventually, the carbon fibers were replaced by tungsten, although the US Navy kept using carbon filaments until the early 60's (American Chemical Society, 2018).

As the concept evolved, it was proven to have properties that made it suitable for applications in automotive, aerospace, wind turbines, and sports. That is, applications where it has use for its high strength-to-weight ratio. Figure 2.1 shows the distribution of annual carbon fiber demand globally as of 2013.

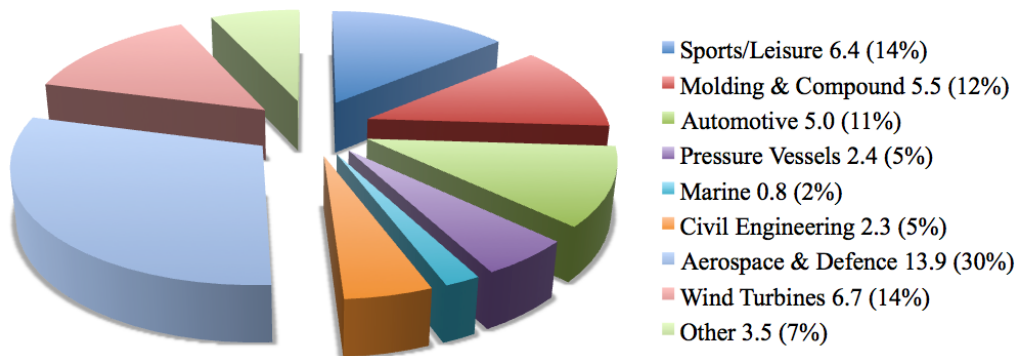


**Figure 2.1:** *Global demand for carbon fibers by application in 2013 [ktonnes] (Holmes, 2014).*

## 2.2 Components of the Composite

FRP is a composite material, that is, it consists of two or more materials that act together as one material, with desired properties. Stiff fibers, such as carbon, aramid, or glass fibers, act as reinforcement. A polymer matrix consisting of resin, additives and fillers hold the fibers in place and make them act together. The resin is the main part of the matrix; the most commonly kinds resins being epoxy, vinylester, and polyester (Jain & Lee, 2012; Potyrala, 2011). Additives and fillers can be added in order to modify the properties of the composite, such as resistance to the environment in terms of fire, corrosion and ultraviolet radiation (Potyrala, 2011). Even a slight price adjustment can be obtained using fillers. The main components of an FRP composite are illustrated in Figure 2.2.

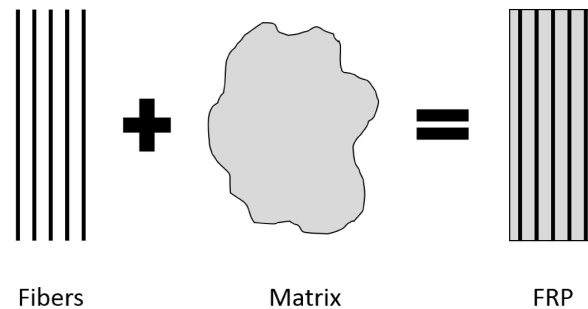


**Figure 2.2:** *The principle of fiber reinforced polymers (FRP).*

## 2.3 Fiber Reinforcement

The essence of the fibers in the FRP composite is to provide strength, stiffness and thermal stability, where the fibers work as reinforcement and need to carry the load along the composite. To do so, the fibers need to be strong and stiff; they also need to have little variation in properties between them, both geometrically and structurally (Tuakta, 2015).

FRP composites where the fibers are made of carbon are called CFRP's; for glass fibers, it is GFRP's or GRP's; and for aramid fibers, the composites are called AFRP's.

A fiber is a long filament, usually with a diameter around  $10\ \mu m$  (Tuakta, 2015). The size of the fibers is of importance, as few fibers with large diameters are easier to impregnate and less pricy, compared to many fibers with small diameters (Clarke, 1996). However, an increased diameter also has drawbacks, such as decreased strength and higher risk for surface defects (Potyrala, 2011). The industry

of today is moving towards manufacturing fibers with enlarged diameter, for economic reasons; however, a diameter above  $30\ \mu\text{m}$  is not recommended (Clarke, 1996).

The fibers usually correspond to 30–70 % of the total volume, and about 50 % of the total weight of the composite (Potyrala, 2011). As the fibers are the reinforcement of the composite, the direction of the fibers are of great importance for the material properties. The fiber orientation can be divided into mainly three groups, shown in Figure 2.3: Unidirectional (UD), bidirectional and multidirectional (Clarke, 1996).

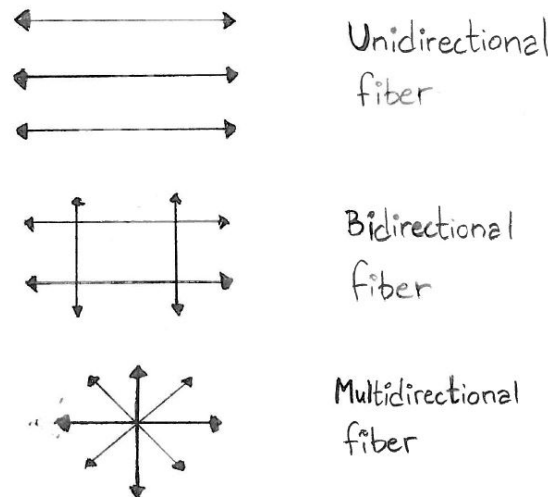


**Figure 2.3:** *Various fiber directions.*

If the majority of the fibers in a laminate are oriented in the same direction, they are referred to as unidirectional. If they are arranged in two directions, either at  $0^\circ$  and  $90^\circ$  or at  $\pm 45^\circ$  (Clarke, 1996), they are referred to as bidirectional fiber orientation. Bidirectional fibers are generally delivered as woven fabrics or as bundles called rovings (in case of glass fibers) or tow (carbon fibers). Multidirectional fiber orientation is when the fibers are arranged at both  $0^\circ$ ,  $90^\circ$ , and  $\pm 45^\circ$ . Multidirectional fibers can also be randomly distributed and delivered in chopped strands and mats (Clarke, 1996).

As mentioned in Section 2.2, the most commonly used fibers in civil engineering industry as of today are carbon, aramid, and glass fibers (Jain & Lee, 2012; Potyrala, 2011). These fibers have different material properties and are suitable for different applications. In Table 2.1, the properties of various fibers are presented. As can be seen in the table, carbon fibers have a higher modulus of elasticity than the other fibers. Moreover, carbon fibers have a higher resistance to fatigue than glass fibers (Tuakta, 2015), and according to studies, carbon fibers are considered better in service life than both aramid and glass fibers (Potyrala, 2011). Furthermore, one of the essential characteristics of carbon fibers is the specific modulus. As can be seen in Table 2.1, the specific modulus is much higher for carbon fibers than for the other fibers. In the longitudinal direction, the specific modulus is also a lot higher than that of steel (Clarke, 1996). However, the composite including the matrix (the

## 2. Carbon Fiber Reinforced Polymers (CFRP)

polymers) has a lower Young's modulus. Specific modulus is the elastic modulus divided by the density of the material, also known as the stiffness-to-weight ratio (Clarke, 1996).

**Table 2.1:** *Properties of carbon, glass, and aramid fibers (Clarke, 1996; Tuakta, 2005).*

Material	Density $\rho$ [ $kg/m^3$ ]	Young's modulus $E$ [ $GPa$ ]	Tensile strength $\sigma$ [ $MPa$ ]	Ultimate tensile strain $\varepsilon$ [%]	Specific modulus $E/\rho$ [ $Mm^2/s^2$ ]
Carbon HS	1700	240	2600	1.7	140
Carbon HM	1900	400	1800	0.7	200
E-glass	2540	70	3450	4.8	27
S-glass	2500	86	4500	5.7	34.5
Kevlar 29 (aramid)	1450	80	2800	4.0	55.5
Kevlar 49 (aramid)	1450	130	2800	2.4	89.5

### 2.3.1 Carbon Fibers

As mentioned, carbon fibers are strong and stiff, compared to other materials, including other kinds of fibers. Among the disadvantages of carbon fibers are the manufacturing process, which requires a high energy consumption, and a high cost (Jain & Lee, 2012; Potyrala, 2011). However, for the rest of this report, carbon fibers will be the only kind of fibers considered, as this master thesis concerns carbon fiber reinforced polymers in footbridges.

Carbon fibers are recognized from the coal black color, see Figure 2.4, and from being transversely isotropic due to their two-dimensional atomic structure. Thus, the structural properties of CFRP are significantly different in the longitudinal and transverse directions (Bank, 2006).



**Figure 2.4:** *Carbon fiber tow on a spool (Gurit, 2018a). Published with permission.*

Furthermore, carbon fibers can be produced in different grades; with standard mod-

ulus, high strength modulus, ultra high modulus and intermediate modulus, where properties for these grades are presented in Table 2.2.

**Table 2.2:** *Properties of various carbon fiber grades (Bank, 2006).*

Grade of carbon	Density $\rho$ [ $kg/m^3$ ]	Young's modulus $E$ [ $GPa$ ]	Tensile strength $\sigma$ [ $MPa$ ]	Ultimate tensile strain $\epsilon$ [%]
Standard, SM	1,700	250	3,700	1.2
High strength, HS	1,800	250	4,800	1.4
High modulus, HM	1,900	500	3,000	0.5
Ultra high modulus, UHM	2,100	800	2,400	0.2

Carbon fibers are manufactured from three different precursor materials: Rayon, pitch, and polyacrylonitrile (PAN), where manufacturing requires temperatures between  $1200^\circ C$  and  $2400^\circ C$  (Tuakta, 2015). Rayon based fibers are made from natural cellulosic textile fibers, and PAN based fibers from synthetic textile fibers (Bank, 2006). Pitch based fibers, on its hand, are made of a by-product from petroleum processing and usually have a lower manufacturing cost than PAN and rayon, due to a lower temperature during manufacturing (Bank, 2006). However, in commercial use, PAN based fibers are in majority (Potyrala, 2011).

The advantages of carbon fibers are not only their high performance in terms of strength and stiffness. Carbon fibers also perform well against fatigue loads, in hot and moist environment, and are a very durable material (Bank, 2006). Thus, it is considered as a material with low maintenance needs.

## 2.4 Matrix

The second component of an FRP composite is the polymer matrix, which needs to have a lower modulus of elasticity than the fibers, in order for the fibers to be able to carry maximum load (Potyrala, 2011). Furthermore, the matrix has the important purpose of holding the fibers together, transferring load between the fibers, separating the fibers within the composite, increasing the ductility, and protecting the fibers from the environment (Clarke, 1996; Potyrala, 2011). The polymer matrix is made up of resin, additives, and fillers; see Sections 2.4.1 through 2.4.3.

### 2.4.1 Resin

The resin is the main part of the matrix and is usually refereed as polymer resin, or just resin. It is the binding agent of the composite (Bank, 2006). The two most commonly used resins types are thermosetting polymers and thermosoftening polymers, categorized depending on properties and manufacturing techniques factors, as curing and hardening (Potyrala, 2011).

#### 2.4.1.1 Thermosoftening Polymers

Thermoplastic polymers (also referred to as thermoplastics) can be softened and reshaped by heating. Subsequently, it can be hardened again by cooling. This procedure can be repeated several times for thermoplastic resins without changing the material properties (Potyrala, 2011).

#### 2.4.1.2 Thermosetting Resins

Thermosetting polymers (commonly referred to thermosets) are more commonly used for FRP composites than thermoplastics. Epoxy, polyester, vinylester, and phenolic resins are the most popular thermosets for this application (Clarke, 1996; Potyrala, 2011). In contrast to thermoplastics, the properties of thermosets are irreversible. They are formed from a chemical reaction under heat, becoming a cured product. After curing, it will not soften or lose any other of its properties, unless heated to the so-called glass transition temperature,  $T_g$ . At this temperature, the mechanical properties of the thermoset change considerably and loss in stiffness and creep are expected (Gurit, 2018a). Service temperature, manufacturing process, and intended application are of interest when choosing the type of resin (Potyrala, 2011). Furthermore; adhesive properties, mechanical properties and degradation from water ingress are all important aspects to have in mind (Gurit, 2018a).

Thermosets are manufactured as a liquid or a semi-solid precursor. Moreover, thermoset polymer resin is usually a brittle material, but it offers a high rigidity, thermal and dimensional stability (Potyrala, 2011). Epoxy is the strongest thermoset, while polyester is the stiffest. In Table 2.3, typical mechanical properties of epoxy, vinylester, polyester and phenolic resin are presented.

**Table 2.3:** *Properties of various thermosetting polymer resins (Bank, 2006).*

Resin	Density $\rho$ [ $kg/m^3$ ]	Young's modulus $E$ [ $GPa$ ]	Tensile strength $\sigma$ [ $MPa$ ]	Ultimate tensile strain $\varepsilon$ [%]
Polyester	1200	4.0	65	2.5
Epoxy	1200	3.0	90	8.0
Vinylester	1120	3.5	82	6.0
Phenolic	1240	2.5	40	1.8

Adhesive properties describe how well the resin bonds with the fiber reinforcement or the core material. Comparing epoxy, polyester, and vinylester resin systems,



polyester have the lowest adhesive properties (Gurit, 2018a). Epoxy system on the other hand have the best adhesion properties and are often used where high strength is required (Gurit, 2018a). This is the main reason why epoxy is the most common choice for CFRP (Allroth, 2018, pers. comm., February 27<sup>th</sup>; Armstrong, 2018, pers. comm., February 27<sup>th</sup>).

Resin systems degradation from water ingress characteristics describe how the resin withstands water and moisture (Gurit, 2018a). However, all resin systems will absorb moisture to some extent and loss in mechanical properties are expected. As for previously mentioned characteristics, epoxy shows the best properties for degradation from water ingress among the popular thermosets. For instance, an epoxy laminate immersed in water for a period of one year is expected to have approximately 90 % of its original inter-laminar shear strength, which can be compared to only 60 % for a laminate with polyester (Gurit, 2018a).

### 2.4.2 Fillers

Adding fillers to the matrix is a common way to decrease the total cost of the composite, by reducing the content of more expensive materials such as fibers and resin (Clarke, 1996). That is, they have the same purpose as fillers in an album, see Figure 2.5. Fillers are an inorganic, non-structural material. Some commonly used fillers are calcium carbonate (limestone), kaolinite, and aluminum oxide (Potyrala, 2011). The filler content in a composite should be limited, since fillers usually reduce the durability and long term structural properties (Clarke, 1996).



**Figure 2.5:** Back cover of "The Album" by Haddaway, released in 1993, featuring one hit and eleven fillers.

### 2.4.3 Additives

Additives are, unlike fillers, added to improve the matrix and thereby the composite properties. Can may consist of colorants, catalysts, flame retardants and other ingredients. Additives can be categorized in two groups; process-related additives and function-related additives, which have advantageous effects on the manufacturing process and the finished product, respectively. Sometimes, improving one characteristic yields a drawback in another. The mechanical properties, corrosion resistance, and fire resistance will always be influenced when additives are added (Potyrala, 2011).

## 2.5 Composite

The fibers and the matrix act as a composite. One normally distinguish between CFRP, GFRP, and AFRP. The composite properties are determined from the properties of the fibers and the matrix, the ratio of fibers/matrix in the composite, and the geometry and orientation of the fibers (Gurit, 2018a). The combined stress-strain property of the composite is shown in Figure 2.6, where the property for the composite is in between fiber and resin stress-strain property independently (Gurit, 2018a).

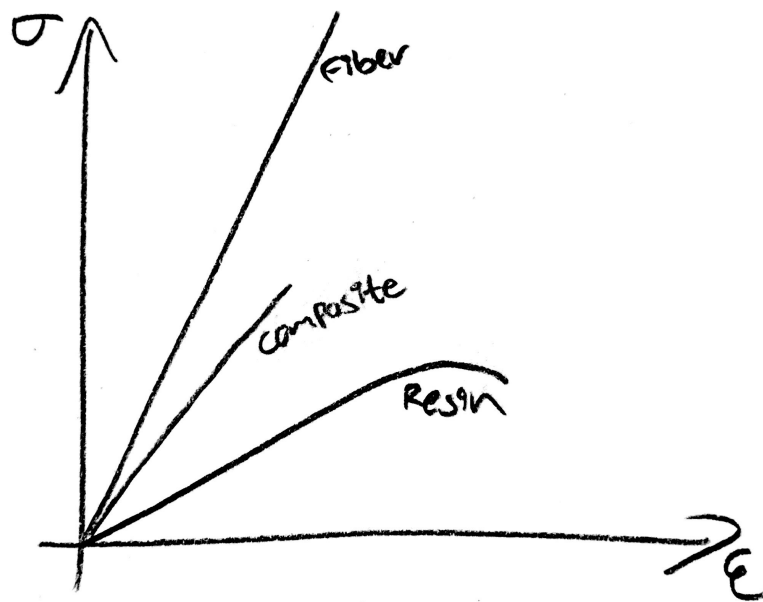


**Figure 2.6:** *Stress-strain behavior of fiber, resin, and composite.*

### 2.5.1 Rule of Mixture

Properties for a composite material can easily be estimated from a simple equation, the so called Rule of mixture (RoM), where the contribution for each component of the composite can be determined, by knowing the volume of fraction for each part (Gurit, 2018a). Furthermore, the sum of the volume fractions is 1, see Equation 2.1.

$$V_f + V_m = 1 \quad (2.1)$$

where

$$\begin{aligned} V_f &= \text{volume fraction of fibers} \\ V_m &= \text{volume fraction of matrix} \end{aligned}$$

Using the RoM, the composite properties are determined by weighting the respective properties of the fibers and the matrix, see Equation 2.2.

$$P_c = P_f V_f + P_m V_m = P_f V_f + P_m (1 - V_f) \quad (2.2)$$

where

$$\begin{aligned} P_c &= \text{property of the composite} \\ P_f &= \text{property of the fibers} \\ P_m &= \text{property of the matrix} \end{aligned}$$

Using Equation 2.2, properties such as density, tensile strength, and Poisson's ratio can be determined (Potyrala, 2011). However, for the Young's modulus of a composite, there are two different equations, depending on whether the Young's modulus parallel or perpendicular to the fiber direction is of interest (Gurit, 2018a). For the Young's modulus parallel to the fibers, Equation 2.2 is used. For the Young's modulus perpendicular to the fibers, however, 2.3 applies.

$$\frac{1}{E_2} = \frac{V_f}{E_f} + \frac{V_m}{E_m} \quad (2.3)$$

where

$$\begin{aligned} E_2 &= \text{Young's modulus perpendicular to fibers} \\ E_f &= \text{Young's modulus of the fibers, longitudinally} \\ E_m &= \text{Young's modulus of the matrix (isotropic)} \end{aligned}$$

The rule of mixture is considered as a conservative method for determining the properties of the composite, because the method is based on simplifications of uniform stress and strain (Clarke, 1996). The strengths and stiffnesses of the composites will always be a bit higher than those estimated with the rule of mixture (Clarke, 1996).

## 2.6 Sandwich Structures

In construction of FRP components, sandwich structures are commonly used, in order to increase structural efficiency. To do so, a core material is bonded between two outer FRP skins. This makes the structure a lot lighter than if the deck was a solid FRP member (Clarke, 1996). See Figure 2.7.

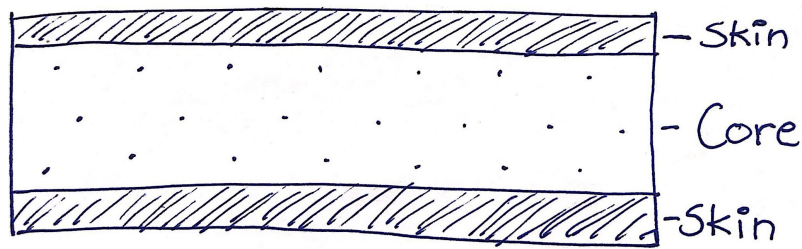


**Figure 2.7:** *Sandwich structure.*

Furthermore, characteristics of importance for a core materials are; low density, high shear modulus, and high shear strength (Clarke, 1996). These characteristics are different for different core systems, where core materials are available in three different forms: Foams, honeycombs, and solids. Foam core material can be made out of polymers, as for example polyvinyl chloride (PVC), styrene acrylonitrile (SAN) and polyethylene terephthalate (PET). Foam cores material are made out of open or closed cell materials, where the density of a commonly used foam core material are in the range from  $30 \text{ kg/m}^3$  to  $300 \text{ kg/m}^3$  (Gurit, 2018a).

Honeycomb core materials are usually produced from extrusion in a hexagon shape, see Figure 2.8, out of metal foil, impregnated resin sheets from paper or glass fabric (Clarke, 1996). Honeycomb cores give stiffness at low weight, so in lightweight constructions, honeycomb is considered as a good option. The density of honeycombs is in the range  $30 \text{ kg/m}^3$  to  $150 \text{ kg/m}^3$  (Clarke, 1996).

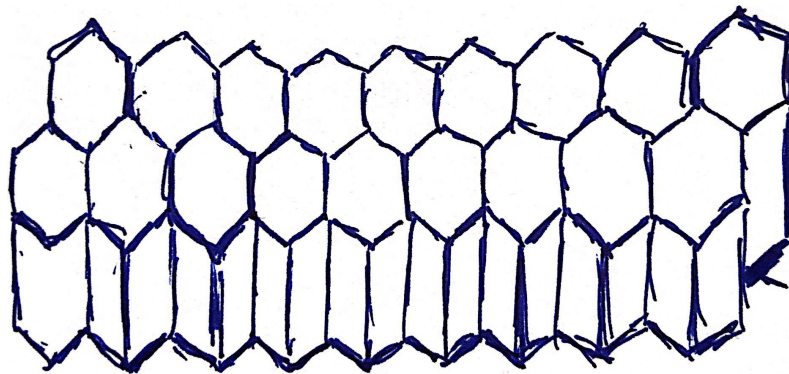


**Figure 2.8:** *Principle structure of a honeycomb core.*

In application of solid core materials for sandwich structures, end-grain balsa is the strongest and stiffest option due to its high compressive properties. Hence, balsa core is still used in lightweight constructions, but are being replaced by synthetic materials (Clarke, 1996). Furthermore, although the density of balsa is relatively low compared to other wooden materials, it is high compared to other core materials, ranging from  $100 \text{ kg/m}^3$  to  $160 \text{ kg/m}^3$  (Gurit, 2018a; Porter, 2004).

## 2.7 Manufacturing Techniques

Fiber reinforced polymer composites can be produced using various techniques. Likewise, there is a lot of materials that can vary between different composites: Resin, fibers, additives, fillers, and core. Altogether, the manufacturing technique and material options influence the composites' final properties (Gurit, 2018a). Some commonly used manufacturing techniques are:

- Hand lay-up.
- Spray lay-up.
- Pultrusion.
- Resin transfer molding (RTM).
- Prepreg.

The various manufacturing processes can be divided in classification, depending whether they are molded in an open or a closed environment. Another classification is whether the process is a manual, semi-automated, or a fully automated method (Clarke, 1996). However, the choice of manufacturing technique is of importance and will influence both cost and material properties of the composite (Potyrala, 2011).

### 2.7.1 Hand Lay-up

Hand lay-up is one of the first processes to manufacturing FRP (Clarke, 1996). It is a messy and labor intensive process; however, it is still widely used, due to low requirements of equipment and its flexibility for complex shapes (Kolstein, 2008). However, hand lay-up is not a good solution when a large number of quantities are desired, high fiber content desired or when a finished surfaces on both sides are wanted. Furthermore, hand lay-up is not a good manufacturing technique in a health and environment concern, because of styrene emissions (Potyrala, 2011). Hand lay-up is also refereed to as wet lay-up and the manufacturing technique can be seen in Figure 2.9. First, a gel-coat of resin can be applied to the mold; further, the fiber reinforcement is added. Afterwards the resin, which is mixed by hand in a bucket, are applied to impregnate the dry fiber reinforcement by using a roller or a brush. Alternate layers of fibers and resin are then applied to the desired thickness, and are then cured in normal atmospheric conditions (Gurit, 2018a).

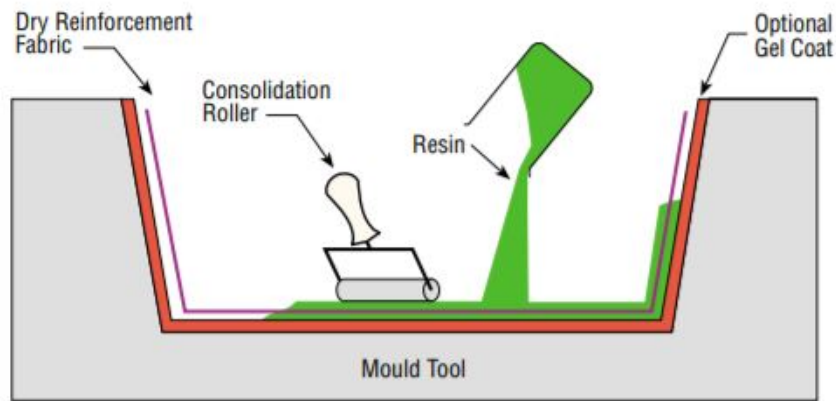


**Figure 2.9:** *Hand lay-up process (Gurit, 2018a). Published with permission.*

### 2.7.2 Spray Lay-up

The spray lay-up process is similar to hand lay-up, the considerable difference is that the spray lay up is a quicker and less expensive method (Clarke, 1996). In a spray lay-up, the fibers are chopped to a length of 10–40 *mm* in a chopper gun, and then simultaneously applied with the air pressurized resin in the mold (Kolstein, 2008). See Figure 2.10 for the spray lay-up process. Thereafter, similar as for hand lay-up, the member is cured in normal atmospheric conditions.

In contrast to hand lay-up, the spray lay-up method are only used for glass roving fibers and polyester are primarily used for the resin (Gurit, 2018a). Furthermore, a disadvantage of using this method is difficulties controlling the volume fraction of fibers and the thickness. Moreover, the process is dependent on a skilled operator and are therefore not suitable for critical products (Kolstein, 2008).

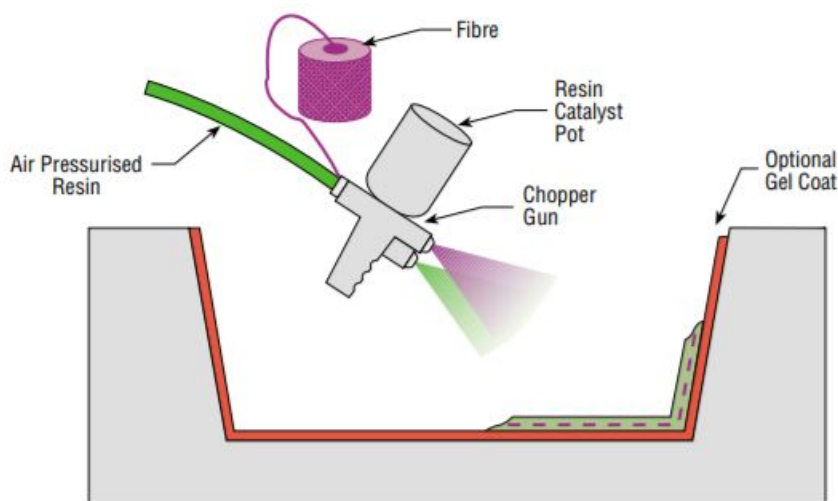


**Figure 2.10:** *Spray lay-up process (Gurit, 2018a). Published with permission.*

### 2.7.3 Pultrusion

Pultrusion is a fully automated and closed mold manufacturing technique, in contrast to hand and spray lay-up techniques, which are manual and open mold environment. Pultrusion enables continuous profiles, with constant cross section at high production speed, hence a labor and cost efficient manufacturing technique, when performed in large scales (Clarke, 1996).

The manufacturing process of pultrusion differs from the previously discussed processes. Firstly, the fibers are pulled from continuous fiber racks through a performing guides to achieve desired fiber content throughout the cross section. Secondly, the resin is applied either through a resin bath or by injection; the sooner being the most common method (Clarke, 1996). Subsequently, the composite is pulled through a heated die, which impregnates and cures the product to its final geometry and material properties. Finally the member is cut at its desired length (Gurit, 2018a). See Figure 2.11. Although pultrusion is a labor and cost efficient process, a quantity of 5000 meters of profiles is required, in order to make it economically favorable (Clarke, 1996).

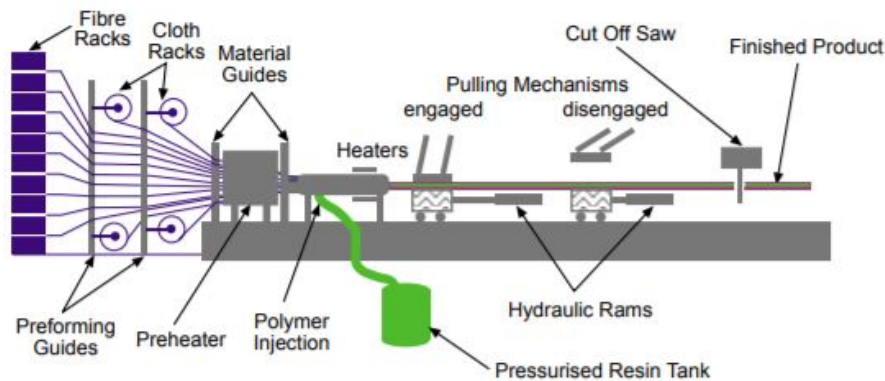


**Figure 2.11:** *Pultrusion process (Gurit, 2018a). Published with permission.*

### 2.7.4 Resin Transfer Molding (RTM)

Resin transfer molding (RTM) is an closed mold and fully automated manufacturing technique, such as pultrusion. Hence, various processes of RTM can be offered. Depending on how the resin is implemented in the mold, different mechanical properties can be achieved (Potyrala, 2011). For example, some variations can be vacuum infusion and vacuum-assisted resin transfer molding (VARTM).

In the RTM process, dry fabrics are first added in a mold tool as a dry stack of material, where the dry fabrics can be prestressed to the mold, with help from a binder (Clarke, 1996). Then, a second mold tool is applied and clamped over the first mold tool, and subsequently, resin is injected into the mold, as can be seen in Figure 2.12. Finally, the composite can be cured in the mold, at normal or raised temperature (Gurit, 2018a). This process can be achieved with help from vacuum, to draw the resin into the fabrics and is then called vacuum-assisted resin injection



(VARI). Further, advantages of using RTM are that a high fiber content can be achieved and that both sides of the product get a molded surface (Gurit, 2018a).

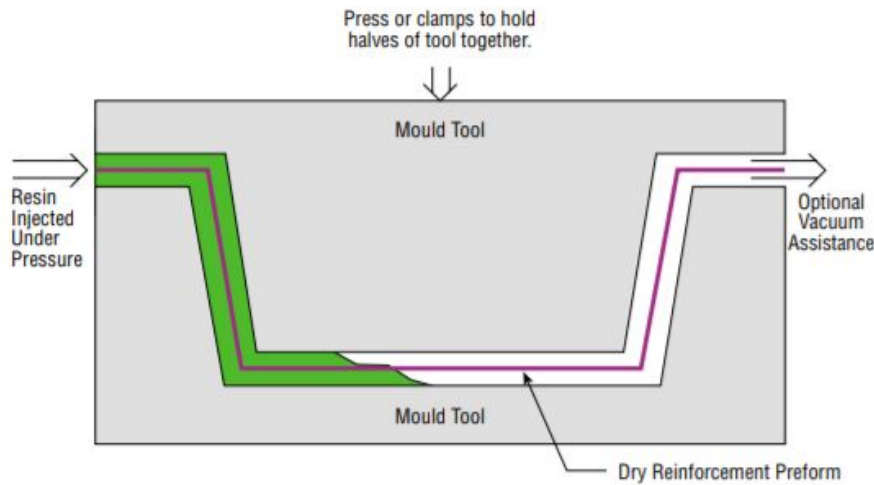


**Figure 2.12:** *Resin transfer molding (RTM) process (Gurit, 2018a). Published with permission.*

Another infusion process mentioned earlier is VARTM, which is a kind of RTM. The dry fabrics are put in a mold tool as a dry stack material (Potyrala, 2011). Thereafter, a peel ply or a resin distribution fabric is added outside of the dry stack. The main difference from regular RTM is that a second mold piece is not used. Instead, a vacuum bag is applied. This vacuum bag reduces the tooling costs and allows for extra large components to be produced (Gurit, 2018a). See Figure 2.13.

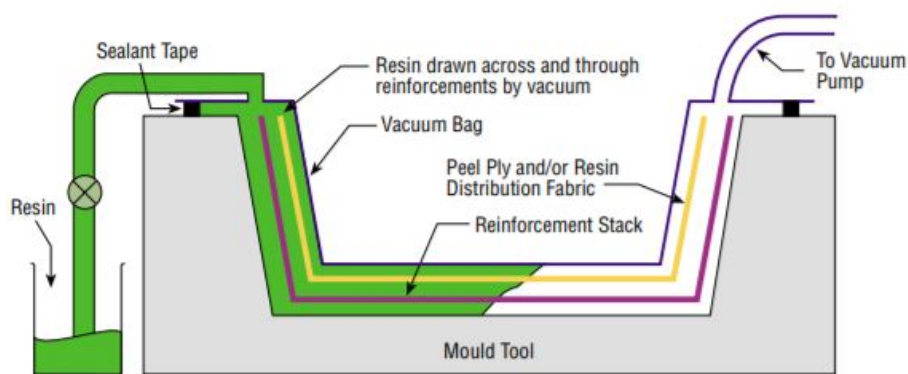


**Figure 2.13:** *Vacuum-assisted resin transfer molding (VARTM) process (Gurit, 2018a). Published with permission.*

### 2.7.5 Pre-impregnated Laminates (Prepreg)

Prepregs are a pre-impregnated fiber reinforcement or fabrics, impregnated with a matrix that is not fully cured on delivery. These prepregs can be laid up to desired applications and then consolidated and cured in temperatures over  $70^{\circ}\text{C}$  (Clarke, 1996). Prepregs are used where high performance is needed; hence a high fiber



fraction and a low void content. Usually, prepregs are delivered on rolls. To extend the shelf life, they are stored frozen. Prepregs can be delivered as unidirectional tapes, woven fabrics in  $0/90^\circ$ , and  $\pm 45^\circ$ . See Figure 2.14 Moreover, the structural ply thickness of each prepreg layer can vary, depending on the proportion of fibers to resin. Thick prepreg layers may increase manufacturing time on site for composite parts, due to less layers needed. Although, layers that are too thick are hard to handle, and are therefore not manufactured (Armstrong, 2018, pers. comm., March 26<sup>th</sup>).



**Figure 2.14:** *Unapplied prepreg laminate.*

Manufacturing of composite with prepregs is done by hand or with help from machines. They are placed in a mold, one layer at a time, in accordance with a laminate plan. A laminate plan illustrates what kind of prepregs and how many layers shall be applied (Allroth, 2018, pers. comm., February 27<sup>th</sup>). Subsequently, the products are vacuum bagged, and the air is removed with help from a vacuum pump. Afterwards, the products are cured at elevated temperatures, either in an autoclave – a pressurized oven, see Figure 2.15 – or in a regular oven. Curing in an autoclave yields the highest possible quality (Magnusson, 2018, pers. comm., February 16<sup>th</sup>). See Figure 2.16 and 2.17 for manufacturing processes of prepregs in an autoclave and in an oven.

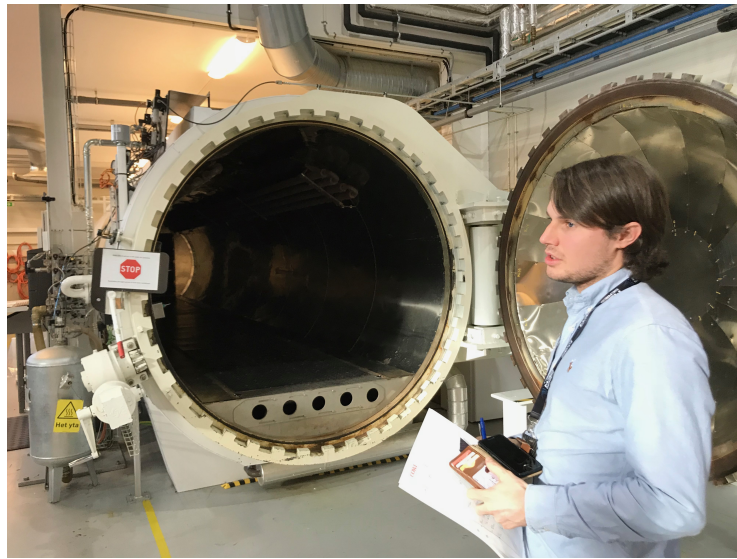


**Figure 2.15:** *An autoclave.*

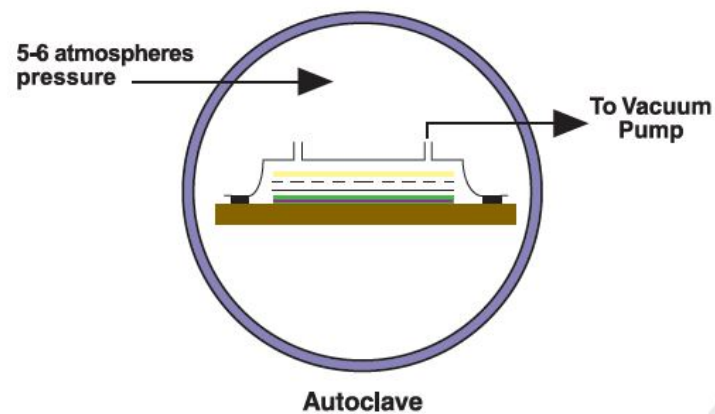


**Figure 2.16:** *Prepreg molding process in an autoclave (Gurit, 2018a). Published with permission.*

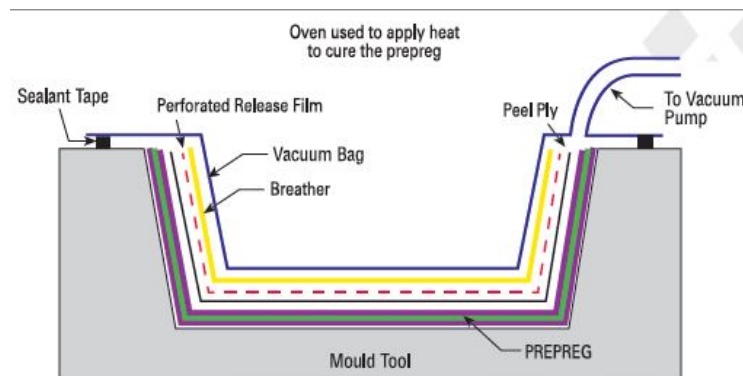


**Figure 2.17:** *Prepreg molding process in an oven (Gurit, 2018a). Published with permission.*

The main difference between the two curing processes are that in an autoclave, an enhanced air pressure can be applied (Gurit, 2018a). This curing process is used where high quality composites are wanted. Therefore, autoclaves are close to only used for prepreg materials (Kolstein, 2008). However, the manufacturing of prepreg is a time and labor consuming procedure, where the sizes of the components are limited to the size of the autoclave available (Clarke, 1996).

## 2.8 Regulations

As of 2018, there is no officially accepted design code and guideline for FRP composites in Europe. This is due to all the various combinations of fibers, resin matrices, suppliers, and manufacturing techniques of the composite (Kolstein, 2008). Altogether, the final product properties may vary depending on the manufacturer and the applications. This complicates the application of general design procedure guidelines for FRP, in contrast to more commercial materials, such as steel and concrete, whose material properties have a lesser variation (Kolstein, 2008).

However, as the use of FRP composites in construction is increasing, there is a need for a generally accepted design code. It is believed that such a design code will help the use of FRP in construction applications increase even more (Haghani, 2018, pers. comm., february 27<sup>th</sup>). As of today, manufacturers and designers tend to use their own "design handbooks", while some countries apply national guidelines for specific applications (Kolstein, 2008). Some examples of existing FRP guidelines are:

- Eurocomp Design Code and Handbook.
- CUR 96 Fibre Reinforced Polymers in Civil Load Bearing Structures.
- Fiberline Design Manual.

These guidelines are not widely used, and not yet officially accepted, such as Eurocode for steel, timber and concrete. Currently, an prospect for a Eurocode for FRP structures, "Prospect for New Guidance in the Design of FRP Structures", is being revised and waiting for approval.

### 2.8.1 Prospect for New Guidance in the Design of FRP Structures

To establish European technical rules and a standard for design in FRP, an working group has been appointed by the CEN Technical Committee 250 (CEN/TC250). the group is known as CEN Working Group WG4 and features people from various European engineering institution (Haghani et al, 2017). This working group, together with the CEN Technical Committee, has publish a prospect report at the Joint Research Center (JRC). This prospect report is under development to eventually become an EN Eurocode for FRP structures. This prospect for European technical rules will not be self standing rules, but complementing rules to existing, relevant Eurocodes (Haghani et al, 2017).



# 3

## CFRP in Civil Applications

### 3.1 Introduction

From Figure 2.1 in Section 2.1, it can be told that civil engineering is a relatively small field regarding the use of carbon fibers, compared to, for instance, aerospace and sports. 5 % of the global carbon fiber tonnage corresponds to 2300 tonnes annually. The corresponding figure for steel is about 700 million tonnes (OECD, 2010; Bergsten, 2016, pers. comm., March 21<sup>st</sup>).

### 3.2 FRP Strengthening of Existing Structures

A relatively common application of carbon reinforced polymers within civil engineering is strengthening of existing reinforced concrete (RC) structures. The method itself was invented in the United States in the mid-70's and started to engage FRP composites in Japan in the late 80's. Aramid, glass, and carbon fibers have been used. The need for strengthening can be due to poor maintenance, accidental load cases, change in application of the structures, increased traffic load, or mistakes committed during the design or construction phase. Even timber and steel structures can be strengthened with FRP, although concrete structures is the most common subject to this kind of reinforcement (Täljsten, 2011).

The traditional kind of CFRP strengthening, where the laminates are attached to the concrete girders by adhesive bonding, is beneficial with regards to the ultimate limit state (ULS). Before yielding of the steel reinforcement, both the RC member and the glued-on FRP show a linear-elastic behavior. As the steel reinforcement yields, however, a stress redistribution takes place and the FRP starts to take over a significant load (Täljsten, 2011).

In the traditional strengthening method just described, the FRP is sometimes referred to as "passive" as it only contributes slightly as long as the RC beam behaves linear-elastically. In recent years, FRP reinforcements have also been made "active" by prestressing. The effect of such an act is similar to that of pre-tensioning or post-tensioning concrete. That is, it takes use of the high tensile strength and has effects in the serviceability limit state (SLS). It stiffens the structure and also helps to reduce cracks, which is useful in corrosive environments (Ahlgren & Edwijn, 2017).



## 3.3 Examples of Existing Structures

### 3.3.1 Gangbroa, Fredrikstad, Norway

210 km north of Gothenburg – in Fredrikstad, Norway, the low self-weight of CFRP was taken advantage from by constructing a drawbridge. The bridge, made for pedestrians, is named Gangbroa, which simply means the footbridge. It has two 28-meter segments, which were both manufactured in a factory in Arendal, 236 km away. The two segments together make a 58-meter span across River Vesterelva. The structural system is made up of a parabolic sandwich system with made of CFRP and with both glass and carbon fiber stiffeners (Fireco, 2018). The bridge has a core of balsa, a wooden material with a relatively high density – from 100 to 160 kg/m<sup>3</sup> – in order to increase stiffness (Fireco, 2018; Gurit, 2018; Porter, 2004). Each of the two cantilevers, however, is so lightweight the bridge can be pushed open by two hydraulic cylinders. That is, no counterweights are needed to open the FRP bridge. See Figure 3.1.



**Figure 3.1:** CFRP drawbridge in Fredrikstad, Norway. (Grängfors & Myhre, 2018). Published with permission.

### 3.3.2 Bridge 254, Malmö, Sweden

The first ever CFRP bridge built in Sweden was installed in March, 2017. It was made as part of a scientific joint venture project between a couple of companies within architecture and civil engineering. Being a simply-supported, 17.6-meter-long sandwich structure, Bridge 254 spans the Risberga Creek in Malmö, Sweden. It consists of 28 short lightweight concrete beam segments, jointed together into seven

beams with the full span length using preimpregnated, CFRP laminates pieces with the angles  $\pm 45^\circ$ . The seven beams have then been wrapped in  $\pm 45^\circ$  for webs and unidirectional, prepregs for flanges and are afterwards cured in an autoclave. Subsequently, the seven beam elements were bonded together on-site, before the railing was attached and the bridge lifted in place (Carlsson, 2018).



**Figure 3.2:** *CFRP footbridge 254 in Malmö, Sweden (Hjelmgren, 2018). Published with permission.*

The main purpose of giving the bridge some extra self-weight. This is due to the fact that lightweight bridges tend to have problems with vibrations (Eriksson & Pagander Tysnes, 2013).

On the bottom side, FRP laminates were attached in order to hold the beams together. However, as the bridge started to deflect transversally, the adhesive was proven not to be sufficient and the laminates tends to loosen. According to expertise, the failure could have been avoided by wrapping the laminates all around the whole bridge section (Haghani 2018, pers. comm., February 15<sup>th</sup>).





# 4

## Dynamics of Footbridges

### 4.1 Introduction

Footbridges are normally used both by pedestrians and cyclists. However, for the rest of this report, only pedestrians will be considered with respect to dynamic behavior. This is because a cyclist crossing a bridge does it smoothly and with a close to constant load distribution between the two wheels. That is, the force from a cyclist does not vary in amplitude, neither vertically nor laterally. A pedestrian, on the other hand, crosses a bridge by frequently imposing footsteps. These steps are impulses that may cause the bridge to vibrate. The tendency of a bridge to vibrate depends mainly on four factors: Its stiffness, its mass, the magnitude of the external force that oscillates on the structure, and the damping properties of the bridge.

### 4.2 Basics of Structural Dynamics

The simplest way to describe the dynamic behavior of a structure is using a single-degree-of-freedom (SDOF) mass–spring–damper (MSD) system, referring to the so-called equation of motion; see Equation 4.1 and Figure 4.1 (Rupakhety & Sigbjörnsson, 2017).

$$m\ddot{u}(t) + c\dot{u}(t) + ku(t) = F(t) \quad (4.1)$$

where

$m$	=	modal mass [kg]
$c$	=	damping [Ns/m] (sometimes referred to as $b$ )
$k$	=	stiffness [N/m]
$\ddot{u}$	=	acceleration [ $m/s^2$ ]
$\dot{u}$	=	velocity [ $m/s$ ]
$u$	=	displacement [ $m$ ]
$F(t)$	=	external, dynamic force [N]

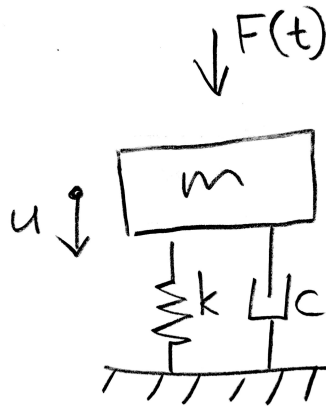


**Figure 4.1:** *SDOF MSD system.*

The modal mass of a structure is defined differently depending on the kind of structure and the boundary conditions. For a simply supported bridge with uniform self-weight, the modal mass equals half of the total mass of the bridge (Hallgren, 2018, pers. comm., April 25<sup>th</sup>). An SDOF system has one eigenfrequency, given by Equation 4.2.

$$f_0 = \frac{1}{2\pi} \sqrt{\frac{k}{m}} \quad (4.2)$$

which can also be expressed as the angular eigenfrequency,  $\omega_0$ :

$$\omega_0 = 2\pi f_0 = \sqrt{\frac{k}{m}} \quad (4.3)$$

In case of a multi-degree of freedom (MDOF) system, the equation of motion looks very similar to that of an SDOF system. The difference is that this time, mass, stiffness, and damping are all given as matrices; while the displacement and its derivatives, and the force, are given as vectors (de Kraker, 2013).

$$\mathbf{M}\ddot{\mathbf{u}}(t) + \mathbf{C}\dot{\mathbf{u}}(t) + \mathbf{K}\mathbf{u}(t) = \mathbf{F}(t) \quad (4.4)$$

As a simplification, a bridge can be seen as a simply-supported MDOF system with several eigenmodes and eigenfrequencies. For such a system, the vertical eigenfrequencies can be calculated using Equation 4.5 (Blevins, 1979), assuming a uniform bending stiffness and weight per unit length along the length of the bridge.

$$f_0 = \frac{i^2 \pi}{2L^2} \sqrt{\frac{EI}{m_{tot}/L}} \quad (4.5)$$

where  $i$  is the order of the eigenmode and the fraction  $m_{tot}/L$  is the mass per unit length.

Equation 4.4 suggests that high values for mass, stiffness, and damping give little vibrations, under a given load. Thus, it is a reasonable assumption that a lightweight system, such as a CFRP footbridge, might have vibration problems. However, a

low mass also yields a high eigenfrequency, as can be told from Equation 4.5. Even the mass of the pedestrians might affect the eigenfrequency along with the bridge's own mass, see Section 4.5. If the excitation frequency is far enough below the first eigenfrequency, the bridge will act decently stable. However, if the eigenfrequency is matched by the frequency of the exciting force, the bridge will end up in resonance, unless sufficiently damped. Regulations and limits regarding eigenfrequencies, velocity response, and accelerations are discussed in section 4.6.

### 4.3 Vibrations in Footbridges Imposed by Pedestrians

On impact, a pedestrian's foot is not only moving downwards and forwards. Since the center of mass is moving from side to side as a person walks, forces are imposed even in the lateral direction of the bridge. As a result, the force that a walking human imposes on a footbridge has three components. These three components are illustrated in Figure 4.2 and furthermore, Figure 4.3 explains how the lateral forces appear.

#### 4.3.1 Load Frequencies in Vertical, Longitudinal, and Lateral Directions

The load frequency in the vertical and longitudinal directions are the inverse of the period between two consecutive footfalls. Both the right and the left foot are moving forwards and downwards on impact. In the lateral direction, however, the period is that between two consecutive footfalls of the same foot; that is, the left or the right one. This is because the lateral forces from the right and the left foot have opposite directions (right and left, respectively), hence a twice as long period. As a consequence, the load frequency in the lateral direction equals half of those in the vertical and longitudinal directions (Sétra, 2006). This is the main reason why a lower eigenfrequency is generally accepted laterally than vertically.

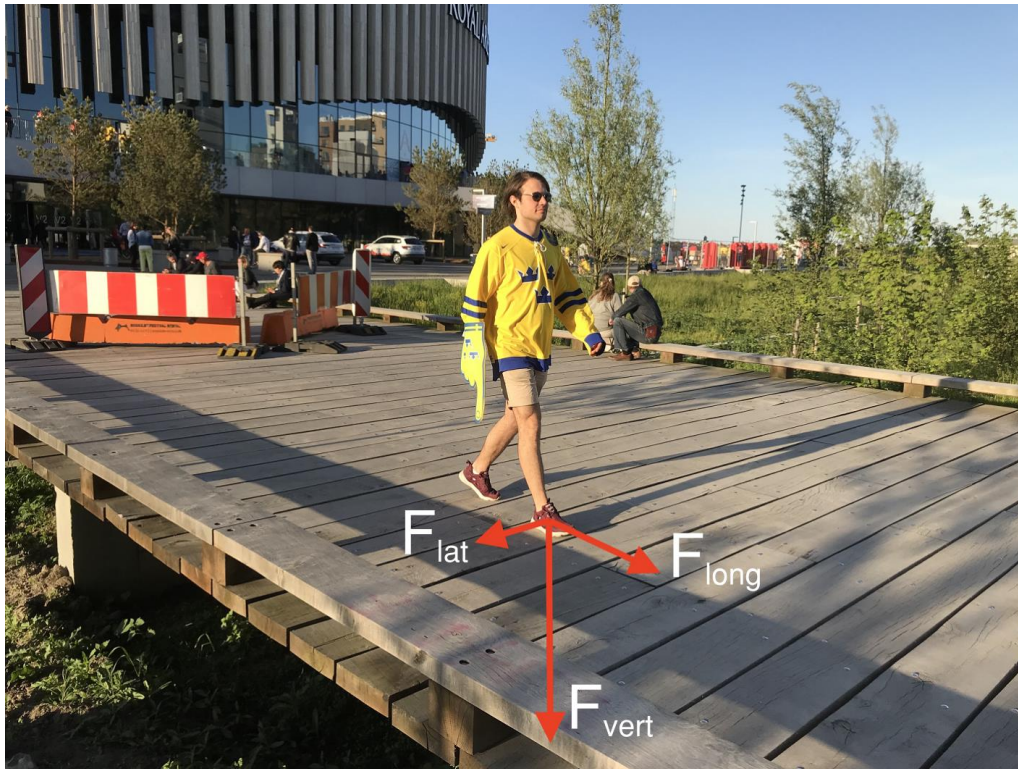


**Figure 4.2:** *Lateral, longitudinal, and vertical force components from a footfall.*

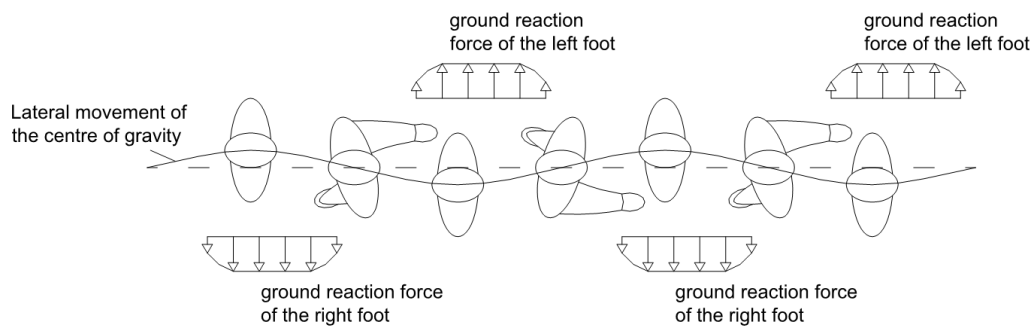


**Figure 4.3:** *Lateral forces imposed by walking human (Heinemeyer, 2008). Published with permission.*

Typically, the vertical component of the footfall force corresponds to about 40 % of the body weight. The lateral component is about a tenth of the vertical one (Dallard et al, 2001). As of the late 20<sup>th</sup> century, there were few documented examples of lateral and longitudinal dynamic forces that cause vibration problems. Thus, structural engineers have put more focus on vertical vibrations than horizontal ones. Bridges tend to be less stiff in the lateral direction than in the vertical (Dallard et al, 2001; Jansson & Svensson, 2012). Lately, the lateral vibrations has been given more focus. A phenomenon that got widely known in 2000 is called lateral lock-in.

#### 4.3.1.1 Lateral Lock-in

The Millennium Footbridge, crossing river Thames in downtown London, United Kingdom, was opened in June of 2000. During the opening weekend, the steel suspension bridge was crowded with up to 2,000 people simultaneously. At its total length of 332 *m*, that corresponds to a density of 1.5 *pedestrians/m*<sup>2</sup>. Soon after opening, the lateral forces from the pedestrians made the bridge start to sway. In order to keep their balance, the pedestrians intended to match the vibrations, that is, follow the bridge as it moved from side to side. They also spread their legs apart in order to maintain their balance, making the lateral loads extra significant. This caused immense lateral, synchronized force components, hence a great amplitude of the deformations. The phenomenon is called lateral lock-in, as the people are locked into their excitation frequency by the movement of the bridge. The mutual frequency from the thousands of pedestrians matched the lateral eigenfrequency of the footbridge, which swayed laterally with an amplitude of up to 70 *mm* (Dallard et al, 2001). Subsequently, the London Millennium Footbridge was closed three days after opening, and remained closed for more than one and a half years. The modification taken on included 37 viscous dampers and 54 tuned mass dampers, at a total additional cost of 55 million Swedish crowns (SEK) – more than 25 % of the construction cost of the bridge (Reynolds, 2002).



**Figure 4.4:** *The London Millennium Footbridge (Heineman, 2011). Published with permission.*

## 4.4 Damping

A bridge that is exposed to dynamic load at its eigenfrequency experiences resonance. Theoretically, the deformations at resonance should approach infinity, even at small dynamic loads, as suggested by a typical so-called frequency response function (FRF), see Figure 4.6. In practice, however, this does not happen, due to the phenomenon of damping.

Damping is the dissipation of kinetic energy in a vibrating structure, caused by

friction. This can be expressed as the damping force,  $c\dot{u}$ , confer Equations 4.1 and 4.4. Normally, the damping force is proportional to the velocity  $\dot{u}$  (Thorsson et al, 2008). Hence,  $c$  can be seen as constant for the particular system.  $c$  [Ns/m] is the damping coefficient, which shall not be mistaken for the damping ratio. If a structure is vibrating without being exposed to an external force, damping will eventually make it come to rest.

A structure also has a so-called critical damping coefficient,  $c_c$ . If the damping coefficient, hypothetically, equals the critical damping coefficient, the oscillation decays at the highest possible rate. That is, the structure comes to rest the soonest possible after being excited by an external force. As the amplitude of the deformation reaches zero, the structure will not oscillate beyond its original position. This is called critical damping. In such a case, the unit-less damping ratio,  $\xi$ , equals one. See Equations 4.6 and 4.7 (Sétra, 2006).

$$\xi = \frac{c}{c_c} \quad (4.6)$$

$$c_c = 2\sqrt{km} \quad (4.7)$$

If the damping ratio is lower than one, the structure is underdamped and will sway back and forth before it comes to rest. In an overdamped scenario, that is,  $\xi > 1$ , the structure does not oscillation. However, the deformation does not decay as quickly as in the critically damped case. See Figure 4.5 for an illustration of the three categories of damping.

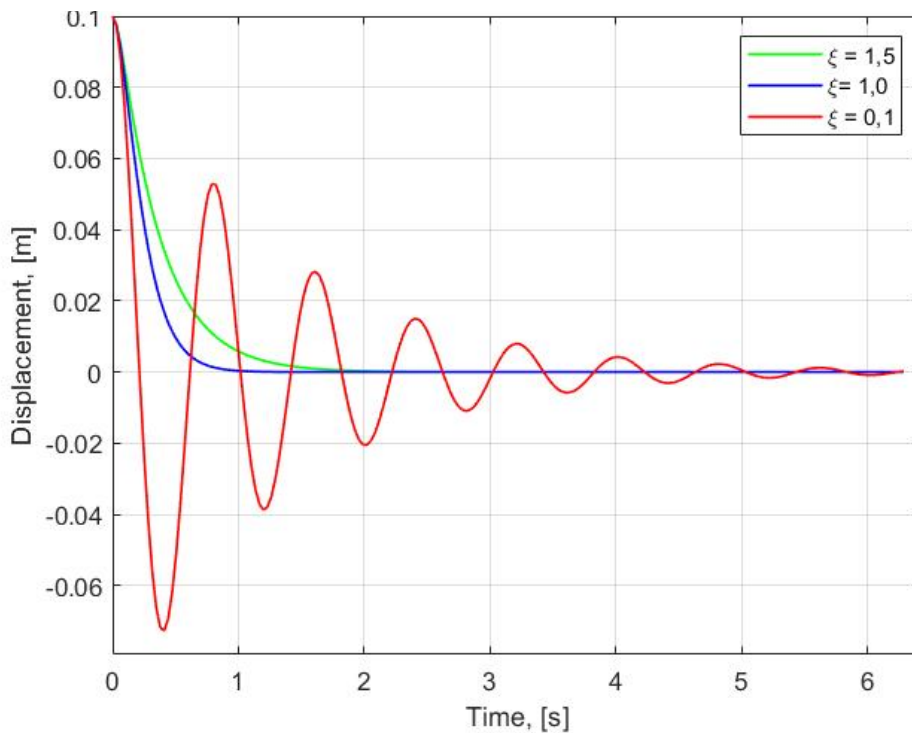


**Figure 4.5:** Overdamped (green), critically damped (blue), and underdamped (red) vibrations.

Figure 4.6 shows how damping reduces the amplitude in deformation of a vibrating structure, which is vital in the case that resonance is striking a bridge.

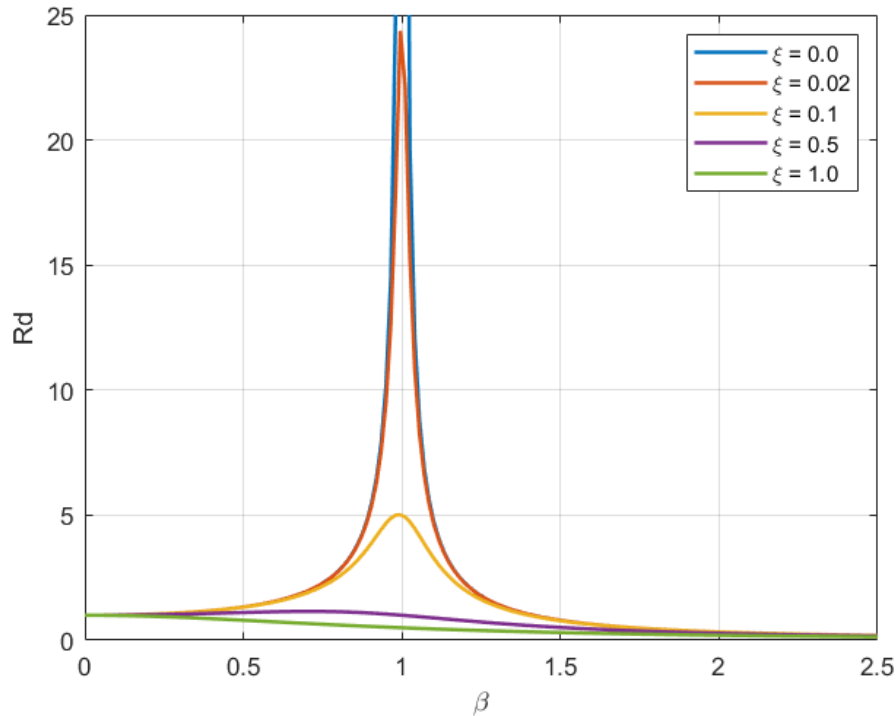


**Figure 4.6:** FRF's showing displacement response factor ( $R_d$ ) as a function of the ratio between the excitation frequency and the eigenfrequency ( $\beta$ ). The five functions all have different damping ratios ( $\xi$ ). Zero damping (blue) yields a response that approaches infinity at resonance.

#### 4.4.1 Aspects that Influence the Damping Behavior of Footbridges

?? The damping ratio of a particular structure cannot be calculated theoretically. It has to be measured from acceleration tests on existing bridges. However, bridge designers are allowed to make experience-based assumptions, taking into account various properties of the bridge. The damping contribution is sorted into two main categories, namely structural damping and material damping. The structural damping includes geometry, mass, structural system, dampers, and structural detailing. Even human–structure interaction (HSI) has an important influence, see Section 4.5.

##### 4.4.1.1 Structural Damping

The accelerations of a vibrating structure are inversely proportional to the weight of the structure. That is, the higher the mass, the smaller the accelerations. As a consequence, adding a heavy deck or wearing course is a popular way to increase the damping tendency.



Damping is also achieved by friction in the connections of a structure. Therefore, the choice of connections is vital. For example, bolted connections are more flexible – unless prestressed – than welded ones. A lot of kinetic energy is dissipated in such a connection, hence a high damping ratio. Generally, a flexible structure has a higher damping ratio than a stiff one. Following that principle, prestressed concrete is assumed to have a lower damping ratio than non-prestressed concrete. The statements given in this paragraph are suggested by codes and regulations, which will be introduced in Section 4.6.

### 4.4.1.2 Mechanical Dampers

Installing the mechanical dampers in the Millennium Footbridge, described in Section 4.3.1.1, was a necessary action to make the dynamic behavior acceptable. The solution is rather expensive and thus not desirable (Haghani, 2018, pers. comm., February 5<sup>th</sup>). Therefore, dampers should normally not be included in the preliminary design of a bridge. Because of the difficulty in predicting the damping behavior, however, it is common that room for dampers is prepared when constructing a bridge. Consequently, dynamic assessment can be carried out. If, and only if, the structure does fail to fulfill vibration criteria, dampers are post-installed (Hallgren, 2018, pers. comm., March 20<sup>th</sup>).

The two most popular kinds of dampers are viscous dampers and tuned mass dampers. The sooner follow the principle of the shock absorbers of a car; that is, excitation forces are dissipated as a piston back and forth inside of a pipe filled with hydraulic oil. The latter is a mass–spring system, which simply uses its weight to damp the vibrations in question. However, in the case of a footbridge, tuned mass dampers is not an efficient solution since the excitation force is large compared to the self-weight (Sétra, 2006).

### 4.4.1.3 Material Damping

Different materials have different damping behavior. As hinted in Section 4.4.1.1, a steel structure can be assumed to have a different damping ratio than, for instance, a reinforced concrete structure. However, as also hinted in the same section, the damping ratio does not only depend on the material itself, but also on other aspects associated with each kind of structure (for example self-weight, connections, etc.). Therefore, manufacturers cannot state a damping ratio of a particular material. There are reasons to believe that rubber-modifications of the resin can significantly change the damping behavior of a FRP structure. The phenomenon can be studied on an advanced micromechanic level. However, material manufacturers put little effort into experimental measurements aiming to predict material damping in terms of numbers for rubber-modified resins (Haghani, 2018, pers. comm., February 28<sup>th</sup>, March 15<sup>th</sup>).

In the cases that material manufacturers do announce numbers of the material's damping contributions, this is typically by means of the so-called  $\tan \delta$ , or loss factor.  $\tan \delta$  is defined by Equation 4.8.



$$\tan\delta = \frac{E''}{E'} \quad (4.8)$$

where

$$\begin{aligned} E'' &= \text{loss modulus [GPa]} \\ E' &= \text{storage modulus [GPa]} \end{aligned}$$

That is,  $\tan \delta$  is the fraction between the energy dissipated and the energy stored within the material. These properties are very temperature dependent at temperatures above  $100^\circ\text{C}$  (Saba et al, 2015).

## 4.5 Human–Structure Interaction (HSI)

Due to the presence of pedestrians on a footbridge, the amount of mass that is to oscillate is increased compared to the empty structure. When occupying a bridge, the pedestrians can be seen as integrated in the bridge system. This phenomenon, which was briefly mentioned in Section ??, is called human–structure interaction (HSI). Equations 4.4, and 4.5 remind of the importance of mass for the dynamic behavior of a bridge. As a consequence of these equations, the pedestrians tend to decrease the eigenfrequency but, on the other hand, increase the damping ratio. This conclusion is supported by three independent studies, carried out by Wang et al (2011), Shahabpoor and Pavić (2012), and Pedersen (2012).

### 4.5.1 Experiments that Support the HSI Effect

Wang et al excited a 3-meter timber beam using an electric shaker in three different setups:

- Empty beam.
- Beam occupied at midspan by an active person.
- Beam occupied at midspan by a passive person.

Due to the interaction between the human and the structure, the damping ratio rose from 0.6 to 8 % for the active person. When the person was standing still, the interaction was even more significant, yielding a damping ratio of 11.4 % (Eriksson & Pagander Tysnes, 2013). The first vertical eigenfrequency decreased from approximately 6.3  $\text{Hz}$  to around 4.5  $\text{Hz}$  when interacting with a human. The importance of the person’s activity was not significant for the eigenfrequency, however.

Shahabpoor and Pavić’s approach was similar, although in a bigger scale. They used a 2-meter wide, prestressed concrete bridge spanning 10.8  $\text{m}$ . Being excited by another electric shaker, the unoccupied bridge had a first vertical eigenfrequency of 4.5  $\text{Hz}$  and a damping ratio of 0.98 %. Occupied by people, the eigenfrequency decreased to 4.37  $\text{Hz}$  and the damping ratio rose to 1.71 %.

Pedersen (2012) studied the impact of the amount of people occupying the floor in a gymnasium. The floor was a composite structure with prestressed concrete atop steel girders. It was simply supported in a 16-meter span and the width was 21.6 m. The amount of people on the floor varied from 0 to 15 and the impact on the damping ratio is illustrated in Figure 4.7. The tendency is clearly that the relationship is linear, at least for the limited amount of people considered in Pedersen's experiment.

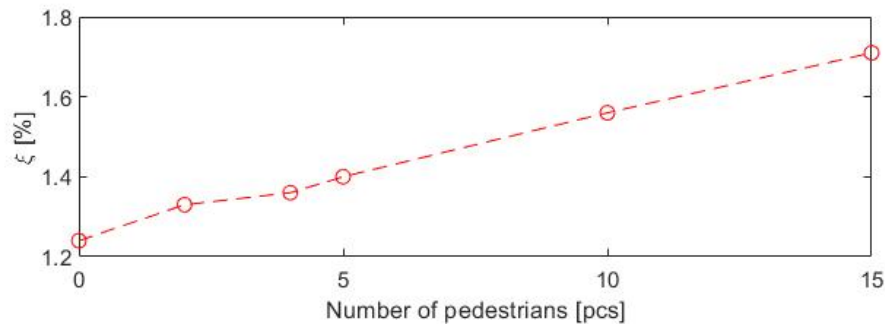


**Figure 4.7:** Results of the study made by Pedersen (2012) showing that the damping ratio of a structure increases with the amount of people occupying it.

#### 4.5.2 New Calculation Models Accounting for HSI

For the first vertical mode, Petersen (2012) describes the floor as an SDOF MSD system and people on the floor as another SDOF MSD system on top of the first one, see Figure 4.8. By addition, this yields a two-degree-of-freedom (2DOF) system. A whole range of later studies follow to the same approach. Zäll (2018) published a licentiate thesis at the Royal Institute of Technology in Stockholm, Sweden, suggesting two calculation models that consider the pedestrians as SDOF MSD's to account for the HSI.

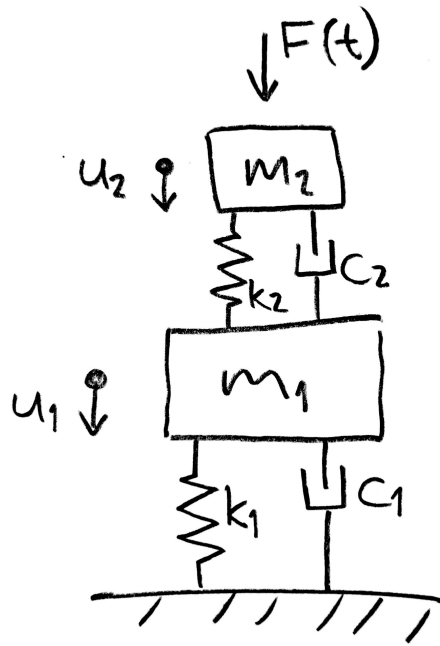


**Figure 4.8:** *HSI illustrated as an SDOF MSD system (the structure) with another one (the structure) on top of it, that is, a 2DOF system.*

## 4.6 Regulations in Footbridges

Within the European Union, the Eurocode is the default code library for structural design. In Sweden, structural engineers normally follow the requirements given in the Eurocode, while they use another code, called Sétra, for the load model (Hallgren, 2018, pers. comm., May 17<sup>th</sup>). It can also be up to the customer to require design in accordance with particular guidelines, in order to achieve optimal comfort. Following is a brief overview of some of the most popular guidelines for footbridge dynamics.

### 4.6.1 Eurocode

The Eurocode presents lower limit values for the eigenfrequencies. The values are 5 Hz for the vertical eigenfrequencies and 2.5 Hz for the horizontal and torsional ones. For bridges with eigenfrequencies below the limits, further dynamic studies have to be carried out. In such a case, the following acceleration limits apply: 0.7 m/s<sup>2</sup> for vertical vibrations and 0.2 m/s<sup>2</sup> for horizontal (SIS, 1990). If the eigenfrequencies are above the limits, there is – by definition – no dynamic load acting on the structure, according to the Eurocode (Hallgren, 2018, pers. comm., March 20<sup>th</sup>).

In earlier days, design regulations for footbridges, such as Bro 94 (Bridge 94) och Bro 2004 (Bridge 2004) did not take lateral vibrations into consideration. As a consequence, several footbridges still standing are relatively easy for one person to put into lateral resonance. A local example is Erik Johannesson's Footbridge in

Gothenburg, Sweden. Being a continuous steel truss footbridge, it crosses the Oscar Highway, not far from the Swedish head quarter of Cowi AB. At the time of its design process, the Eurocode did not apply; instead, the bridge was designed in accordance with older codes. A minor field study was carried out at the site, see Figure 4.9.



**Figure 4.9:** *Erik Johannesson's Footbridge being put into resonance by the actions of one person. The significant lateral displacements can be seen looking at the webs.*

The Eurocode emphasizes that the dynamic behavior of a footbridge is hard to predict; thus also refers to the possibility of post-installing dampers as suggested by Hallgren (see Section 4.4.1.2). However, it does state assumable values for the damping ratios of different kinds of bridges. The values are listed in Table 4.1. Since the Eurocode, up to this date, does not treat CFRP structures, there are neither any  $\xi$  values for this material. However, there is an update to come, See Section 2.8.

**Table 4.1:** *Recommended for the dimensionless damping ratio,  $\xi$ , where  $L$  is the length of the bridge (SIS, 1991; SIS, 1995).*

Kind of Bridge	$L < 20m$	$L > 20m$
Steel	$0.5 + 0.125(20 - L)$	0.5
Steel/concrete composite	$0.5 + 0.125(20 - L)$	0.5
Prestressed concrete	$1.0 + 0.07(20 - L)$	1.0
Filler beam & reinforced concrete	$1.5 + 0.07(20 - L)$	1.5
Timber w mech. connections	1.5	1.5
Timber w/o mech. connections	1.0	1.0

### 4.6.2 Sétra

Sétra (2006) is a review of other commonly used codes, which also gives its own design recommendations. It refers to a design procedure, presented in the rapidly

illustrated Figure 4.10. To summarize, it says the same as the Eurocode, namely that bridges under a certain eigenfrequency should have its dynamic behavior assessed under the desired load case.

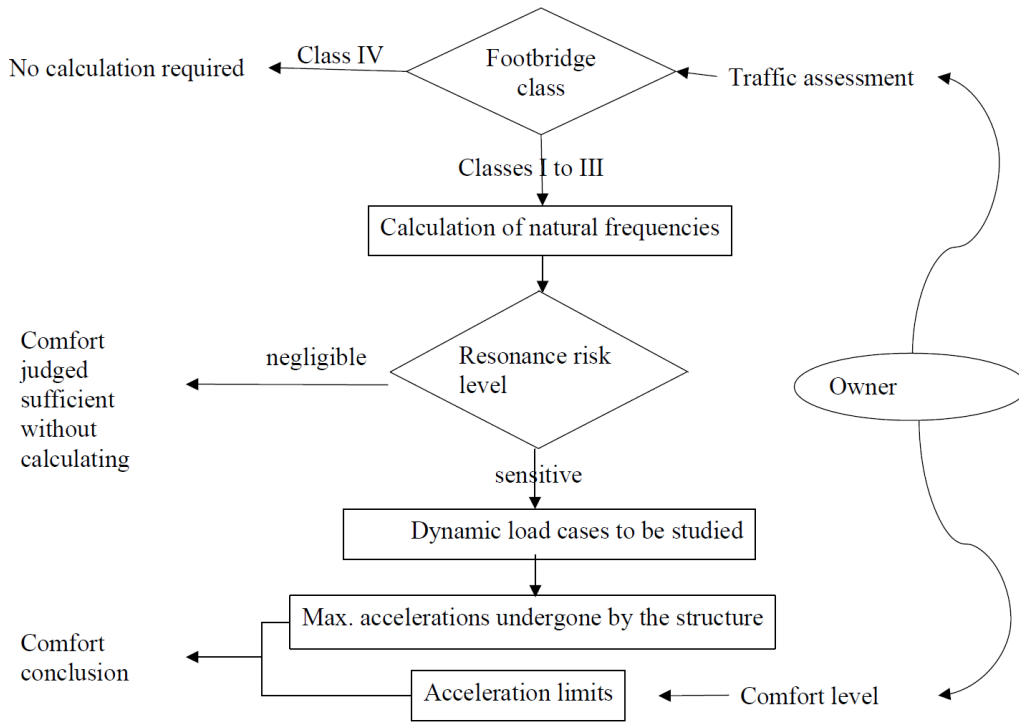


**Figure 4.10:** *Dynamic design process for footbridges according to Sétra (2006).*

#### 4.6.2.1 Resonance Risk by Frequency Range

According to Sétra, bridges risk for resonance depends on the eigenfrequency in accordance with the ranges presented in Tables 4.2 (vertically and longitudinally) and 4.3 (laterally). The values will be recognized in the tables for the load reduction factor  $\psi$ , see Figure 4.12 and Tables 4.7 and 4.8. These checks shall be done for two cases, making two different systems, namely the bridge with no additional mass and the bridge loaded with additional masses from pedestrians in accordance with the bridge class chosen (Sétra, 2006).

**Table 4.2:** *Eigenfrequency ranges and for vertical and longitudinal eigenmodes with corresponding resonance risks (Sétra, 2006).*

$f_0 < 1.0 \text{ Hz}$	Negligible risk of resonance.
$1.0 \text{ Hz} < f_0 < 1.7 \text{ Hz}$	Medium risk of resonance.
$1.7 \text{ Hz} < f_0 < 2.1 \text{ Hz}$	Maximum risk of resonance.
$2.1 \text{ Hz} < f_0 < 2.6 \text{ Hz}$	Medium risk of resonance.
$2.6 \text{ Hz} < f_0 < 5.0 \text{ Hz}$	Low risk of resonance.
$5.0 \text{ Hz} < f_0$	Negligible risk of resonance.

**Table 4.3:** *Eigenfrequency ranges and for lateral eigenmodes with corresponding resonance risks (Sétra, 2006).*

$f_0 < 0.3 \text{ Hz}$	Negligible risk of resonance.
$0.3 \text{ Hz} < f_0 < 0.5 \text{ Hz}$	Medium risk of resonance.
$0.5 \text{ Hz} < f_0 < 1.1 \text{ Hz}$	Maximum risk of resonance.
$1.1 \text{ Hz} < f_0 < 1.3 \text{ Hz}$	Medium risk of resonance.
$1.3 \text{ Hz} < f_0 < 2.5 \text{ Hz}$	Low risk of resonance.
$f_0 > 2.5 \text{ Hz}$	Negligible risk of resonance.

#### 4.6.2.2 Comfort Levels

The acceleration limits recommended by Sétra are categorized in four different comfort levels, presented in Table 4.4. The levels of acceptable comfort have the following definitions (Sétra, 2006):

- Max: Accelerations undergone by the structure are practically imperceptible to the users.
- Mean: Accelerations undergone by the structure are merely perceptible to the users.
- Min: Under loading configurations that seldom occur, accelerations undergone by the structure are perceived by the users, but do not become intolerable.

It should be noted, however, that these comfort levels are not used in Sweden (Hallgren, 2018, pers. comm., May 17<sup>th</sup>).

**Table 4.4:** *Comfort levels and associated acceleration limits [ $m/s^2$ ] (Sétra, 2006).*

Comfort level	Vertically	Horizontally
Max	0–0.5	0–0.15
Mean	0.5–1	0.15–0.3
Min	1–2.5	0.3–0.8
Not acceptable	2.5–	0.8–

It shall be borne in mind, that the direction of the load has to be adjusted to fit into the mode shape in order to model the worst case scenario. That is, except for the first bending mode, the loads shall have different directions, see Figure 4.11

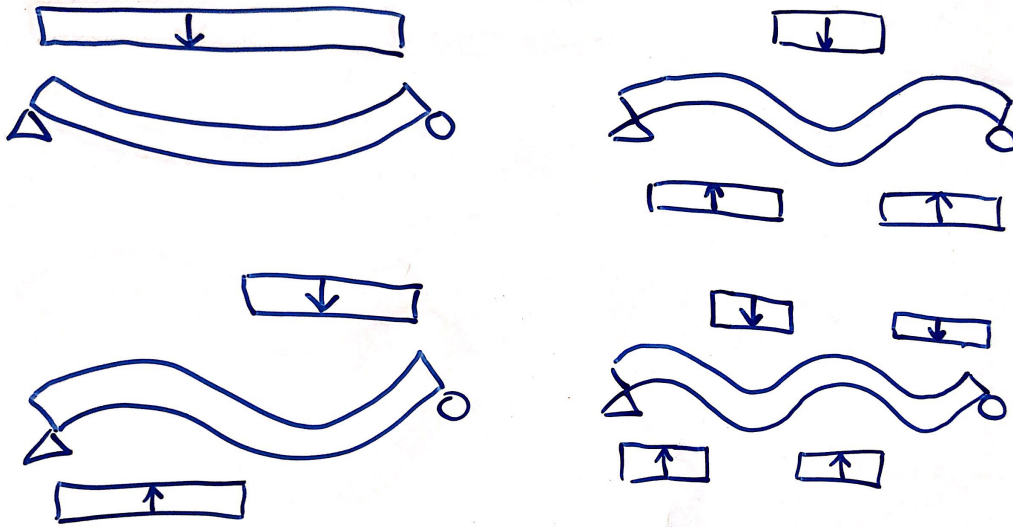


**Figure 4.11:** Load directions depending on mode cases, here presented for the first four bending modes (Sétra, 2006).

For dynamic loading, Sétra refers to three different load cases:

- Case 1: Dense and sparse crowds (footbridge class II and III).
- Case 2: Very dense crowd (footbridge class I).
- Case 3: Second harmonic effect.

The footbridge class – and thereby the crowd density – are chosen with respect to the location of the footbridge; a high class and pedestrian density in busy environment and the other way around for urban areas. In all load cases, the pedestrians are assumed to be uniformly distributed over the area of the footbridge. It is considered as very unlikely that all pedestrians walk with the same frequency and phase shift. Hence equivalent numbers for the amount of pedestrians, assuming that these all do walk in the same frequency and phase. The pedestrian densities and equivalent numbers of pedestrians for the three footbridge classes are listed in Table 4.5. A pedestrian's mass is assumed to be 70 kg (Sétra, 2006).

**Table 4.5:** Dynamic crowd classes and associated pedestrian densities and equivalent amount of people walking with the same step frequency and phase.  $\xi$  is the damping ratio and  $S$  is the total area of the bridge (Sétra, 2006).

Class	$d$ [pedestrians/m <sup>2</sup> ]	$N_{eq}$ [pedestrians]
I	1	$1.85\sqrt{Sd}$
II	0.8	$10.8\sqrt{\xi Sd}$
III	0.5	$10.8\sqrt{\xi Sd}$

In Sweden, load crowd III is by far the most common one (Hallgren, 2018, pers. comm., May 23<sup>rd</sup>). The equations for equivalent numbers of pedestrians are used to derive the three different components of the pedestrian load – vertical, longitudinal, and lateral – for the three different load cases. For load case 1, unlike load case 2, the dynamic load is dependent on the damping ratio of the structure. For the two cases, the load is defined in Table 4.6.

**Table 4.6:** Equations for dynamic load  $F(t)$  caused by the pedestrians (Sétra, 2006).  $f_{step}$  is the vertical step frequency as defined in Section 4.3.1.

Load case	Dynamic load $[N/m^2]$	Load amplitude $[N/m^2]$
1	$10.8dF_0\psi\sqrt{\frac{\xi}{S_d}}\cos(2\pi f_{step}t)$	$10.8dF_0\psi\sqrt{\frac{\xi}{S_d}}$
2	$1.85dF_0\psi\sqrt{\frac{1}{S_d}}\cos(2\pi f_{step}t)$	$1.85dF_0\psi\sqrt{\frac{1}{S_d}}$

The values for  $F_0$  are listed in Table 4.9. The factor  $\psi$  is eigenfrequency dependent and it is there to reduce, or even eliminate, the load for eigenfrequencies outside of the critical range for the particular load case, according to Figure 4.12 and Tables 4.7 and 4.8.

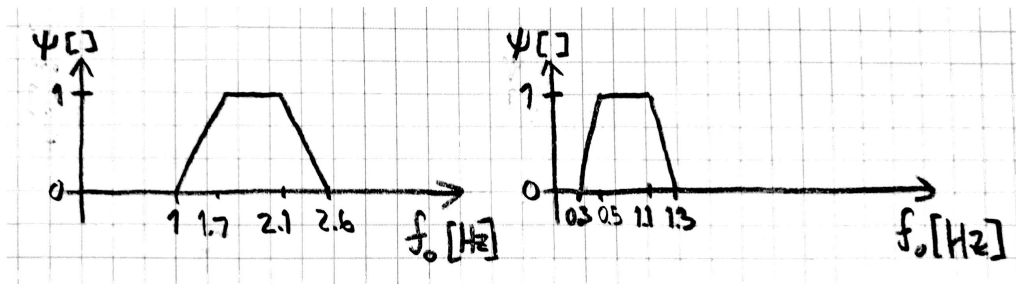


**Figure 4.12:** Reduction factor  $\psi$  for vertical and longitudinal vibrations (left) and lateral vibrations (right) (Sétra, 2006).

**Table 4.7:** Equations for the reduction factor  $\psi$  [ ] for load cases 1 and 2, for vertical and longitudinal vibrations (Sétra, 2006).

$\psi = 0$	for	$f_0 < 1.0 \text{ Hz}$
$\psi = \frac{f_0 - 1 \text{ Hz}}{0.7 \text{ Hz}}$	for	$1.0 \text{ Hz} < f_0 < 1.7 \text{ Hz}$
$\psi = 1$	for	$1.7 \text{ Hz} < f_0 < 2.1 \text{ Hz}$
$\psi = 1 - \frac{f_0 - 2.1 \text{ Hz}}{0.5 \text{ Hz}}$	for	$2.1 \text{ Hz} < f_0 < 2.6 \text{ Hz}$
$\psi = 0$	for	$2.6 \text{ Hz} < f_0$

**Table 4.8:** Equations for the reduction factor  $\psi$  [ ] for load cases 1 and 2, for lateral vibrations (Sétra, 2006).

$\psi = 0$	for	$f_0 < 1.0 \text{ Hz}$
$\psi = \frac{f_0 - 0.3 \text{ Hz}}{0.2 \text{ Hz}}$	for	$0.3 \text{ Hz} < f_0 < 0.5 \text{ Hz}$
$\psi = 1$	for	$0.5 \text{ Hz} < f_0 < 1.1 \text{ Hz}$
$\psi = 1 - \frac{f_0 - 1.1 \text{ Hz}}{0.2 \text{ Hz}}$	for	$1.1 \text{ Hz} < f_0 < 1.3 \text{ Hz}$
$\psi = 0$	for	$1.3 \text{ Hz} < f_0$

Load case 3 includes crowd classes I and II. In this case, the frequency is higher than in case 1 and 2. Thus, the second harmonic is considered and Figure 4.13 (or Tables 4.10 and 4.11, if preferred) is used for the  $\psi$  factor. For the dynamic load, Table



4.6 still applies. However, for this load case, there is a reduction in the dynamic load from the pedestrians. Hence, the values of  $F_0$  are replaced by those in the right column of Table 4.9. In summary; case 3 is just like cases 1 and 2, but with reduced  $F_0$ 's. It is rarely, however, that the second harmonic causes problems for footbridges (Hallgren, 2018, pers. comm., May 17<sup>th</sup>).

**Table 4.9:** Values for  $F_0$  [N] depending on load case and direction considered (Sétra, 2006).

Direction	Case 1 & 2	Case 3
Vertical	280	70
Longitudinal	140	35
Lateral	35	7

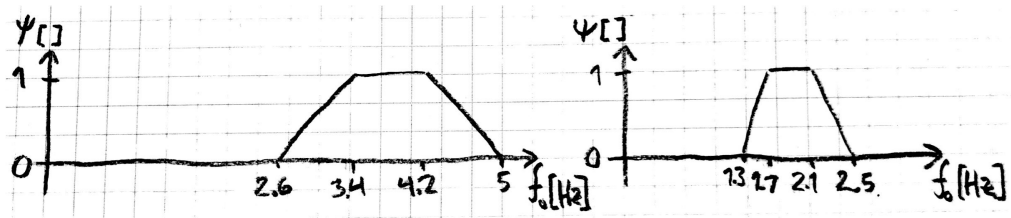


**Figure 4.13:** Reduction factor  $\psi$  [ ] for load case 3 (second harmonic), for vertical and longitudinal vibrations (left) and lateral vibrations (right) (Sétra, 2006).

**Table 4.10:** Equations for the reduction factor  $\psi$  [ ] for load case 3 (second harmonic), for vertical and longitudinal vibrations (Sétra, 2006).

$\psi = 0$	for	$f_0 < 2.6 \text{ Hz}$
$\psi = \frac{f_0 - 2.6 \text{ Hz}}{0.8 \text{ Hz}}$	for	$2.6 \text{ Hz} < f_0 < 3.4 \text{ Hz}$
$\psi = 1$	for	$3.4 \text{ Hz} < f_0 < 4.2 \text{ Hz}$
$\psi = 1 - \frac{f_0 - 4.2 \text{ Hz}}{0.8 \text{ Hz}}$	for	$4.2 \text{ Hz} < f_0 < 5.0 \text{ Hz}$
$\psi = 0$	for	$5.0 \text{ Hz} < f_0$

**Table 4.11:** Equations for the reduction factor  $\psi$  [ ] for load case 3 (second harmonic), for lateral vibrations (Sétra, 2006).

$\psi = 0$	for	$f_0 < 1.3 \text{ Hz}$
$\psi = \frac{f_0 - 1.3 \text{ Hz}}{0.4 \text{ Hz}}$	for	$1.3 \text{ Hz} < f_0 < 1.7 \text{ Hz}$
$\psi = 1$	for	$1.7 \text{ Hz} < f_0 < 2.1 \text{ Hz}$
$\psi = 1 - \frac{f_0 - 2.1 \text{ Hz}}{0.4 \text{ Hz}}$	for	$2.1 \text{ Hz} < f_0 < 2.5 \text{ Hz}$
$\psi = 0$	for	$2.5 \text{ Hz} < f_0$



# 5

## Suitable Applications for CFRP Footbridges

The aim of this chapter is to determine criteria for a case in which a carbon fiber footbridge is believed to be more suitable than a bridge made of a more conventional material, such as concrete or steel. These criteria have to take the greatest possible advantage of the beneficial aspects of CFRP, to compensate for the fact that CFRP is an expensive material (Hjelm & Karlsson, 2014). Even factors that limit the applications possible are looked at. Subsequently, an evaluation is made by comparing an existing steel truss bridge in Norrköping, Sweden, to a hypothetical substitute made out of CFRP. This is done in Chapter 6.

### 5.1 Manufacturing

There are several restrictions on the environmental conditions when manufacturing a CFRP structure, both regarding the temperature and the relative humidity. For that reason, an envelope is required for the manufacturing site, that is, a temporary factory would be needed in case of in-situ lay-up and casting of a CFRP bridge. For economic and logistic reasons, such a solution is hard to justify for a bridge project (Gledhill, 2018, pers. comm., February 5<sup>th</sup>). The reasonable alternative is to build the bridge to the largest possible extent in a factory and then transport it to the site, hence a size-wise limitation with respect to the capacity of a factory and that of a truck with a trailer. If the highest possible quality is desired, the products shall cure in an autoclave, see Section 2.16. In such a case, the size of each part is obviously limited to the size of the autoclave.

### 5.2 Supports

The opportunity of constructing a lightweight bridge can be taken advantage of on a foundation level. A lightweight bridge simply does not require a foundation as solid as in the case of a heavy bridge. This fact was taken into account when proposing a CFRP solution for the so-called Caponier Bridge in downtown Gothenburg. The 45-meter bridge was to be built on weak quays above a clay ground. Although paused at the time of master's thesis writing, the project referred to geotechnics as a main reason to the choice of material (Falk, 2014). Another project saved an alleged 3.3 million SEK by not constructing new piers and piles for a GFRP bridge crossing a railway in Thornaby, near Middlesbrough, United Kingdom (Fiberline, 2014).

### 5.3 Transportation

In the Kingdom of Sweden, there is no official limit to how oversized cargos one can transport by road. Allegedly, road transportation of 70-meter wind power blades has been performed in Sweden (Molnar, 2018, pers. comm., April 9<sup>th</sup>), which yields a total carriage length of about 74 m. Further, a width of up to 7 m is manageable, if the route is well-planned. Special permits are required for oversized cargo; however, it is the responsibility of the transporter to make sure that the particular operation is possible. There are rules on the amount of escort that cargos of various sizes require. In principle, escort vehicles are needed in front of the carriage if it is wide, and behind it if it is long. If the cargo is wider than 3.1 m or longer than 30 m, it requires an escort vehicle, where the driver has a driver's license of category C. If the measurements are beyond 4.5 m or 35 m, respectively, a so-called police license escort is needed. These are driven either by police officers or by traffic directors, that is, people who have undergone an education putting her or him on the same authority level in traffic as a police officer (Svanberg, 2018, pers. comm., May 15<sup>th</sup>). In total, if the cargo is both wider and longer than the measurements mentioned, four escort vehicles are needed.

The rules are summarized in Table 5.1. Additionally, when transporting even more oversized cargos, the transportation company might choose to use a supervisor, that is, a fifth vehicle accompanying the carriage (Svanberg, 2018, pers. comm., May 9<sup>th</sup>).

**Table 5.1:** *Escorting vehicles required for particular cargo measurements (Trafikverket, 2018a; Svanberg, 2018, pers. comm., May 9<sup>th</sup>).*

● Escort

● Police license escort

Width \ Length	–3.1	3.1–4.5	4.5–
–30		●	● ●
30–35	●	● ●	● ● ● ●
35–	● ●	● ● ● ●	● ● ● ● ● ●

If the cargo is wider than 4.5 m, the route in question should be analyzed to see if any particular obstacles have to be dealt with. For example, ditches may have to be filled up, or road signs might have to be temporarily demounted. The cost for demounting a road sign is normally between 10,000 and 20,000 SEK. The weight of the cargo is not of high importance as long as it corresponds to those of steel truss bridges and lighter (Molnar, 2018, pers. comm., April 9<sup>th</sup>; Svanberg, 2018, pers. comm., May 9<sup>th</sup>). In extreme occasions, however, the lightweight characteristic can be taken advantage of in a rather spectacular way. In 2013, two GFRP bridges were flown in by helicopter at a difficultly accessed water reservoir, 51 km north of Glasgow, United Kingdom (Fiberline, 2013).

## 5.4 Installation

Once the bridge in question is at the site where it shall be used, it must be lifted in place. The cost of the installation depends mainly on the kind of crane needed for the lift, what kind of traffic the process affects, and for how long.

### 5.4.1 Crane

Typically, an all-terrain crane or a regular mobile crane is capable enough to lift and lower a footbridge in place. The choice of crane, however, depends on the weight of the bridge and from where the site is accessed. If possible, the best option is to lower the bridge into position with the bridge's long side facing the crane vehicle. Such a scenario does not require a very long crane radius, hence a moderate moment force at the base of the crane. If not possible, the vehicle has to stand at the short end of the bridge and have a reach greater than half of the bridge length. This also yields a higher moment force and requires a bigger vehicle, see Figure 5.1 (Hagstrand, 2018, pers. comm., May 3<sup>rd</sup>).

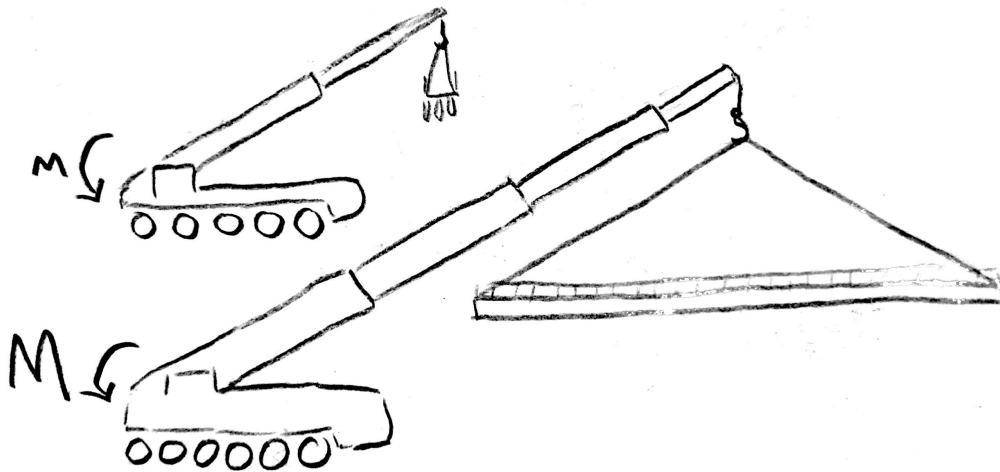


**Figure 5.1:** Principle sketch of how the required crane capacity depends on way of access. Access at the long end of the bridge (top), and at the short end (bottom).

### 5.4.2 Traffic Disruptions

A well-planned installation is important, in order to cause the smallest possible disruption in the surrounding traffic. Any interference in roads, railways, and other facilities at or around the site can be converted into a cost (Johansson, 2018, pers. comm., May 7<sup>th</sup>). The Swedish Traffic Administration (Trafikverket) has default numbers for the cost of delaying of people or cargo, expressed in SEK per person hour or SEK per tonne hour (Trafikverket, 2018b). If a road is closed, these numbers are put in calculation sheets along with the distance of the detour that the traffic has to take. If a railway cannot operate, supplementary buses have to be used and the cost for this must be accounted for (Johansson, 2018, pers. comm., May 7<sup>th</sup>).

If a stop is not well-planned, the disruption might yield very high expenses (Sundbom, 2018, pers. comm., May 14<sup>th</sup>). Normally, one aims to install a bridge at night (Karlsson, 2018, pers. comm., April 30<sup>th</sup>); and a bridge design that allows a quick installation is of high priority in busy environments, exempli gratia in cities, across heavily loaded freight railways, and across highways. In such cases, it also makes sense not to build an intermediate support, since such a construction most likely requires a capacity reduction or a shutdown of the road that the bridge is to cross. The busy traffic on a downtown highway makes such a barrier a reasonable obstacle to span for a lightweight, quickly-installed, footbridge (Jansson, 2017, pers. comm., December 6<sup>th</sup>).

### 5.5 Maintenance

One advantage of using CFRP as a structural material is the low need for maintenance. Since the use of fiber composites in footbridges only started in the 1990's (Reeve, 2017), it is hard to verify such a statement. However, characteristics that indicate it are the high resistance against corrosion and UV radiation, along with good impact strength and fatigue resistance (Kolstein, 2008; Peeters, 2011). The latter, however, is not a benefit that applies to footbridges, since such structures are generally not designed for fatigue loading (Jansson, 2018, pers. comm., March 9<sup>th</sup>).

The corrosion and UV resistance means that a CFRP bridge does not have to be re-painted during its lifetime. This yields an advantage when placed in a location that is sensitive to traffic disruptions, both on and underneath the bridge. Steel structures have to be re-painted using epoxy-based paint, which must not end up in the surroundings. That is, some kind of envelope has to be made around the bridge, possibly by making a temporary tunnel for the traffic (Darholm, 2018, pers. comm., May 17<sup>th</sup>). This could be a difficult and expensive process.

Despite the little maintenance needs, the Traffic Administration does not suggest any difference in requirements on inspection intervals for CFRP bridges than other bridges. That is, a CFRP bridge should be inspected as often as a typical bridge made of other materials. This is supported by Haghani & Yang (2016). The inspection intervals stated by the Traffic Administration are one year for minor inspections and six years for major inspections (Rutgersson, 2014).

## 5.6 Summarized Criteria for Suitable Applications of CFRP Footbridges

With the aspects referred to in Section 5.1 through 5.5 in mind, the application in which a CFRP footbridge is believed to be a good option is characterized by the following bullets:

- A span of up to 70 *m*. At least a span corresponding to the width of a downtown highway.
- No intermediate support.
- A busy environment, where time can be saved from a quick installation. Preferably downtown or on busy roads and railroads.
- A corrosive environment, that is, in coastal locations.
- A weak foundation.





# 6

## Economic Comparison Between Existing Steel Truss Bridge and CFRP Alternatives

The aim of this chapter is to assess how competitive a CFRP footbridge is in means of economy, by comparing the costs of two different CFRP design options (described in Chapter 7) to an existing bridge of a more conventional kind.

### 6.1 Introduction

In Åby, a suburb located 10 *km* north of Norrköping, Sweden, a steel truss footbridge crosses a single-track railway. The span is 30 *m*. The official name of the bridge is 581-909-1. Parallel to the footbridge is a road bridge carrying the Humpegård Road. East of the railway is the district of Humpegården, with residential houses, a kindergarden, a soccer field, and a sewage treatment facility. West of the railway is downtown Åby (Google Maps, 2018). Installed in 2010, the bridge is not designed for vertical vibration requirements (Darholm, 2018, pers. comm., May 25<sup>th</sup>). The location in question fulfills some of the criteria stated Section 5.6. The railway connects the city of Norrköping to Kolmården Wildlife Park and the nearby town of Nyköping (Google Maps, 2018), and is therefore important for the municipality. An intermediate support is not an option because of the railway itself.



**Figure 6.1:** *Satellite view of bridge 581-909-1 in Åby, Sweden (Google Maps, 2018).*

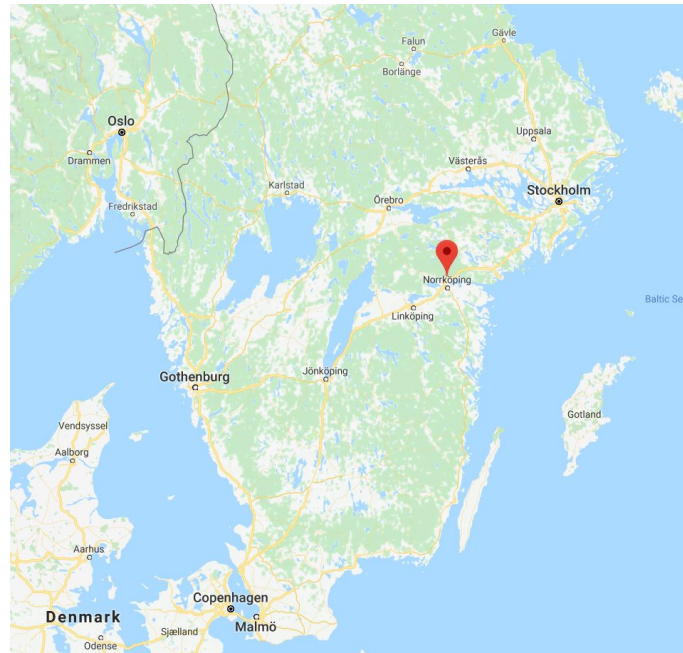


**Figure 6.2:** *The location of bridge 581-909-1 in Åby, Sweden (Google Maps, 2018).*

### 6.2 Bridge 581-909-1

Up to this day, a steel truss solution is the most common choice for a footbridge in a spot with the characteristics given. Bridge 581-909-1 was designed by Cowi and prefabricated by Lecor in Kungälv, Sweden. It is 30 m long, 3.4 m wide and has a total mass of 28.5 tonnes, hence a mass of 950 kg per meter (Appendix A; Karlsson, 2018, pers. comm., April 30<sup>th</sup>).



**Figure 6.3:** *Bridge 581-909-1 in Åby in the foreground, adjacent road bridge in the background (Trafikverket, 2018c). Published with permission.*

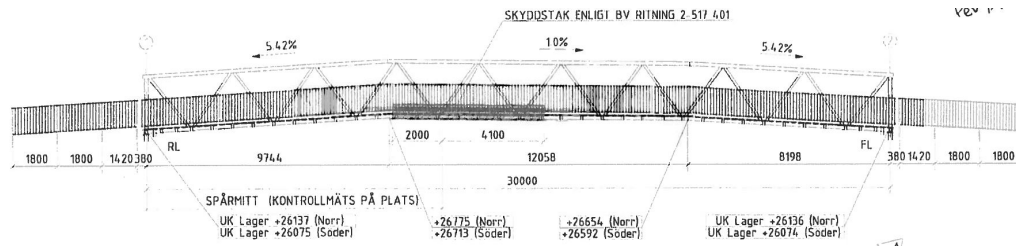


**Figure 6.4:** *Elevation of bridge 581-909-1 in Åby (Appendix A). Published with permission.*

## 6.3 Comparison

In this section, the estimated costs of bridge 581-909-1 are compared to those of two hypothetical substitutes, made out of CFRP. The aim is to figure out whether the benefits of CFRP make it an economically better choice than a steel truss bridge, despite its high manufacturing cost. With the previously stated criteria in mind, the CFRP bridge is designed in the upcoming Chapter 7. A slender CFRP design will occasionally be referred to in short as "CFRP1". A bulky, more stable but heavier CFRP design will, likewise, be shortcut "CFRP2". Bridge 581-909-1 will in short be called "truss". The input data for calculating the prices are given in this chapter; however, the calculations are carried out in parallel to the thesis.

Specialists within civil engineering suggests the service life of the CFRP bridges to be 100 years (Haghani, 2018, pers. comm., May 22<sup>nd</sup>; Olsson, 2018, pers. comm., May 22<sup>nd</sup>) and that of the truss bridge to be 80 years (Darholm, 2018, pers. comm., April 23<sup>rd</sup>). Since the suggested service life is different to that of a truss bridge, the overall cost of each alternative is subsequently divided by the amount of years in operation, see Section 6.5.

### 6.3.1 Manufacturing

The prefabrication is the activity in which CFRP is far more pricy than a steel truss, since the process is time consuming and the material expensive. Since the concept of steel truss bridges is very widely applied, typical numbers can be used to calculate the manufacturing cost with a very decent accuracy. The cost of the truss bridge is calculated using the numbers stated in Table 6.1.

**Table 6.1:** *Estimated costs for a truss bridge (Karlsson, 2018, pers. comm., April 30<sup>th</sup>). Please note that the cost for surface finishing is given in SEK per unit bridge mass, and that the acrydur cost includes application.*

Product/activity	Unit cost	Unit
Materials	10	SEK/kg
Manufacturing	15	SEK/kg
Surface finishing	8	SEK/kg
Acrydur coarse	1,400	SEK/m <sup>2</sup>

The approach used to calculate the manufacturing cost of the CFRP alternatives was different. A cost estimation was made by Allroth (2018, pers. comm., May 22<sup>nd</sup>), based on design option 1, presented in the next chapter, although in a 25-meter span. The estimated material cost for this is 6,450,000 SEK and the estimated manufacturing time is 2,520 working hours. A total of 14,000 m<sup>2</sup> of prepreg laminates are laid up for the first CFRP design, while the corresponding number for CFRP2 is 26,700 m<sup>2</sup>, as Hand calculated made by the master's thesis group indicates that the total area of laid-up prepreps is almost twice as big for CFRP2 as for CFRP1. According to Allroth, both the personnel cost and the material cost for structures like the ones considered can be approximated as linearly dependent on the total area of prepreg laminates to be applied. Therefore, several simplifications can be made to consider differences like size, span length, et cetera. This is also the basis on which the costs for manufacturing CFRP2 are made. An estimated 50 % should be added in the calculation, representing molds, personnel, planning, et cetera. The cost of the acrydur sheeting is subsequently added in the calculations.

**Table 6.2:** *Estimated manufacturing costs [SEK].*

Activity	Truss	CFRP1	CFRP2	Relationship
Manufacturing	1,066,500	11,800,000	22,230,000	1/11.1/20.8

### 6.3.2 Supports

Considering the location, between two roads and just a few meters from a road bridge, it is assumed that no geotechnical effort is saved by using a lightweight bridge. Thus, the same numbers apply for all three bridge alternatives. According to Karlsson (2018, pers. comm., April 30<sup>th</sup>; April 15<sup>th</sup>), constructing the two abutments costs approximately 45,000 SEK, and the bearings some 30,000, that is, a total of 75,000 for either alternative.

**Table 6.3:** *Estimated costs for the supports [SEK].*

Activity	Truss	CFRP1	CFRP2	Relationship
Supports	75,000	75,000	75,000	1/1/1

### 6.3.3 Transportation

In order to make a decently fair comparison, the three bridge options are assumed to be transported from the same factory, although the factory where the truss bridge was built does not manufacture CFRP products. That is, the transportation distance considered is that between the Lecor factory in Rollsbo Industrial Park in Kungälv, 23 *km* north of Gothenburg, to Kroktorp Road in Åby. The distance is 340 *km* (Google Maps, 2018).

Due to the moderateness of the bridge sizes considered, no cost difference should apply in the transportation phase. All three bridges have the same length and width, namely 30 and 3.4 *m*, respectively. In accordance with Table 5.1, this requires one escorting vehicle behind the carriage and one in front of it.

Uddevalla Specialtransporter is a transportation company based 63 *km* north of the Lecor factory. The costs calculated in this section are based on their price list. The price for the carriage is 25 *SEK/km*, measured as a round trip between the starting point and the end point of the shipping route. Each escort vehicle is 7.5 *SEK/km*. Two hours of unloading are included in the price (Svanberg, 2018, pers. comm., May 9<sup>th</sup>). This yields a transportation cost of 27,200 *SEK* for either case.

**Table 6.4:** *Transportation costs [SEK].*

Activity	Truss	CFRP1	CFRP2	Relationship
Transportation	27,200	27,200	27,200	1/1/1

### 6.3.4 Installation

Looking at Figure 6.1, it becomes clear that the crane has to be placed by either one of the ends of the footbridge. It cannot access the railway; the overhead lines being one of several reasons. Standing on the adjacent road bridge is not an option. The crane has to be braced by its outriggers while lifting the bridge, and can therefore not drive onto the road bridge with the footbridge hanging.

Thus, a crane radius corresponding to half of the span length plus approximately 5 *m*, that is, 20 *m* in total, is required. The bigger the reach and the heavier the bridge, the greater the counter-weight needed. That is: A bigger crane truck is needed.

For the considered radius, Hagstrand (2018, pers. comm., May 3<sup>rd</sup>) proposes three different cranes, depending on the weight of the footbridges. These are listed in Table 6.5, with associated prices provided by lifting service company Havator.

**Table 6.5:** *Cranes suggested for a radius of 20 m and various footbridge weights. The numbers are approximate. Prices provided by Havator (Hagstrand, 2018, pers. comm., May 3<sup>rd</sup>).*

Weight [t]	Crane model	Crane type	Lift prize [SEK]
–11	Liebherr LTM 1100-5.2	Mobile crane	28,000
11–17	Tadano 130G-5	All-terrain crane	32,000
17–	Tadano 400G-6	All-terrain crane	100,000

The total mass of CFRP1 is about 10 tonnes and that of CFRP2 is slightly below 17 tonnes. With respect to the self-weights, a Liebherr LTM 1100-5.2 for the slender CFRP bridge, a Tadano 130G-5 for the bulky CFRP bridge, and a Tadano 400G-6 for the truss bridge are recommended. This yields a cost difference between the three alternatives. As an addition, there are operation costs for supervision personnel, a traffic arrangement plan (TA plan), et cetera, of approximately 100,000 SEK (Janssen, 2018, pers. comm., May 14<sup>th</sup>; Karlsson, 2018, pers. comm., May 16<sup>th</sup>).

One of the biggest benefits of a CFRP solution is claimed to be a quick installation, that is, a short amount of time that surrounding road and rail traffic has to be shut down. However, this advantage may not be significant. Bridges of the kind that is present in Åby are also marketed as lightweight structures which require little installation time. It is generally lifted in place during a six-hour shutdown at night (Karlsson, 2018, pers. comm., April 30<sup>th</sup>). A comparable example is the GFRP bridge mentioned in Section 5.2. Even that bridge was installed during a six-hour time frame (Fiberline, 2014). It is reasonable to believe that the considered CFRP bridge, in question, would take a corresponding amount of time to install. Therefore, costs for closing the railway and the surrounding roads during installation are not calculated more in detail.

**Table 6.6:** *Installation costs [SEK].*

Activity	Truss	CFRP1	CFRP2	Relationship
Installation	200000	128000	132000	1/0.64/0.66

## 6.4 Maintenance

It is suggested that a steel truss bridge is repainted with intervals of up to 40 years (Darholm, 2018, pers. comm., April 23<sup>rd</sup>). Thus, it is assumed that the truss bridge is re-painted once during its 80-year service life. A local painting company in Norrköping, Målerit, estimates the cost of painting the particular bridge in-situ to be 82,400 SEK (Alkin, 2018, pers. comm., May 28<sup>th</sup>).

The wearing coarse should be replaced the same rate as the truss bridge is re-painted (Darholm, 2018, pers. comm., April 23<sup>rd</sup>). A very rough estimation made by Dahllöf (2018, pers. comm., May 22<sup>th</sup>), indicates that the previously stated 1,400 *SEK*/m<sup>2</sup> for applying the new layer, plus another 200 *SEK*/m<sup>2</sup> for removing the old one, add up to a reasonable cost for replacing the acrydur wearing coarse.

As far as inspection is concerned, inspection costs are estimations based on an LCCA made on a planned 12.4-meter culvert road bridge concept. For the minor inspections, required to take place once a year, the cost is 3,240 *SEK*. The major inspections, required once every six years, are 18,900 *SEK* (Haghani & Yang, 2016).

**Table 6.7:** *Maintenance costs [SEK].*

Activity	Truss	CFRP1	CFRP2	Relationship
Maintenance	737,600	718,200	718,200	1/0.974/0.974

## 6.5 Cost Adjustments

This category is meant to account for additional factors that should be considered. According to Karlsson (2018, pers. comm., May 21<sup>st</sup>), an approximate 10 % should be added to the total cost, paying respect to unforeseen extra expenses. Besides that, 20 % is removed from the CFRP bridges, taking into account that the service life of the CFRP bridges is assumed to be 25 % longer than that of the truss bridge.

**Table 6.8:** *Price Adjustments [SEK].*

Activity	Truss	CFRP1	CFRP2
Adjustments	210,600	-1,530,000	-2,782,000

The total costs for the three alternatives are summed in Section 9.1, in the result chapter, and commented on in Section 10.1.





# 7

## Bridge Design

A first workshop on took place on March 12<sup>th</sup>, 2018, engaging Svensson, Darholm, and the master's thesis group. With attention paid to the summarized criteria for reasonable use of a lightweight CFRP footbridge, stated in Section 5.6, a preliminary design was developed. This design includes a sandwich deck with a foam core, supported by three main box girders. The deck has no edge beams; however, it does have edge stiffeners outside of the railings. For the sake of aesthetics, the main girders are given a slightly elliptic cross-section, see Figure 7.1. A geometrically simplified version is also presented. In order to make hand calculations and FE modeling time-efficient, this is the model that the master's thesis will henceforth refer to.

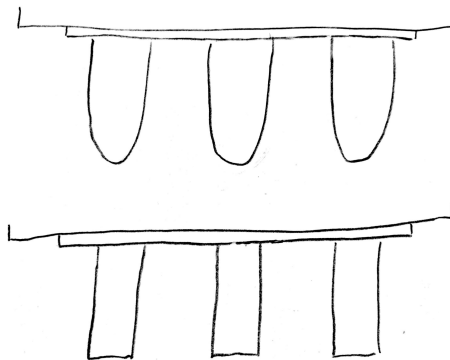


**Figure 7.1:** *Rough sketch of the preliminary design of the CFRP footbridge's structural system (top); simplified version for calculations and FE modeling (bottom).*

There is a desire to have the structural system consist of CFRP to the biggest possible extent (Darholm, 2017, pers. comm., July 12<sup>th</sup>). Therefore, the option of integrating a lightweight concrete core to the beams, as for Bridge 254 in Malmö, was not considered as an option. Thus, the only member of the structural system not made of CFRP is the deck core, made of PVC foam. Although not modeled, the railing posts are suggested to be made of aluminum, with wires of CFRP, and a handrail made of CFRP. The wearing coarse is proposed to be made of acrydur (Darholm, 2018, pers. comm., March 12<sup>th</sup>).

### 7.1 Fiber Orientation

Since CFRP is a highly orthotropic material, the orientation of the fibers in the laminates are of high significance for the design of the footbridge. Mainly, the

choice of orientations is based on suggestions by Jens Allroth, naval architect of CFRP product manufacturer Aston Harald (2018, pers. comm., March 26<sup>th</sup>), and Erik Olsson, CFRP bridge specialist at Chalmers University of Technology (2018, pers. comm., April 20<sup>th</sup>). For the deck (including the edge stiffeners), which is loaded both in the longitudinal and the lateral direction of the bridge span, a combination of  $\pm 45^\circ$  and  $0/90^\circ$  laminates are used. At the preliminary design stage,  $\pm 45^\circ$  solely makes up the webs, which shall resist both large moment forces and large shear forces. For the flanges, unidirectional fibers are used since they are the strongest solution for longitudinal forces, both in compression (the upper flanges) and in tension (the bottom flanges).

### 7.2 Manufacturing

The idea is to manufacture the bridge of pre-impregnated laminates and curing in either an autoclave or an oven. In order to remove the hardened beams from the mold, it is important that the beams have a shape that does not lock them to it; see Figure 7.2. For the same reason, the top flanges for the box beam girders are chosen to be pointing outwards, leaving the beams open at the top.

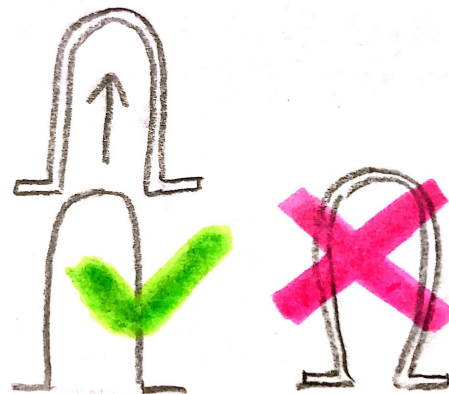


**Figure 7.2:** *How the beam profiles should and should not be shaped, considering molding workability.*

If the same beam mold can be used for sections less deep than for the ones considered, the manufacturing process could be made more cost- and time-efficient. The opportunity has been considered, but not further investigated.

### 7.3 Sizing

The first sizing and the first checks are based on hand calculations, using Mathcad, in accordance with the Eurocode and a pending prospect for an update of the Eurocode introducing the material of FRP, a work in progress by Haghani et al (2018). This prospect is described in Section 2.8.1. However, the final checks are done with the finite element method (FEM), since the simplified hand calculations assume full interaction, an assumption that is hard to verify for a CFRP structure.

Additionally, models that feature orthotropic materials are hard to calculate accurately by hand (Haghani, 2018, pers. comm., May 2<sup>nd</sup>). For this reason, the FE model is verified by assigning an isotropic material to all parts of the model, see Section 8.4.1. After that, a reliable FE model can be used for the final sizing procedure.

Following a limitation of the master's thesis, local buckling is not designed for. The hand calculations consider stresses, moment force resistance, and shear force resistance in the ULS, and deflection in the SLS. For the reason stated in the previous paragraph, the bridge is designed for a margin in the deflection utilization. Hence, a deflection that turns out to be greater in the FE analysis may still be acceptable.

In Section 8.2.4.2, eigenfrequencies are determined using FEM. Subsequently, the dynamic behavior in terms of accelerations is evaluated, see Section 8.2.4.2 and 8.2.4.3.

## 7.4 Two Final Designs

After improving the preliminary design, two final, geometrically simplified, bridge design alternatives are proposed. Many measurements are in common; what sets them apart is the slenderness. One slender section is given deep beams with thin webs and flanges. One bulky version, which is supposed to have a better buckling resistance, has lower beams with thicker plates. This design also has thicker deck skins and a greater self-weight. Since the slender bridge design is considered as alternative 1 and the bulky one as alternative 2, they will be referred to as CFRP1 and CFRP2, respectively.

Both alternatives are 30-meter simply supported bridges. The length is chosen with the comparison in Chapter 6 in mind. However, for the dynamic analysis, a slight expansion in length is applied in order to make the analysis extra interesting. Regular truss bridges, without horizontal bracing trusses, generally tend to get dynamic problems at spans beyond 30 *m* (Darholm, 2018, pers. comm., March 9<sup>th</sup>).

The bridge has a total width of 3.4 *m* and a free walking path width of 3.0 *m*. The main box girders are 0.4 *m* wide; including the top flanges a total width of approximately 0.8 *m* and have a center-to-center distance of 1.0 *m*. The beams of CFRP1 are 1,550 *mm* deep; those of CFRP2 are 1,050 *mm*. These girders interact throughout the span of the bridge with help from six diaphragms, with a center-to-center distance of 6.4 *m*. In practice, these diaphragms act as vertical stiffeners inside of and between the three box girders, in order to increase the resistance against buckling and torsion. Sketches of the final bridge designs are given in Figures 7.3 and 7.4.

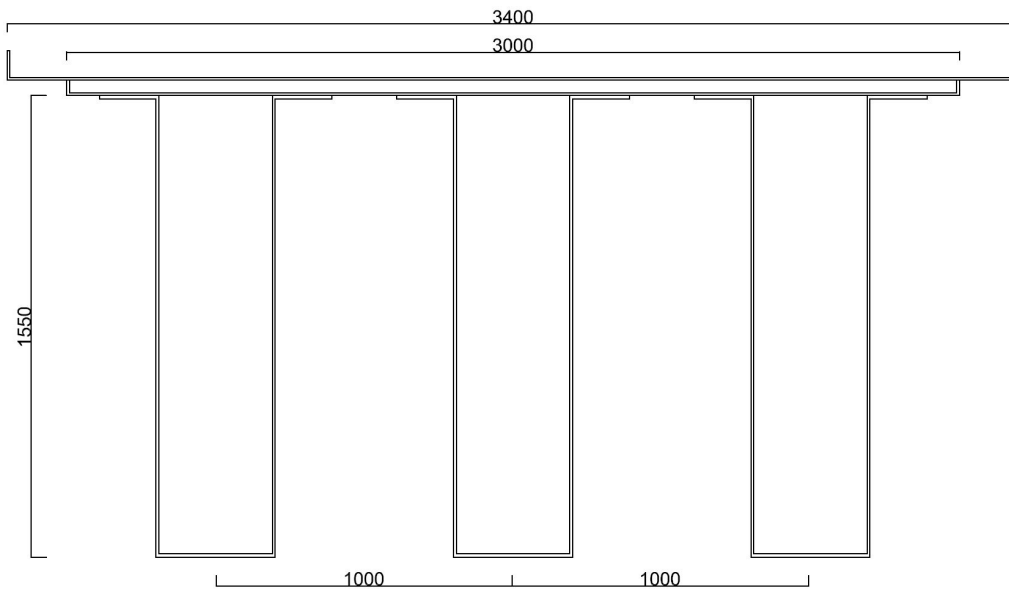


**Figure 7.3:** *Final sketch of the bridge design, alternative CFRP1. Measurements given in mm.*

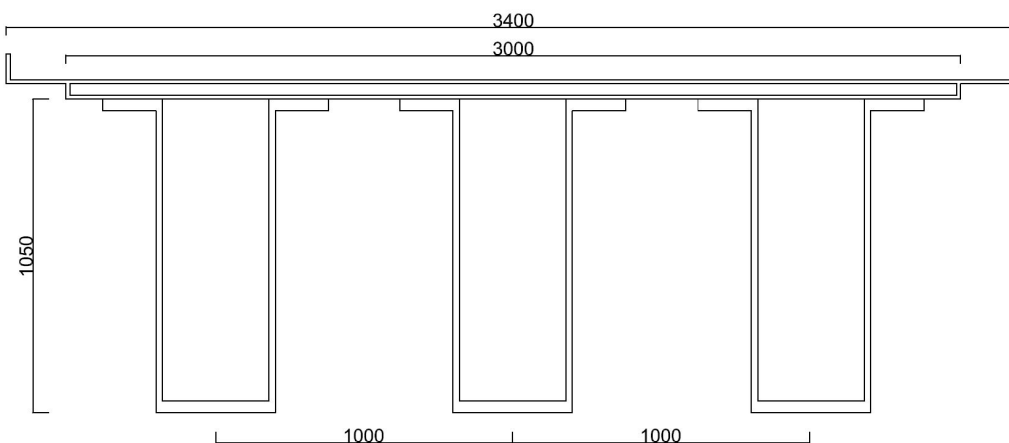


**Figure 7.4:** *Final sketch of the bridge design, alternative CFRP 2. Measurements given in mm.*

### 7.4.1 Deck

The main part of the bridge decks is a sandwich construction made up of two outer CFRP skins (upper and lower) and a foam core made of PVC between them. On both sides of the cross-section, the top skin continues as 0.2-meter edges outside of the foam core, in order to leave room for the railing posts. This can be done because the sandwich construction is only needed underneath the walking path, which has the greatest design load, and therefore does not have to continue along with the top skin. As mentioned earlier in this section, the deck has no edge beams; instead, it has edge stiffeners. Besides stiffening the edges, they take care of the rain, allowing no water to fall off the edges of the bridge. Using stiffeners instead of edge beams also has aesthetic and economic reasons. Furthermore; on top of the deck, a 6 mm

acrydur S sheeting is added as a wearing coarse. Dimensions of the two alternatives of the final bridge deck are presented in Figure 7.5 and the material selection is presented in Section 7.5.

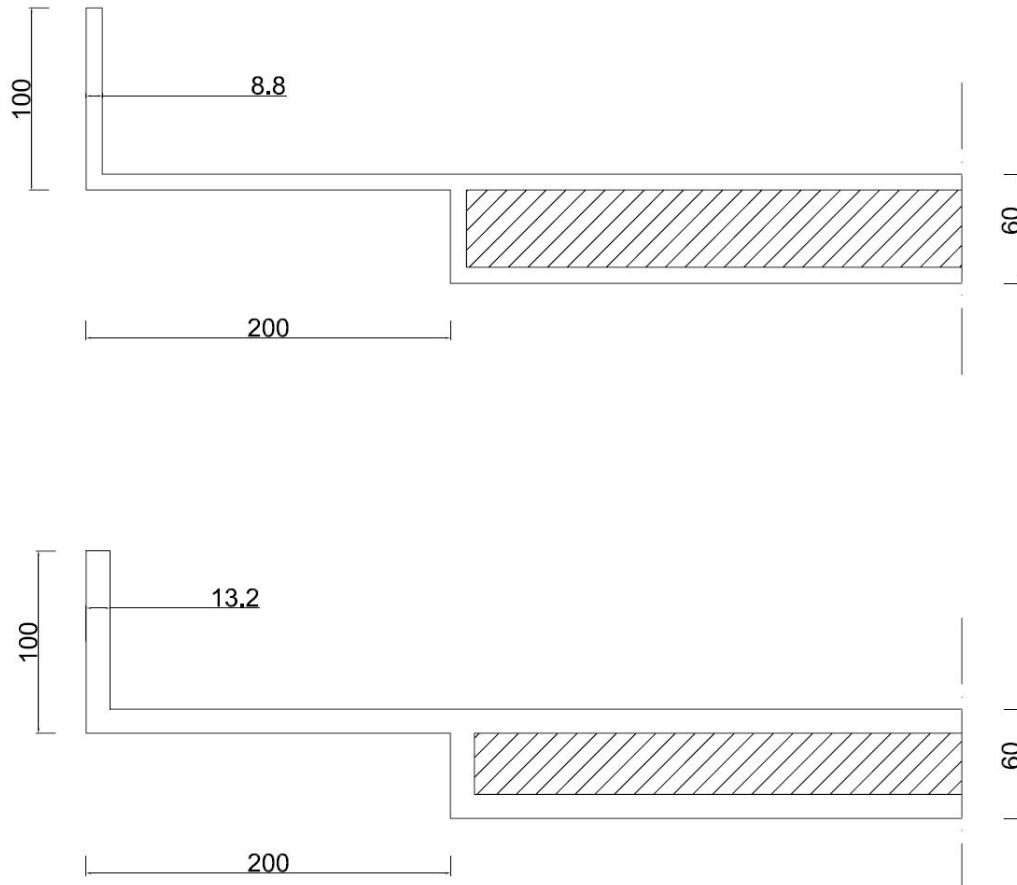


**Figure 7.5:** *Dimensions of the bridge deck [mm]. CFRP1 (top) and CFRP2 (bottom).*

### 7.4.2 Girders

The final bridge design consists of three main box girders, all with the same dimensions. Each girder is a U-shaped beam with two upper flanges pointing outwards. Dimensions of the two versions of the box girders are presented in Figure 7.6 and the materials are presented in Section 7.5.

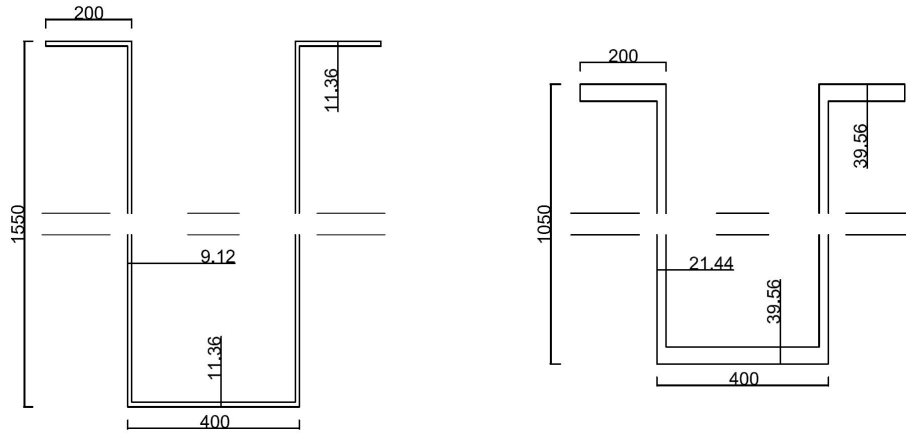


**Figure 7.6:** Dimensions of the girders [mm]. CFRP1 (left) and CFRP2 (right).

## 7.5 Materials

Mechanical properties for the materials used are presented in Tables 7.1 for composite laminates parts, 7.2 for the core material and 7.3 for the wearing course. Carbon fibers used in composite laminates are of standard modulus, in order to keep the cost reasonable. For the same reason, fiber reinforcement of larger ply thicknesses than presented in Table 7.1, 0.3 and 0.44 mm, are used, in order to reduce the lay-up time during manufacturing. However, for design and calculations these laminate properties will be used. The drawback of using thicker laminates may be that they are hard to lay up accurately in the corners (Armstrong, 2018, pers. comm., March 26<sup>th</sup>). That problem, however, is more significant for small CFRP products, such as automotive parts, than for a major structure like a footbridge.

**Table 7.1:** Properties of UD (0°), 0/90°, and ±45° laminates (Gurit, 2018b).

Fiber arrangement	UCHEC300	RC416	XC411
Resin type	SE84	SE84	SE84
Material type	UD (0°)	0/90°	±45°
Ply thickness [mm]	0.30	0.44	0.44
Density [kg/m <sup>3</sup> ]	1,514	1,491	1,485
Longitudinal Poisson's ratio [ ]	0.337	0.037	0.037
Longitudinal tensile modulus [GPa]	130.33	63.63	63.95
Longitudinal tensile strength [MPa]	1,433.6	604.5	607.5
Longitudinal compressive modulus [GPa]	122.35	62.36	62.67
Longitudinal compressive strength [MPa]	1,003.3	498.9	501.4
Transverse tensile modulus [GPa]	7.22	63.63	63.95
Transverse tensile strength [MPa]	32.5	604.5	607.5
Transverse compressive modulus [GPa]	7.22	62.36	62.67
Transverse compressive strength [MPa]	108.3	498.9	501.4
In-plane shear modulus [GPa]	4.23	4.18	3.80
In-plane shear strength [MPa]	76.1	68.1	67.6

**Table 7.2:** *Mechanical properties of PVC 250 foam core (Gurit, 2018c).*

Material name	PVC250
Nominal density [ $kg/m^3$ ]	250
Possion's ratio [ ]	0.32
Tensile modulus [ $GPa$ ]	0.439
Tensile strength [ $MPa$ ]	7.19
Compressive modulus [ $GPa$ ]	0.296
Compressive strength [ $MPa$ ]	6.88
Shear modulus [ $GPa$ ]	0.098
Shear strength [ $MPa$ ]	4.37

**Table 7.3:** *Mechanical properties of Acrydur S (Hagmans, 2005).*

Material name	Acrydur S
Density [ $kg/m^3$ ]	950

In order to optimize each composite part of the structure, various fiber orientations have been used in the lay-up. These laminate plans have been worked out after suggestions from Allroth of Aston Harald and Olsson of Chalmers University of Technology. For the outer layers of the composite, it is reasonable to have one layer of  $0/90^\circ$  and one layer of  $\pm 45^\circ$  as symmetry around the main laminate layers, in order to achieve a stronger and more protective surface (Olsson, 2018, pers. comm., March 28<sup>th</sup>). In Sections 7.5.1 through 7.5.3, a laminate plan for each part of the two bridge alternatives is presented.

### 7.5.1 Deck

For the deck, a combination of  $0/90^\circ$  and  $\pm 45^\circ$  laminates is used. The decks, including the edge stiffeners, are given uniform thicknesses all over, namely 8.8 mm for CFRP1 and 13.2 mm for CFRP2. Hence, 20 and 30 layers, respectively, for each skin, half of the layers being  $0/90^\circ$  and half being  $\pm 45^\circ$  laminates, as illustrated in Figure 7.7.

$$\begin{bmatrix} 0/90^\circ \\ \pm 45^\circ \end{bmatrix}_{10} \quad \begin{bmatrix} 0/90^\circ \\ \pm 45^\circ \end{bmatrix}_{15}$$

**Figure 7.7:** *Configuration of  $0/90^\circ$  and  $\pm 45^\circ$  laminates in the deck skins. CFRP1 (left) and CFRP2 (right).*

### 7.5.2 Webs and Diaphragms

In the webs, another combination of laminates is made, as the webs shall resist both moment and shear forces. They mainly consist of  $\pm 45^\circ$  laminates, although a layer

of  $0/90^\circ$  and two layers of unidirectional laminates are added on each surface. The total numbers of plies for the webs in CFRP1 and CFRP2 are 22 and 50, respectively. The laminate plans for the webs are illustrated in Figure 7.8. Furthermore, the same laminate plans and thicknesses are used for the six diaphragms mentioned in Section 7.4.

$$\left[ \begin{array}{c} 0/90^\circ \\ \pm 45^\circ \\ 0_2 \\ \pm 45^\circ_7 \end{array} \right]_s \quad \left[ \begin{array}{c} 0/90^\circ \\ \pm 45^\circ \\ 0_2 \\ \pm 45^\circ_{21} \end{array} \right]_s$$

**Figure 7.8:** Configuration of unidirectional ( $0^\circ$ ),  $0/90^\circ$ , and  $\pm 45^\circ$  laminates in the webs and the diaphragms, with symmetry. CFRP1 (left) and CFRP2 (right).

### 7.5.3 Flanges

Both upper and lower flanges have the same laminate plan for each alternative and consists mostly of unidirectional laminates, plus one layer each of  $0/90^\circ$  and  $\pm 45^\circ$  at the surfaces. The total numbers of plies in the flanges are 36 and 130, respectively. The laminate plans for the flanges are illustrated in Figure 7.9.

$$\left[ \begin{array}{c} 0/90^\circ \\ \pm 45^\circ \\ 0_{16} \end{array} \right]_s \quad \left[ \begin{array}{c} 0/90^\circ \\ \pm 45^\circ \\ 0_{63} \end{array} \right]_s$$

**Figure 7.9:** Configuration of unidirectional ( $0^\circ$ ),  $0/90^\circ$ , and  $\pm 45^\circ$  laminates in the flanges with symmetry. CFRP1 (left) and CFRP2 (right).

## 7.6 Static Loads

In this master's thesis, various configurations, according to Eurocode 1, for static load combinations in the ULS and the SLS have been applied. Loads considered in the static design are self-weight of the structure, snow load, traffic load from the pedestrians, and the load from a service vehicle. Loads not considered are wind loads and the self-weight of the railings.

The magnitude of each design load is presented in Table 7.4, where the self-weight is expressed in  $kN/m$  along the bridge span. The entire bridges' masses are 9.94 tonnes and 16.6 tonnes. Snow load and traffic load from pedestrians are presented as uniform loads along the span, where the traffic load is applied only on the footpath width, that is, 3 m. The characteristic snow load for a location in Åby (location



chosen with Chapter 6 in mind) is applied over the full width of the bridge, that is, 3.4 meters. The service load is applied as point loads from the four wheels, the front wheels with a magnitude of 20  $kN$  each and the rear wheels with 40  $kN$  each. The distance between the axes is 3.0  $m$ . However, traffic load from pedestrians and the service vehicle load are not considered simultaneously.

**Table 7.4:** *Characteristic static loads on the bridges.*

Load	Unit	Source
Self-weight CFRP1	3.05 $kN/m$	(Brigade/Plus model)
Self-weight CFRP2	5.08 $kN/m$	(Brigade/Plus model)
Snow	1.6 $kN/m^2$	(SIS, 1991)
Pedestrians	5.0 $kN/m^2$	(SIS, 1991)
Service vehicle	120 $kN$	(SIS, 1991)

In the load combinations for ULS and SLS checks, the loads are considered as fundamental unfavorable loads. For variable loading, the traffic load is seen as the main load, due its significantly greater magnitude than the snow load. Moreover, the load case including the pedestrian load is governing before the one including the service vehicle; hence, this load case is used for global checks.

The applied design load combinations for the ULS and the SLS are calculated by Equations 7.1 and 7.2, respectively, with input values for partial safety factors and reduction factors  $\psi_0$  from Table 7.5. On the last row in the same Table, design values for load combinations in the ULS and the SLS are found.

$$Q_{ULS} = \gamma_G G_k + \gamma_{Q.1} Q_{k.1} + \gamma_{Q.i} \psi_{0.i} Q_{k.i} \quad (7.1)$$

$$Q_{SLS} = G_k + Q_{k.1} + \psi_{0.i} Q_{k.i} \quad (7.2)$$

**Table 7.5:** *Partial safety factors  $\gamma$ ,  $\psi_0$  factors for snow load, and design values for ULS and SLS load combinations.*

	ULS	SLS	
$\gamma_G$	1.5	1.0	SIS, 1991
$\gamma_Q$	1.35	1.0	SIS, 1991
$\psi_{0snow}$	0.7	0.7	SIS, 1991
Q [ $kN/m$ ]	32.405	21.914	

## 7.7 Requirements

The static requirements for the ULS and the SLS are in accordance with the Eurocode and the pending prospect for a Eurocode update involving the material of FRP, a work in progress introduced to in Section 2.8.1. Sétra is referred to in the dynamic analyses, see Section 8.2.4.

Characteristic values for strengths given in Table 7.1 need to be turned into design values in order to perform resistance checks. In the design phase, Equation 7.3 must be satisfied, where design values of resistance,  $X_{Rd}$  shall be greater than the calculated effect from the applied loads,  $X_{Ed}$ .

$$X_{Ed} \leq X_{Rd} \quad (7.3)$$

The design strength value in the considered direction is obtained by multiplying the characteristic value by a conversion factor and dividing with a partial factor for the limit state in question.

$$X_d = \eta \frac{X_k}{\gamma_M} \quad (7.4)$$

where

- $X_d$  = design value
- $X_k$  = characteristic value
- $\gamma_M$  = partial factor
- $\eta$  = conversion factor given in Eurocode 0, with FRP specific values in Haghani et al (2017)

The partial factor,  $\gamma_M$ , is a multiplication of various partial factors, accounting for uncertainties in the material properties and the production methods. These partial factors for different limit states are calculated in accordance with Equation 7.5 and Table 7.6 for the bridge in question. The conversion factor,  $\eta$  is a multiplication of several factors considering phenomenons such as temperature changes, humidity, creep, and fatigue effects. However,  $\eta$ , is set equal to 1.0 in this master's thesis (Haghani, 2018, pers. comm., May 2<sup>nd</sup>).

$$\gamma_M = \gamma_{M1} \gamma_{M2} \quad (7.5)$$

**Table 7.6:** *Partial safety factors [ ] for ULS and SLS for the CFRP footbridges considered.*

	ULS	SLS	
$\gamma_{M1}$	1.35	1.0	Haghani et al, 2017
$\gamma_{M2}$	1.35	1.0	Haghani et al, 2017
$\gamma_{M.TOT}$	1.823	1.0	Equation 7.5

### 7.7.1 Moment and Shear Force Resistance in the ULS

For moment and shear force resistance in the ULS, characteristic values for strengths in Table 7.1 were transformed into design values by using Equation 7.4 with associated factors according to Table 7.6. These moment and shear force resistances need to be greater than the moment and shear forces applied on the bridge; that is, Equations 7.6 and 7.7 need to be satisfied.

$$M_{Ed} \leq M_{Rd} \quad (7.6)$$

$$V_{Ed} \leq V_{Rd} \quad (7.7)$$

### 7.7.2 Deflection in the SLS

The maximum deflection allowed for footbridges is a 400<sup>th</sup> of the span length, according to the Traffic Administration (Trafikverket, 2016). See Equation 7.8.

$$\delta < \frac{l}{400} \quad (7.8)$$

## 7.8 Checks

In hand the calculations, the bridge sections are checked for moment force, shear force, and deflection. The moment force from the applied ULS load has been determined and compared to the moment force resistance at three points in each cross-section. These three points have been chosen as critical parts of the cross section. The first point is on top of the edge stiffeners, where the compressive stress is the largest and the deck consist of 0/90° and ±45° laminates. The second and third points are on the top and the bottom of the web, respectively.

The points in question have been chosen to check both compressive and tensile stresses in the girders. However, the flanges have greater stresses than the webs as they are further away from the center of gravity, but they are much stronger than the webs due to the unidirectional fibers. Hence, the flanges are not checked. The points of moment checks are illustrated in Figure 7.10 and the moment force checks are presented in Tables 7.7 and 7.8.

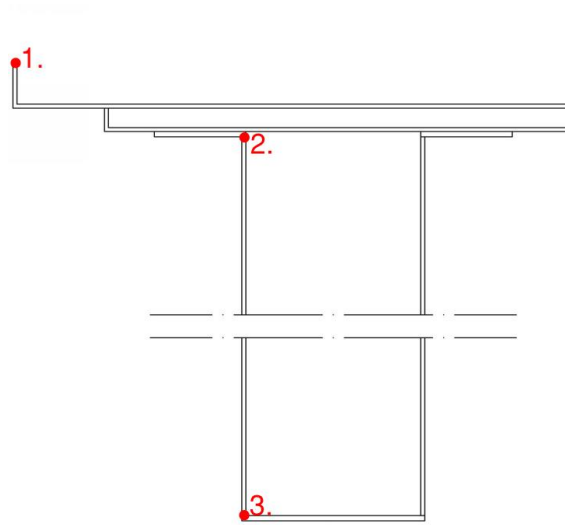


**Figure 7.10:** Points for moment force checks of the cross section. Point 1 is at the top of the edge stiffener. Point 2 is at the top of the web and point 3 at the bottom of the web.

**Table 7.7:** Moment force checks for three points in the cross section of CFRP1, made by hand calculations.

Point	Design moment force [ $kNm$ ]		Moment force resistance [ $kNm$ ]	Utilization ratio [ ]
1.	4,150	<	14,500	0.285
2.	4,150	<	21,500	0.193
3.	4,150	<	14,700	0.282

**Table 7.8:** Moment force checks for three points in the cross section of CFRP2, made by hand calculations.

Point	Design moment force [ $kNm$ ]		Moment force resistance [ $kNm$ ]	Utilization ratio [ ]
1.	4,479	<	18,100	0.247
2.	4,479	<	28,900	0.155
3.	4,479	<	23,200	0.193

The largest shear forces appear at the supports of the bridges. These forces are compared, in the ULS, to the shear resistances of the webs of the main beams and the checks are presented in Tables 7.9 and 7.10.

**Table 7.9:** *Shear checks for the cross section of CFRP1 at end support, made by hand calculations.*

Design shear force [kN]		Shear force resistance [kN]	Utilization ratio [ ]
518	<	8,620	0.06

**Table 7.10:** *Shear checks for the cross section of CFRP2 at end support, made by hand calculations.*

Design shear force [kN]		Shear force resistance [kN]	Utilization ratio [ ]
560	<	12,800	0.044

The maximum deflection allowed is 80 mm in the longitudinal direction for a foot-bridge with a 32-meter span. The deflection checks are presented in Tables 7.11 and 7.12.

**Table 7.11:** *Deflections checks for CFRP1, made by hand calculations.*

Deflection [mm]		Max deflection [mm]	Utilization ratio [ ]
61.6	<	80.0	0.770

**Table 7.12:** *Deflections checks for CFRP2, made by hand calculations.*

Deflection [mm]		Max deflection [mm]	Utilization ratio [ ]
63.7	<	80.0	0.796



# 8

## Finite Element Modeling of the Bridge Alternatives

### 8.1 Brigade Plus

The FE software used for this master thesis is Brigade/Plus, which is a version of Abaqus/CAE with extra features for bridge design. Brigade/Plus has pre-defined loads that represent vehicles and pedestrians. Design codes, such as Eurocode with various national annexes, can be added.

### 8.2 Model Design

In Brigade/Plus, composites structures can be modeled with various techniques, depending on the aim. In a guide written by Mara (2015), three different ways of modeling composites are mentioned, namely microscopic modeling, lay-up modeling and equivalent single layer modeling.

In this master's thesis, the lay-up modeling technique has been chosen for modeling the composite parts. With this technique, material properties for each ply are given as input data, either as experimentally determined values given in data sheets from material suppliers or through mathematical calculations, such as the rule of mixture, mentioned in Section 2.5.1. In Table 8.1 ply properties as input for Brigade/Plus for three different laminates fabrics, UD ( $0^\circ$ ),  $0/90^\circ$  and  $\pm 45^\circ$  are presented.

Footbridge alternatives CFRP1 and CFRP2 are modeled as deformable 3D elements with SI units as input; meters, kilograms, newtons, et cetera. Furthermore, the three global directions in Brigade/Plus are shown in Figure 8.1 and are defined as follows:

- X – Longitudinal direction of the bridge.
- Y – Lateral direction of the bridge.
- Z – Vertical direction of the bridge.

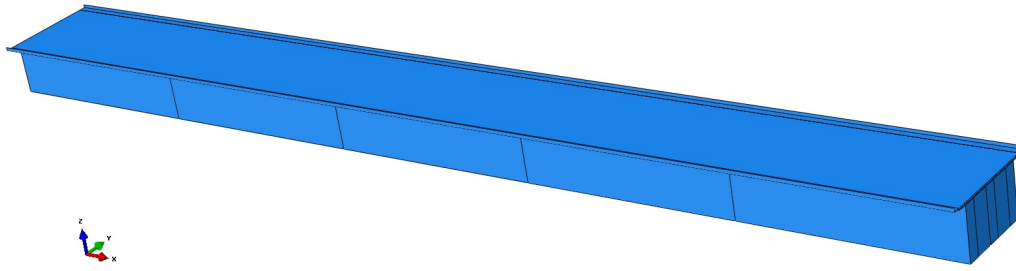


**Figure 8.1:** *Global direction of coordinate system in Brigade/Plus.*

The composite parts of the footbridge are modeled as 3D shell elements, with lamina properties set to "elasticity" in the dialog box. Local fiber orientations for each part of the model are important to specify. This is, as stated in Section 7.1, because composite materials are orthotropic and therefore have different material properties in different directions. The bridge deck is a sandwich structure, where the composite skins are modeled as 3D shell elements and the core material is modeled as a solid 3D element. In contrast to composite materials, core elements have isotropic properties for elasticity and material inputs in Brigade/Plus are given in Table 8.2. Furthermore, the wearing coarse, acrylic sheet is not modeled as a 6-millimeter sheeting with associated mechanical properties in Brigade/Plus; but as a non-structural mass, hence no stiffness is added from the acrylic.

### 8.2.1 Boundary Conditions

The footbridge is modeled as a simply supported bridge, based on an Autocad 2D sketch of the cross-section, the with three main box girders as supports on each side. These main box girders are constrained as lines with different boundary conditions, see Figure 8.2. The boundary conditions for the supports are as follows:

- All supports are free to rotate in all planes (UR1, UR2, UR3).
- All supports are fixed for displacement in the z-direction (U3).
- Both middle supports are fixed for displacement in the y-direction (U2).
- One of the middle supports is fixed for displacement in the x-direction (U1).



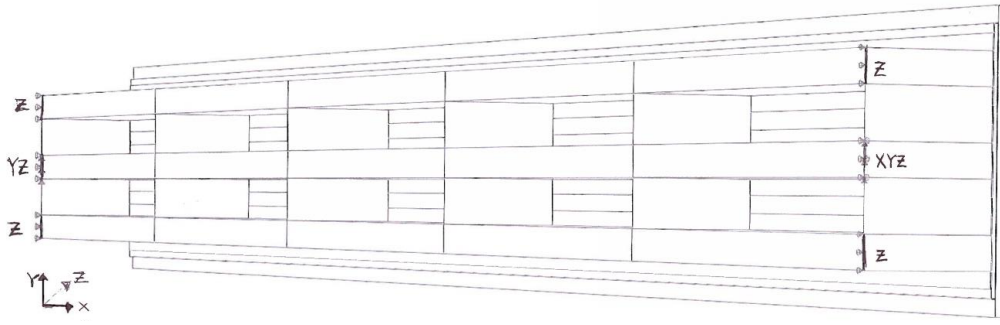


**Figure 8.2:** *Boundary conditions in Brigade/Plus, seen from underneath the bridge, where  $x$ ,  $y$  and  $z$  at the supports indicates directions in which the support is fixed in translation. Top and bottom girders are fixed in the  $z$ -direction at both ends. The middle girder is fixed in the  $x$ -,  $y$ -, and  $z$ -directions at one end and in the  $y$ - and  $z$ -directions at the other end.*

## 8.2.2 Material Input

Material properties needed as input for Brigade/Plus are longitudinal modulus, transverse modulus, in-plane shear modulus, density, Possion's ratio and out-of-plane shear modulus. These values are in accordance with Table 8.1. They are all from Gurit (2018b), except the out-of-plane shear modulus,  $G_{23}$ , which is calculated using Equation 8.1 (Mara, 2015).

$$G_{23} = \frac{E_2}{2(1 + \nu_{23})} \quad (8.1)$$

where

- $\nu_{23}$  = through thickness Poisson's ratio, taken as 0.4 (Mara, 2015)
- $E_2$  = transverse modulus [GPa]

**Table 8.1:** *Material input for prepregs in Brigade/Plus, UD ( $0^\circ$ ), 0/90° and  $\pm 45^\circ$  (Gurit, 2018b).*

Material name Material type	UCHEC300 UD ( $0^\circ$ )	RC416 0/90°	XC411 $\pm 45^\circ$
Ply thickness [mm]	0.30	0.44	0.44
Mass density [ $kg/m^3$ ]	1514	1491	1485
Longitudinal modulus, $E_1$ [GPa]	130.33	63.63	63.95
Transverse modulus, $E_2$ [GPa]	7.22	63.63	63.95
In-plane shear modulus, $G_{12}$ [GPa]	4.23	4.18	3.80
Transverse shear modulus, $G_{13}$ [GPa]	4.23	4.18	3.80
Out-of-plane shear modulus, $G_{23}$ [GPa]	2.578	22.725	22.839
Major Poisson's ratio, $\nu_{12}$ [ ]	0.337	0.037	0.037

**Table 8.2:** Material input for PVC 250 foam core in Brigade/Plus (Gurit, 2018c).

Material name	PVC250
Mass density [ $kg/m^3$ ]	250
Young's modulus [ $GPa$ ]	0.296
Poisson's ratio	0.32

### 8.2.3 Material Lay-up

The composites layers have been modeled with material input from the previous section and are modeled as thick layers, where laminates of the same type have been used, in order to save processing time in Brigade/Plus. Lay-up configurations for the deck, webs, and flanges are illustrated for both footbridge alternatives in Figures 8.3, through 8.5.

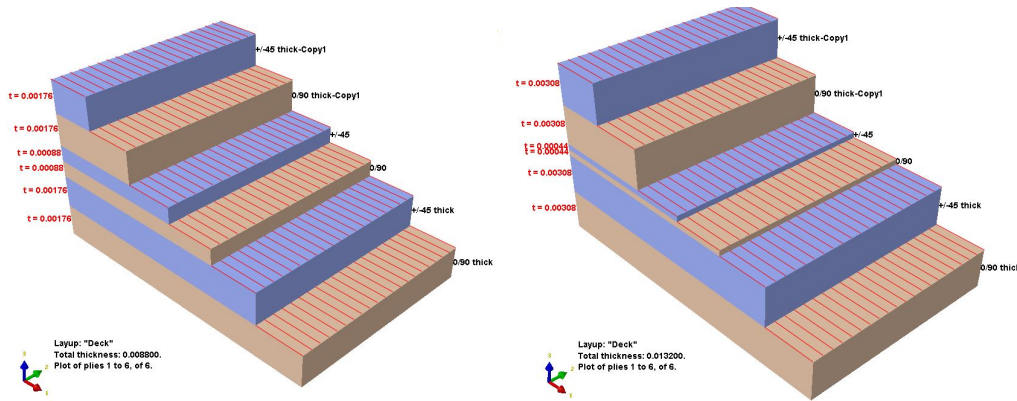


**Figure 8.3:** Lay-up configurations for the decks, CFRP1, with a total thickness of 8.8 mm (left), and CFRP2, with a total thickness of 13.2 mm (right). The figures are not to scale.

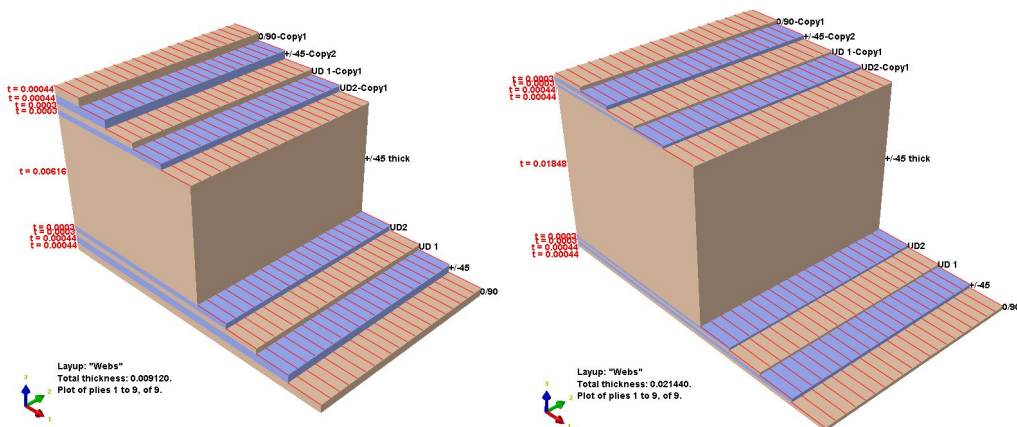


**Figure 8.4:** Lay-up configurations for the webs, with a thick layer of  $\pm 45^\circ$  in the middle. CFRP1, with a total thickness of 9.12 mm (left), and CFRP2, with a total thickness of 21.44 mm (right). The figures are not to scale.

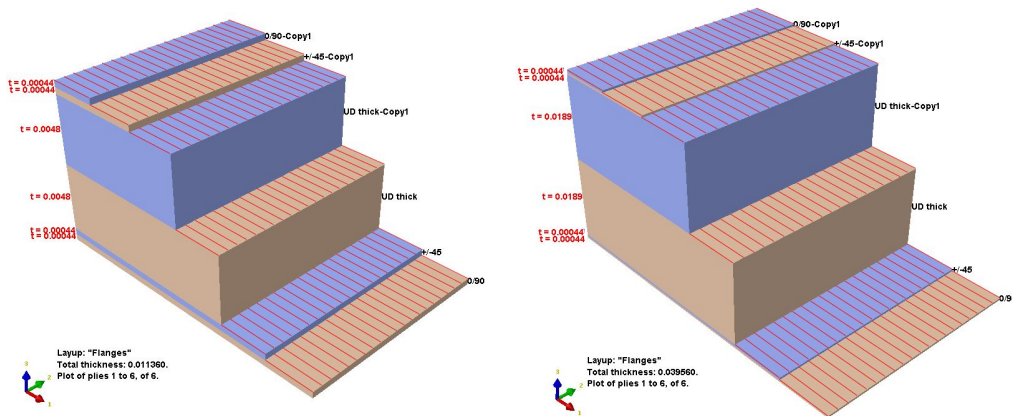


**Figure 8.5:** Lay-up configurations for the flanges, with two thick layers of unidirectional CFRP in the middle, CFRP1, with a total thickness of 11.36 mm (left), and CFRP2, with a total thickness of 39.56 mm (right). The figures are not to scale.

## 8.2.4 Steps

In the step module in Brigade/Plus, all analyses of interest are defined and they are:

- Static analysis.
- Frequency analysis.
- Modal dynamic analysis.

### 8.2.4.1 Static Analysis

Static analysis is considered as a linear perturbation. Loads considered in this analysis are the load combination stated in Section 7.6, for the ULS and the SLS. The loads are the self-weight, traffic load from pedestrians, and snow load. This analysis will present results in terms of stresses, reaction forces, and deflections.

### 8.2.4.2 Frequency Analysis

Frequency analysis is also considered as a linear perturbation procedure type. Frequency analysis will determine the eigenfrequencies and related eigenmodes based on the footbridges' modal properties. This analysis is made three times for each bridge design. It should be two, according to the Sétra model introduced in Section 4.6.2.1; however, this master's thesis considers two different footbridge classes, namely III and II. The first time, the frequency analysis is made without any extra mass from the pedestrians, the second time with masses added from a crowd of 0.5 pedestrians/m<sup>2</sup>, and the third time with masses added from a crowd of 0.8 pedestrians/m<sup>2</sup>. These masses are added as non-structural masses in Brigade/Plus. The fundamental, variable loads stated in Table 7.4 are not accounted for at this point. Each bridge with its associated mass additions is henceforth represented by three different bridge-crowd systems. For the subsequent modal dynamic analysis, the six bridge-crowd systems are labeled as defined in Table 8.6.

### 8.2.4.3 Modal Dynamic Analysis

Based on the frequency analysis, modal dynamic analysis are made for all bridge–crowd systems. According to the Sétra model, a uniform harmonic load, given in Table 4.6, is applied as a pressure on the bridge in the same direction as the mode shape. Moreover, a time period, a time increment, and a damping ratio are entered in the analysis. These values are constant for all considered cases and presented in Table 8.3. Please note that the damping ratio is a conservative value.

**Table 8.3:** *Input parameters in step module for modal dynamic analysis.*

Parameter	Value	Reference
Damping Ratio $\xi$ [ ]	0.01	Haghani et al, 2017
Time Interval $t$ [s]	20	Section 8.3.2
Time Increment $\Delta t$ [s]	0.01	Section 8.3.2

The output from this analysis is accelerations at a location in the middle of the top face of the bridge deck, illustrated in Figure 8.6.

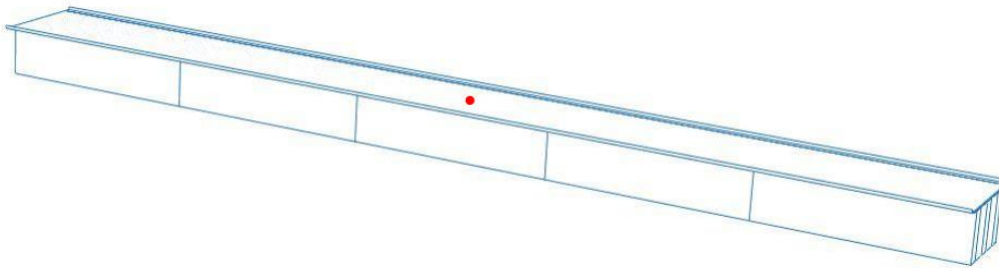


**Figure 8.6:** *Location on top of the bridge deck (red point), where the accelerations have been analyzed.*

### 8.2.5 Interaction

In Brigade/Plus, two connections have been modeled in the interaction module; connection between deck and foam core material in the sandwich structure, and connections between the girders and the deck. Both connections have been modeled in constraint manger as tie constraints, where two surfaces have been tied together with no relative motion between them, hence, full bond between parts. See Figure 8.7 for the tie constraints in Brigade/Plus.

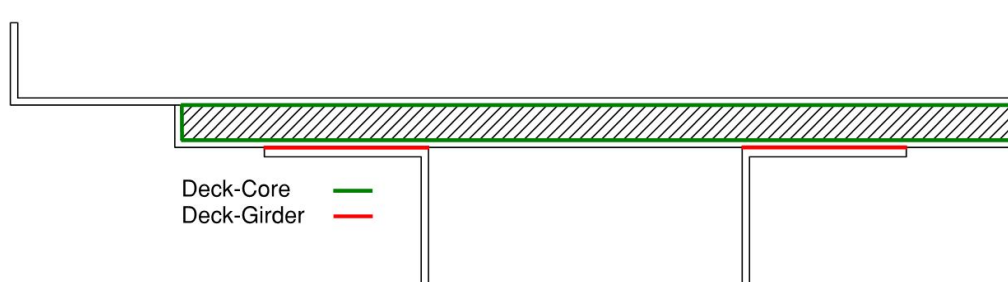


**Figure 8.7:** Tie constraints in Brigade/Plus. The green color is the tie constraint between deck and foam core. The red color is the tie constraint between deck and girders.

## 8.2.6 Loads

### 8.2.6.1 Static Loads

In the load module, all loads mentioned in Section 7.6 are applied. Self-weight is applied as a uniformly distributed gravity force in the z-direction, with an acceleration of gravity equal to  $9.82 \text{ m/s}^2$ . The wearing coarse is, as stated in Section 8.2, added as a non-structural mass. Pedestrian load and snow load are, applied as a uniformly distributed pressure force over the affected surface. Furthermore, the loads are applied for two load cases; the ULS and the SLS depending on what is of interest and in Table 8.4, data about the load applied in Brigade/Plus is presented.

**Table 8.4:** Load applied in Brigade/Plus for the ULS and the SLS.

	ULS	SLS
Acceleration of gravity [ $\text{m/s}^2$ ]	13.26	9.82
Snow load [ $\text{kN/m}^2$ ]	1.68	1.12
Pedestrian load [ $\text{kN/m}^2$ ]	7.50	5.00
Acrydur load [ $\text{kg/m}^2$ ]	6.55	4.85

### 8.2.6.2 Mass Additions and Dynamic Loads

In order to perform a frequency analysis for the loaded cases, the extra masses from the pedestrians have been modeled as non-structural masses in accordance with footbridge classes III and II. These additional crowd masses in Brigade/Plus are presented in Table 8.5. They account for crowd densities of  $0.5$  and  $0.8 \text{ pedestrians/m}^2$ , respectively, and a pedestrian mass of  $70 \text{ kg}$ , as suggested by Sétra (2006).

**Table 8.5:** Non-structural masses applied in Brigade/Plus for loaded footbridge classes II and III.

Footbridge Class	Magnitude [ $\text{kg/m}^2$ ]
II	56
III	35

These additional crowd masses yield three bridge-crowd systems with different modal masses and eigenfrequencies for each footbridge design. These systems are henceforth referred to as stated in Table 8.6.

**Table 8.6:** *Definitions of the new bridge-crowd systems, that is, the bridges with different mass additions from the pedestrians.*

Label	Definition
CFRP1 <sub>0</sub>	CFRP1 with no mass addition
CFRP1 <sub>0.5</sub>	CFRP1 with mass addition from 0.5 <i>pedestrians/m</i> <sup>2</sup>
CFRP1 <sub>0.8</sub>	CFRP1 with mass addition from 0.8 <i>pedestrians/m</i> <sup>2</sup>
CFRP2 <sub>0</sub>	CFRP2 with no mass addition
CFRP2 <sub>0.5</sub>	CFRP2 with mass addition from 0.5 <i>pedestrians/m</i> <sup>2</sup>
CFRP2 <sub>0.8</sub>	CFRP2 with mass addition from 0.8 <i>pedestrians/m</i> <sup>2</sup>

For the modal dynamic analysis, a uniform load in form of a pressure is applied on the bridge in the same direction as the mode shape. Dynamic load models are in accordance with S etra, which are introduced in Table 4.6. Dynamic crowd classes that have been studied are II and III, which are stated in Table 4.5. According to S etra (2006), the load is given a periodic term  $-\cos(2\pi f_{step}t)$ . Corresponding to this term, Brigade/Plus requests the angular frequency of the load  $-f_{step}$ . Since the bridges are checked for the worst case scenario – that of resonance – the step frequency is set as equal to the eigenfrequency of the system. The input values for Brigade/Plus – load amplitude and angular eigenfrequency – are summarized for all considered systems in Table 8.7. In order to determine the load amplitude from the walking crowd, parameters such as reduction factor  $\psi$ , loaded surface area  $S_{load}$  and the amplitude of the harmonic force from one pedestrian  $F_0$  are needed. The reduction factor is eigenfrequency dependent and can be determined from Figure 4.13 after the eigenfrequencies are determined for each of the systems listed in Table 8.6. The force  $F_0$  is also eigenfrequency dependent. In this master’s thesis load case 3, the effect of second harmonic will only be analyzed, due to the high eigenfrequencies. Hence,  $F_0 = 70\text{ N}$  according to Table 4.9. The loaded surfaces for both bridge alternatives are equal, namely the span length multiplied by the width of the walking path,  $S_{load} = 96\text{ m}^2$ .

**Table 8.7:** *Input values in Brigade/Plus for load amplitude and angular eigenfrequency for all considered systems.*

System	$d$ [ped/m <sup>2</sup> ]	$\psi$ [ ]	Load amplitude [N/m <sup>2</sup> ]	$f_{step}$ [Hz]	$w_{step}$ [rad/s]
CFRP1 <sub>0</sub>	0.5	0	0	5.62	35.3
CFRP1 <sub>0</sub>	0.8	0	0	5.62	35.3
CFRP1 <sub>0.5</sub>	0.5	0.179	0.977	4.86	30.5
CFRP1 <sub>0.8</sub>	0.8	0.594	4.10	4.53	28.4
CFRP2 <sub>0</sub>	0.5	0.546	2.98	4.56	28.7
CFRP2 <sub>0</sub>	0.8	0.546	3.77	4.56	28.7
CFRP2 <sub>0.5</sub>	0.5	1.0	5.46	3.96	24.9
CFRP2 <sub>0.8</sub>	0.8	1.0	6.90	4.16	26.1

### 8.2.7 Mesh

Altogether, for the master's thesis designs, the following mesh controls are used in Brigade/Plus:

- Element shape – Quad.
- Technique – Structured.
- Algorithm options – Minimize the mesh transition.
- Mesh approximate global size – 0.2  $m$ .

The value for mesh approximate global size, 0.2  $m$ , is determined from a convergence study made in Section 8.3.1 Although, on edges with only one mesh size have instead been set by numbers, in order to obtain more accurate results, by increasing the number of elements in these parts.

## 8.3 Convergence Study

In order to verify that accurate and reliable results are obtained from the finite element model, without longer computation times than necessary, convergence studies for mesh sizing and time stepping for dynamic response in time domain are carried out. These convergence studies are presented in Sections 8.3.1 and 8.3.2.

### 8.3.1 Mesh Sizing

Mesh sizing for an FE model is of big importance, when talking about accuracy of the results. A convergence study was carried out for deflection in the SLS, along a path at the bottom of the middle girder of bridge CFRP1. This convergence study for various mesh sizes is presented in Figure 8.8 and the greatest deflections from the various mesh sizes are presented in Table 8.8.



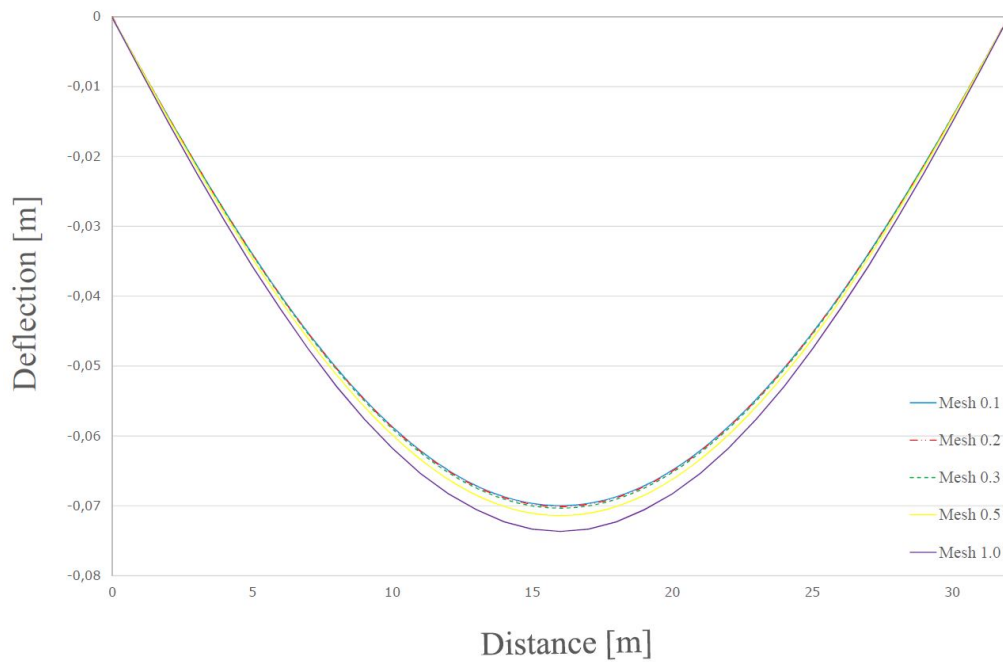


**Figure 8.8:** Convergence study for deflection along the path of bridge alternative CFRP1, for various mesh sizes.

**Table 8.8:** Maximum deflections for various mesh sizes.

Mesh size [m]	Max deflection [m]	Change from previous [%]
1.0	0.0737	
0.5	0.0714	−3.09
0.3	0.0703	−1.49
0.2	0.0701	−0.0304
0.1	0.0700	−0.0189

The convergence study concludes that a mesh size of 0.2 m is fine enough.

### 8.3.2 Time Step

Since the dynamic response analysis is done in the time domain, the time increment has an important role in order to receive true values. Hence, in time domain for finite element software, the equation of motion is solved for each time increment, so if the time increment is not small enough, peaks will be missed. Furthermore, the time interval has to be chosen big enough, in order for the system to stabilize and converge towards its maximum response. To excite this, a convergence study for various time increments and time interval have been tested. In Figures 8.9 through 8.13, the accelerations have been evaluated for an equal dynamic load, with various time increments.

As can be seen, the time increment has significant influence on accelerations obtained. Furthermore, maximum acceleration obtained from Figures 8.9 through 8.13



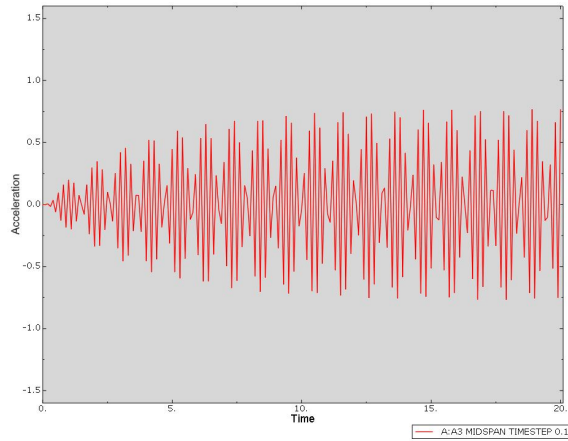


**Figure 8.9:**  $\Delta t = 0.1s$ .

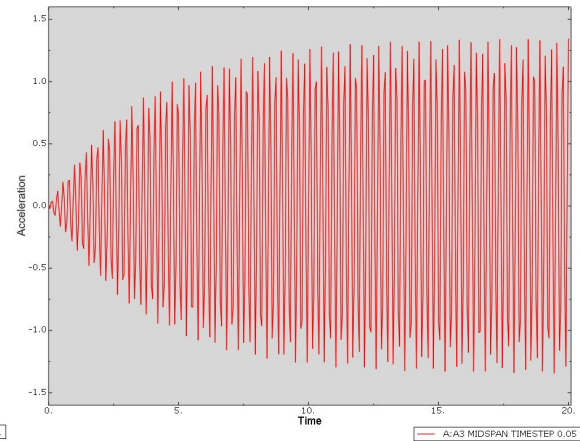


**Figure 8.10:**  $\Delta t = 0.05s$

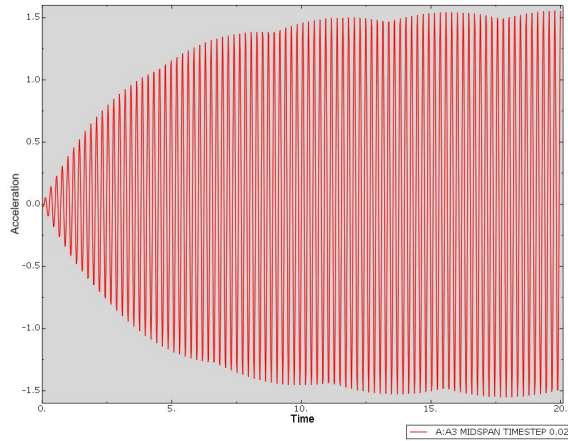


**Figure 8.11:**  $\Delta t = 0.02s$

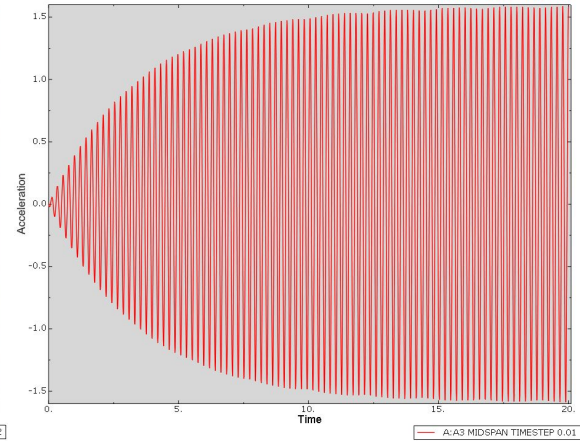


**Figure 8.12:**  $\Delta t = 0.01s$

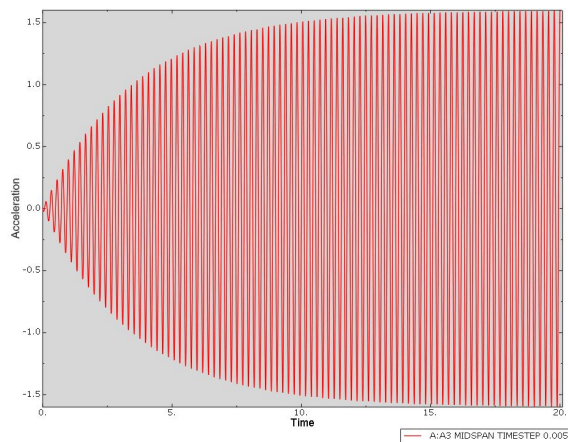


**Figure 8.13:**  $\Delta t = 0.005s$

are summarized in Table 8.9. It turns out that a time increment of  $\Delta t = 0.01$  s gives accurate results enough, without increasing simulation time more than necessary.

**Table 8.9:** *Maximum acceleration responses at various time increments  $\Delta t$  with equal dynamic loads.*

Time increment $\Delta t$ [s]	Max acceleration [ $m/s^2$ ]	Change from previous [%]
0.1	0.772	
0.05	1.347	74.5
0.02	1.556	15.5
0.01	1.588	2.05
0.005	1.596	0.507

## 8.4 Verification of the FE model

### 8.4.1 Verification by Assigning Steel Properties

Since making accurate hand calculations on a CFRP structure is difficult, it is also hard to verify the FE model against such calculations. One reason, mentioned in 7.3, is that CFRP is an orthotropic material, with different strength and stiffness properties in different directions. Even tensile and compressive properties are different. Another reason why hand calculations give a different result is that full interaction is assumed, an assumption that is not actually correct. For instance, the foam core has an in-plane and out-of-plane shear modulus that is far too low to make the upper and lower skins of the deck fully interact. Also, the effective width of the deck has been assumed to be equal to its actual width.

These issues suggest that the hand calculations are most likely to be inaccurate. In order to verify the FE model against more trustworthy hand calculations, all parts were assigned a stiff, isotropic material; in this case steel, with properties according to Table 8.10. This verification of the FE model was performed only for footbridge alternative CFRP1; assuming that CFRP2 is equally accurate.

**Table 8.10:** *Material input for steel properties in Brigade/Plus (Al-Emrani et al, 2013).*

Material name	Steel
Mass density [ $kg/m^3$ ]	7,800
Young's modulus [ $GPa$ ]	210
Poisson's ratio [ ]	0.3

Properties from Table 8.10 were assigned for both the hand calculations and the FE model. Bending stresses in the ULS and deflections in the SLS were checked. Figure 7.10 illustrates the points at which the bending stresses were checked. The results of the verification are summarized in Table 8.11 for bending stresses and in Table 8.12 for deflections in the SLS.

**Table 8.11:** *Bending stresses in the ULS for a cross-section with steel properties; from hand calculations and Brigade/Plus analysis. The points are illustrated in Figure 7.10.*

Point	Hand calculations [MPa]	Brigade/Plus [MPa]	Ratio [ ]
1.	41.84	40.82	1.025
2.	25.81	26.16	0.987
3.	12.48	12.77	0.985

**Table 8.12:** *Deflection check in the SLS for steel properties between hand calculations and Brigade/Plus.*

Hand calculations [mm]	Brigade/Plus [mm]	Ratio [ ]
35.36	36.35	0.973

Altogether, the validation of FE model with hand calculations indicate a good agreement, where the least accurate ratio is 2.7 %. In other words, a reliable finite element model that provide accurate results is claimed to be used.

#### 8.4.2 Verification of FE Model Using Nastran

In order to verify the FE model even more, a comparison of deflection and eigenfrequencies in two FE programs was carried out. The CFRP1 design was modeled in Nastran by Thomas Hallgren, structural engineer at Cowi. The results from the two models for deflection due to self-weight and eigenfrequencies, together with the accordance ratios, are presented in Table 8.13. As can be noticed, the accordance for the two models is good; however, the third eigenfrequency has a slightly higher deviation, but is still decently accurate.

**Table 8.13:** *Verification of CFRP1 with Nastran model made by Hallgren.*

Check	Brigade/Plus	Nastran	Ratio [ ]
Deflection due to self-weight [mm]	9.79	10.3	0.95
1 <sup>st</sup> Eigenfrequency [Hz]	5.10	5.07	1.01
2 <sup>nd</sup> Eigenfrequency [Hz]	5.62	5.56	1.01
3 <sup>th</sup> Eigenfrequency [Hz]	9.46	10.33	0.92
4 <sup>th</sup> Eigenfrequency [Hz]	13.39	13.47	0.99
5 <sup>th</sup> Eigenfrequency [Hz]	18.14	18.49	0.98
6 <sup>th</sup> Eigenfrequency [Hz]	18.92	18.60	1.02

## 8.5 Checks

The Brigade/Plus model is verified as a reliable model in the previous Section 8.4. However, the two bridge designs must be proven to fulfill the requirements stated in Chapter 7.7 in order to proceed.

### 8.5.1 Bending Stress

Bending stress capacities of FE models CFRP1 and CFRP2 were checked at the same three points of the cross-section as for previous checks; see Figure 7.10. These bending stresses with associated utilization factors are presented in Tables 8.14 and 8.15.

**Table 8.14:** *Bending stress checks in the ULS for three points of the cross-section for footbridge alternative CFRP1 in Brigade/Plus.*

Point	Design bending stress [MPa]		Bending stress resistance [MPa]	Utilization ratio [ ]
1.	37.22	<	250.08	0.149
2.	27.20	<	283.60	0.096
3.	54.87	<	357.96	0.153

**Table 8.15:** *Bending stress checks in the ULS for three points of the cross-section for footbridge alternative CFRP2 in Brigade/Plus.*

Point	Design bending stress [MPa]		Bending stress resistance [MPa]	Utilization ratio [ ]
1.	30.98	<	250.08	0.124
2.	22.64	<	264.69	0.086
3.	34.11	<	326.81	0.104

### 8.5.2 Shear Stress

Shear stress checks were done at the end supports of FE models CFRP1 and CFRP2 in Brigade/plus. The results are presented in Tables 8.16 and 8.17.

**Table 8.16:** *Shear stress check in the ULS at the supports for CFRP1 in Brigade/Plus.*

Design shear stress [MPa]		Shear stress resistance [MPa]	Utilization ratio [ ]
10.16	<	34.383	0.295

**Table 8.17:** *Shear stress check in the ULS at the supports for CFRP2 in Brigade/Plus.*

Design shear stress [MPa]		Shear stress resistance [MPa]	Utilization ratio [ ]
5.006	<	34.048	0.147

### 8.5.3 Deflection

The footbridge FE models CFRP1 and CFRP2 in Brigade/Plus fulfills maximum deflection requirements and the checks are presented in Tables 8.18 and 8.19.

**Table 8.18:** *Deflection check in the SLS for CFRP1 in Brigade/Plus.*

Deflection [mm]		Max deflection [mm]	Utilization ratio [ ]
70.33	<	80.00	0.879

**Table 8.19:** *Deflection check in the SLS for CFRP2 in Brigade/Plus.*

Deflection [mm]		Max deflection [mm]	Utilization ratio [ ]
70.70	<	80.00	0.884



# 9

## Results

### 9.1 Economic Comparison Between Existing Steel Truss Bridge and CFRP Alternatives

The costs stated in Chapter 6 are summarized in Table 9.1.

**Table 9.1:** *Total costs for the actual steel truss bridge in Åby and design alternatives CFRP1 and CFRP2 [SEK].*

Activity	Truss	CFRP1	CFRP2	Relationship
Manufacturing	1,066,500	11,800,000	22,230,000	1/11/21
Supports	75,000	75,000	75,000	1/1/1
Transportation	27,200	27,200	27,200	1/1/1
Installation	200,000	128,000	132,000	1/0.64/0.66
Maintenance	737,600	718,200	718,200	1/0.97/0.97
Adjustments	210,600	-1,530,000	-2,782,000	
Total	2,300,000	11,000,000	20,000,000	1/4.8/8.8

### 9.2 Dynamic Response

A frequency and dynamic analyses stated in Sections 8.2.4.2 and 8.2.4.3 have been made. These results for the two bridge alternatives, CFRP1 and CFRP2 are presented in this Sections 9.2.1 and 9.2.2.

#### 9.2.1 CFRP1

From a frequency analysis in Brigade/Plus, the first six eigenfrequencies of each bridge-crowd system featuring footbridge alternative CFRP1 are presented in Table 9.2. For a description of the systems, see Section 8.2.6.2.

**Table 9.2:** *The first six eigenfrequencies [Hz] in Brigade/Plus for three different bridge-crowd systems involving CFRP1; empty bridge, bridge with mass additions from 0.5 pedestrians/m<sup>2</sup>, and bridge with mass additions from 0.8 pedestrians/m<sup>2</sup>.*

Mode	Type	CFRP1 <sub>0</sub>	CFRP1 <sub>0.5</sub>	CFRP1 <sub>0.8</sub>
1.	Torsional/Horizontal	5.10	4.70	4.45
2.	Vertical	5.62	4.86	4.52
3.	Torsional	9.46	7.92	7.31
4.	Torsional/Horizontal	13.4	12.5	12.0
5.	Vertical	18.1	15.7	14.6
6.	Torsional	18.9	18.6	17.6

The first eigenmodes are torsional/horizontal and no further analysis have been made on these, since not needed according to the Eurocode as their eigenfrequencies are greater than 2.5 Hz. The second eigenmodes are the first vertical eigenmodes. According to the Eurocode, no dynamic analysis is needed for CFRP1<sub>0</sub>. However, for CFRP1<sub>0.5</sub> and CFRP1<sub>0.8</sub>, dynamic response analyses are needed, as their first vertical eigenfrequencies are below the limit value of 5.0 Hz. The first vertical eigenmode of CFRP1, in Brigade/Plus, is shown in Figure 9.1.

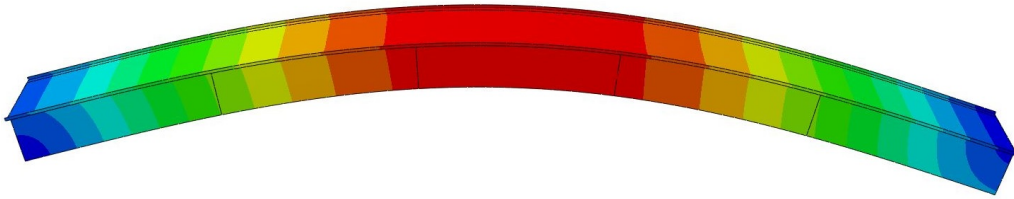


**Figure 9.1:** *First vertical mode shape for footbridge alternative CFRP1.*

Dynamic response analyses have been carried out for the first vertical eigenfrequencies of CFRP1<sub>0.5</sub> and CFRP1<sub>0.8</sub> and the results are presented in Sections 9.2.1.1 through 9.2.1.4.

#### 9.2.1.1 CFRP1<sub>0</sub>, Crowd Class III

No dynamic analysis is needed since the lowest vertical eigenfrequency is greater than 5 Hz. The dynamic load magnitude is assumed to be zero.

#### 9.2.1.2 CFRP1<sub>0</sub>, Crowd Class II

No dynamic analysis is needed since the lowest vertical eigenfrequency is greater than 5 Hz. The dynamic load magnitude is assumed to be zero.



### 9.2.1.3 CFRP<sub>10.5</sub>, Crowd Class III

**Table 9.3:** *Parameters for CFRP<sub>10.5</sub>, with a dynamic load from 0.5 pedestrians/m<sup>2</sup> and in case of the second harmonic.*

Parameter	Value	Reference
First Vertical Eigenfrequency $f_0$ [Hz]	4.86	Table 9.2
Reduction Factor $\psi$ [ ]	0.179	Table 4.10
Load Amplitude [ $N/m^2$ ]	0.977	Table 4.6

The accelerations of CFRP<sub>10.5</sub>, exposed to a dynamic load with an amplitude of  $0.977 N/m^2$ , are presented in Figure 9.2.

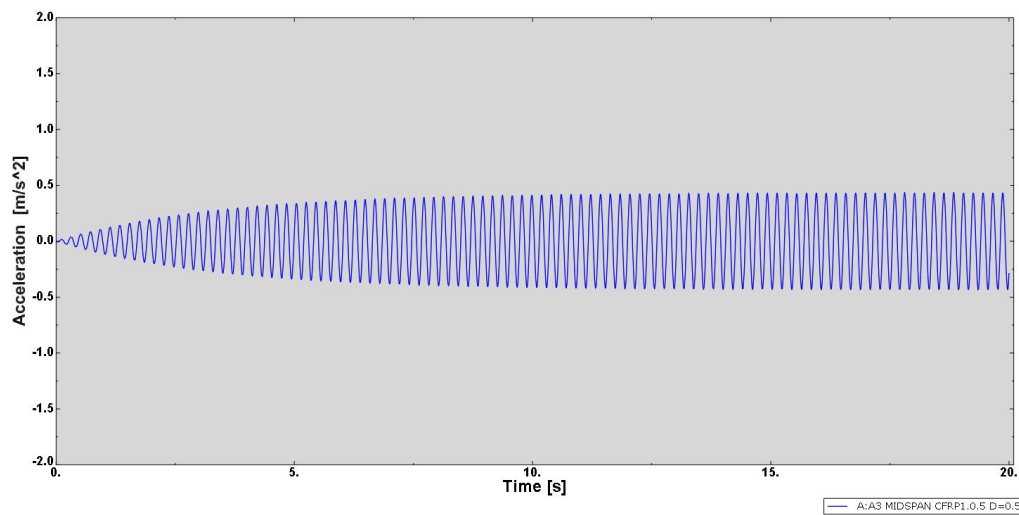


**Figure 9.2:** *Acceleration response for CFRP<sub>10.5</sub>, with a dynamic load from 0.5 pedestrians/m<sup>2</sup> and in case of the second harmonic. The maximum acceleration obtained is  $a_{max} = 0.436 m/s^2$ .*

### 9.2.1.4 CFRP<sub>10.8</sub>, Crowd Class II

**Table 9.4:** *Parameters for CFRP<sub>10.8</sub>, with a dynamic load from 0.8 pedestrians/m<sup>2</sup> and in case of the second harmonic.*

Parameter	Value	Reference
First Vertical Eigenfrequency $f_0$ [Hz]	4.52	Table 9.2
Reduction Factor $\psi$ [ ]	0.594	Table 4.10
Load Amplitude [ $N/m^2$ ]	4.10	Table 4.6

The accelerations of CFRP<sub>10.8</sub>, exposed to a dynamic load with an amplitude of  $4.10 N/m^2$ , are presented in Figure 9.3.

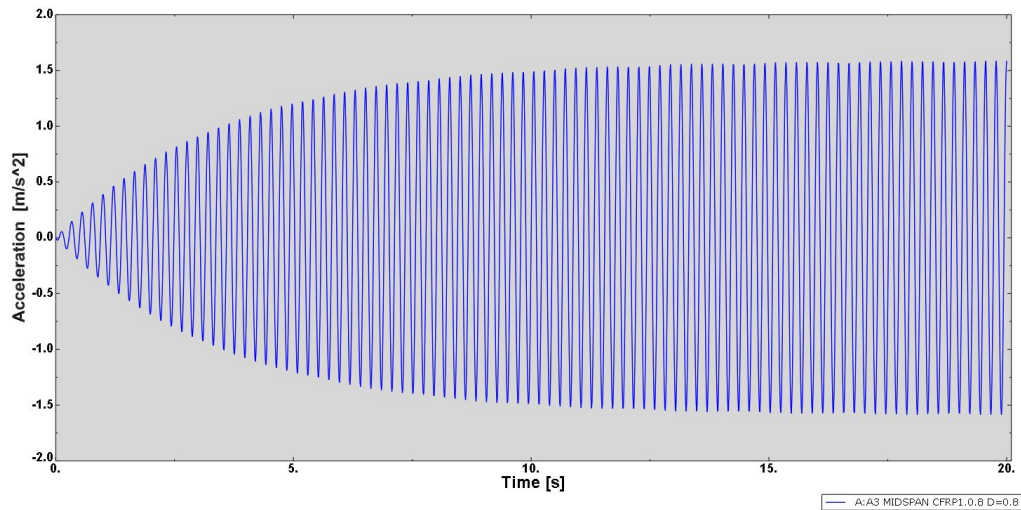


**Figure 9.3:** Acceleration response for  $CFRP1_{0.8}$ , with a dynamic load from 0.8 pedestrians/ $m^2$  and in case of the second harmonic. The maximum acceleration obtained is  $a_{max} = 1.59m/s^2$ .

### 9.2.2 CFRP2

From a frequency analysis in Brigade/Plus, the first six eigenfrequencies of the three bridge–crowd systems associated with CFRP2 are presented in Table 9.5.

**Table 9.5:** The first six eigenfrequencies [ $Hz$ ] in Brigade/Plus for three different bridge–crowd systems involving CFRP2; empty bridge, bridge with mass additions from 0.5 pedestrians/ $m^2$ , and bridge with mass additions from 0.8 pedestrians/ $m^2$ .

Mode	Type	CFRP2 <sub>0</sub>	CFRP2 <sub>0.5</sub>	CFRP2 <sub>0.8</sub>
1.	Vertical	4.56	4.16	3.96
2.	Torsional/Horizontal	5.17	4.86	5.01
3.	Torsional	9.38	8.31	7.82
4.	Torsional/Horizontal	14.3	14.3	13.9
5.	Vertical	16.1	14.6	14.0
6.	Torsional	23.5	20.8	19.6

In contrast to the first bridge alternative, CFRP1, the first eigenmodes are vertical for all systems involving CFRP2. All three systems – CFRP2<sub>0</sub>, CFRP2<sub>0.5</sub> and CFRP2<sub>0.8</sub> – have first vertical eigenfrequencies below the limit of 5  $Hz$ , given in the Eurocode. Therefore, dynamic analyses need to be carried out for all of these systems. However, the first horizontal eigenfrequencies are all greater than 2.5  $Hz$ ; hence, no further investigation of the horizontal vibrations is needed. The first vertical eigenmode of footbridge alternative CFRP2 is shown in Figure 9.4.

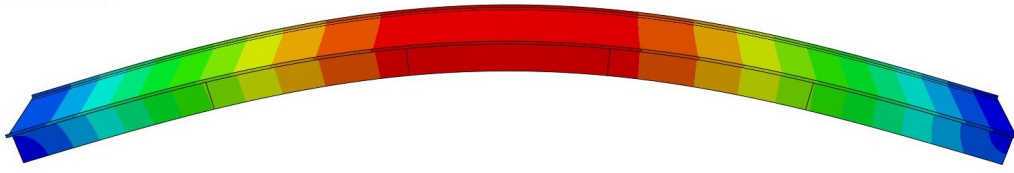


**Figure 9.4:** First vertical mode shape for footbridge alternative CFRP2.

### 9.2.2.1 CFRP2<sub>0</sub>, Crowd Class III

**Table 9.6:** Parameters for CFRP2<sub>0</sub>, with a dynamic load from 0.5 pedestrians/m<sup>2</sup> and in case of the second harmonic.

Parameter	Value	Reference
First Vertical Eigenfrequency $f_0$ [Hz]	4.56	Table 9.5
Reduction Factor $\psi$ [ ]	0.546	Table 4.10
Load Amplitude [ $N/m^2$ ]	2.98	Table 4.6

The acceleration response for CFRP2<sub>0</sub>, exposed to a dynamic load with an amplitude of 2.98  $N/m^2$ , is presented in Figure 9.7.

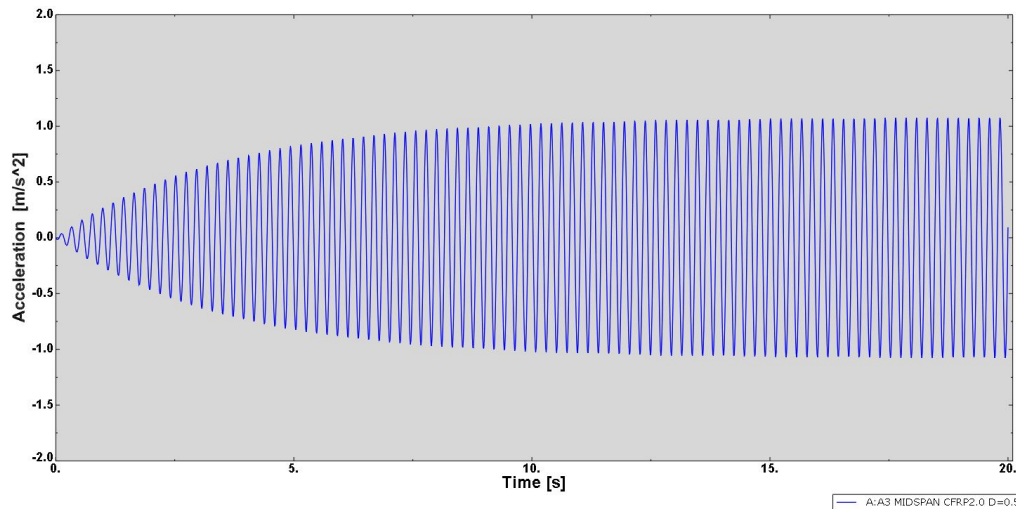


**Figure 9.5:** Acceleration response for CFRP2<sub>0</sub>, with a dynamic load from 0.5 pedestrians/m<sup>2</sup> and in case of the second harmonic. The maximum acceleration obtained is  $a_{max} = 1.08 m/s^2$ .

### 9.2.2.2 CFRP<sub>20</sub>, Crowd Class II

**Table 9.7:** Parameters for CFRP<sub>20</sub>, with dynamic a load from 0.8 pedestrians/m<sup>2</sup> and in case of the second harmonic.

Parameter	Value	Reference
First Vertical Eigenfrequency $f_0$ [Hz]	4.56	Table 9.5
Reduction Factor $\psi$ [ ]	0.546	Table 4.10
Load Amplitude [ $N/m^2$ ]	3.77	Table 4.6

The acceleration response of CFRP<sub>20</sub>, exposed to a dynamic load with an amplitude of 3.77  $N/m^2$ , is presented in Figure 9.6.

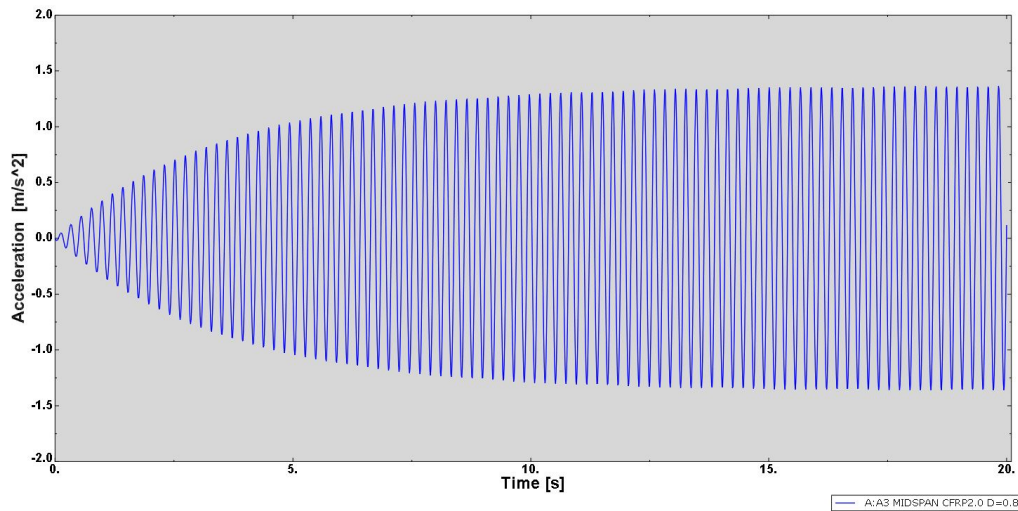


**Figure 9.6:** Acceleration response for CFRP<sub>20</sub>, with a dynamic load from 0.8 pedestrians/m<sup>2</sup> and in case of the second harmonic. The maximum acceleration obtained is  $a_{max} = 1.36m/s^2$ .

### 9.2.2.3 CFRP<sub>20.5</sub>, Crowd Class III

**Table 9.8:** Parameters for CFRP<sub>20.5</sub>, with a dynamic load from 0.5 pedestrians/m<sup>2</sup> and in case of the second harmonic.

Parameter	Value	Reference
First Vertical Eigenfrequency $f_0$ [Hz]	4.16	Table 9.5
Reduction Factor $\psi$ [ ]	1.0	Table 4.10
Load Amplitude [ $N/m^2$ ]	5.46	Table 4.6

The acceleration response for CFRP<sub>20.5</sub>, exposed to a dynamic load with an amplitude of 5.46  $N/m^2$ , is presented in Figure 9.8.

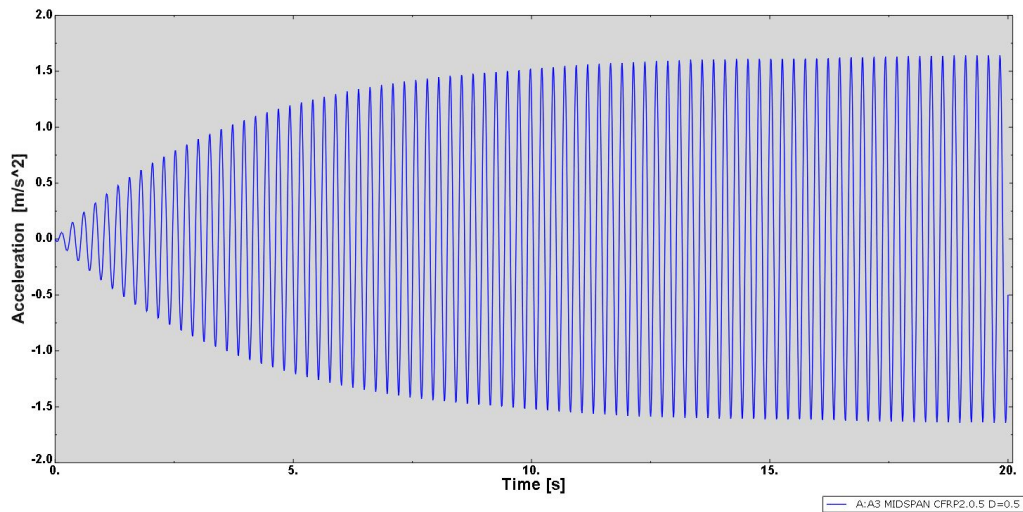


**Figure 9.7:** *Acceleration response for CFRP2<sub>0.5</sub>, with dynamic load from 0.5 pedestrians/m<sup>2</sup> in case of second harmonic. The maximum acceleration obtained is  $a_{max} = 1.64 \text{ m/s}^2$ .*

#### 9.2.2.4 CFRP2<sub>0.8</sub>, Crowd Class II

**Table 9.9:** *Parameters for CFRP2<sub>0.8</sub>, with dynamic load from 0.8 pedestrians/m<sup>2</sup> in case of second harmonic.*

Parameter	Value	Reference
First Vertical Eigenfrequency $f_0$ [Hz]	3.96	Table 9.5
Reduction Factor $\psi$ [ ]	1.0	Table 4.10
Load Amplitude $A$ [N/m <sup>2</sup> ]	6.90	Table 4.6

The acceleration response for CFRP2<sub>0.8</sub>, exposed to a dynamic load with an amplitude of  $6.90 \text{ N/m}^2$ , is presented in Figure 9.8.

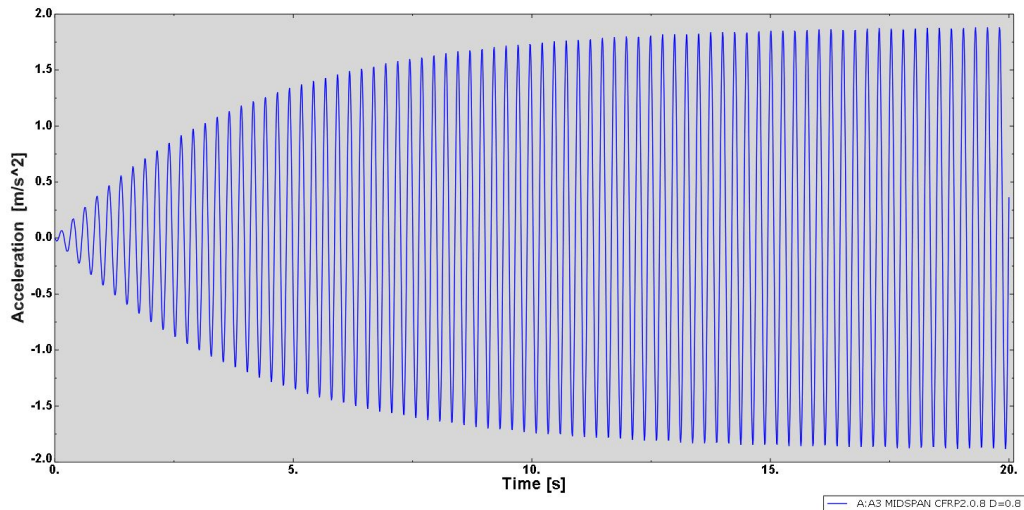


**Figure 9.8:** Acceleration response for  $CFRP2_{0.8}$ , with a dynamic load from 0.8 pedestrians/ $m^2$  and in case of the second harmonic. The maximum acceleration obtained is  $a_{max} = 1.88 m/s^2$ .

### 9.2.3 Summary of Maximum Accelerations

Maximum accelerations from Sections 9.2.1.1 through 9.2.2.4 are summarized in Table 9.10, for both footbridge alternatives CFRP1 and CFRP2, exposed to dynamic loads corresponding to footbridge classes III (0.5 pedestrians/ $m^2$ ) and II (0.8 pedestrians/ $m^2$ ).

**Table 9.10:** Summary of maximum acceleration response according to Sétra for footbridge alternative, CFRP1 and CFRP2, for footbridge classes III and II.

Bridge System	Class	$a_{max} [m/s^2]$
CFRP1 <sub>0</sub>	III	n/a
CFRP1 <sub>0</sub>	II	n/a
CFRP1 <sub>0.5</sub>	III	0.436
CFRP1 <sub>0.8</sub>	II	1.59
CFRP2 <sub>0</sub>	III	1.08
CFRP2 <sub>0</sub>	II	1.36
CFRP2 <sub>0.5</sub>	III	1.64
CFRP2 <sub>0.8</sub>	II	1.88

# 10

## Discussion

### 10.1 The Suitability of CFRP Bridges

It should be observed that all costs associated with the creating of a bridge are not considered. The parameters that have been left out are of such nature, that the costs are believed to be very similar between the three bridge alternatives that have been evaluated. In addition, the immense cost difference in the manufacturing phase makes it obvious that choosing a CFRP solution would not be economically justified for the case studied.

The manufacturing cost is surprisingly high, although it was already expected to be high. The cost of manufacturing the bridges has a significant relationship to the efficiency in bridge design, and the comparison is a bit unfair since the design is not optimized further, but has a constant cross-section. This is discussed in Section 10.2.

The procedure of moving the bridge from the factory and into place was believed to be one of the main opportunities to save money using CFRP instead of steel. The difference turned out to be very small. A total of 72,000 *SEK* are saved by using a smaller mobile crane for the lightest, slender CFRP bridge (CFRP1). For transportation, either of the three designs is lightweight enough for the weight not to have any influence on the cost. And at the site, although a smaller crane is used, no significant time of traffic disruptions is saved. The social costs saved by the use of carbon fibers at this point turned out to be close to nothing.

One source of cost savings not used in the case study is the foundation. If applied on weak grounds or old, worn piers, a significant amount of money can be saved, as indicated in Section 5.2. This is one parameter that has to be taken advantage of. It should even be considered as a requirement for a reasonable application for a CFRP bridge.

When it comes to maintenance, it has been assumed that CFRP needs no maintenance except regular inspections. It is hard to tell, however, if this is really true. As mentioned in Section 5.5, some certain characteristics are known, like the non-existing tendency to corrode, and the high fatigue strength. It is also assumed that the outer layer of each member of the CFRP bridges are made with a matrix that features a UV protection. However, it should not be taken for granted that no maintenance will be needed over the life time. Up to this day, there is literally no



experience on civil FRP structures standing their whole lifetime, since the oldest such structure was built 25 years ago.

As mentioned in Section 5.5, the same inspection intervals are recommended for CFRP bridges as for more conventional bridges. The master's thesis group agrees to this idea, referring to the little amount of experience of LCA of CFRP structures as of today. In the future, however, when there is more experience in maintaining CFRP structures, there might be a bigger confidence with the material's status over time. Consequently, inspections might be carried out with greater intervals than proposed as of today, saving a significant fraction of the inspection cost. Eventually, it could also be reasonable to increase the expected service life; that is, another way to make CFRP more cost-efficient over a lifetime.

A hypothetical scenario is considered, to see if a CFRP solution could be an option in the future, assuming a lot better optimization of the concept and a more matching location of application. The following arbitrary assumptions are made:

- An optimized CFRP design saves 40 % of the manufacturing cost of the structural system (see Section 10.2 for a discussion of the bridge design).
- The structural system of the truss bridge is increased by 20 % to fit the requirements on vertical vibrations (Darholm, 2018, pers. comm., May 25<sup>th</sup>).
- The bridge is installed on old piers, saving a foundation cost similar to that mentioned in Section 5.2.
- Future confidence in the long-term behavior of CFRP allows the intervals between inspections to be doubled.

Hand calculations, provided upon request, suggest that a truss bridge would be just above 6 million *SEK* over a lifetime for this hypothetical case. CFRP1 would be just below 7 million *SEK*. This means that the truss bridge is still significantly cheaper than the slender CFRP option.

The steel truss bridge has been widely used for many decades and it is well optimized as a cost-efficient option for the application considered. It is known, however, for its tendency to have vibration problems in large spans. Slightly beyond 30 meter, the trusses have to be stabilized in by a horizontal truss (Darholm, 2018, pers. comm; May 25<sup>th</sup>; Svensson, 2018, pers. comm; May 25<sup>th</sup>). A big extra cost for a bridge would be added if the span is so long that an intermediate support is needed. Building such a support would most likely mean that the road or railway would have to be closed for several weeks – an operation associated with immense social costs. That is, if a CFRP footbridge could span a distance significantly greater than a truss bridge, still fulfilling the static and dynamic requirements, CFRP could be a good option. How much material can be saved by optimization is briefly discussed in the next section.



## 10.2 Bridge Design

The designs presented in Chapter 7 are not claimed to be finished design concepts. No detailing has been treated and they both have uniform cross-sections throughout the entire length of the bridge span, except the vertical web stiffeners. A more optimized bridge design would have saved a lot of self-weight and money. It is hard to estimate how much material can be saved; however, a reference that gives a hint is the crossbeams of the catamarans manufactured by Aston Harald. They hold the three hulls together and its depth at the ends is only half of that in the middle. Their thickness varies between 6 and 20 mm (Allroth, 2018, pers. comm., May 26<sup>th</sup>). With that in mind, material savings of more than 50 % should not be considered as unrealistic.

Another way to cut the costs might be using a different manufacturing technique. Prepregs have been chosen as that solution yields the highest quality among all manufacturing methods. It is also the most expensive method. Some kind of resin injection technique might fit better for the purpose, having economy in mind. High strength and standard modulus CFRP has been used in the design. It is worth considering a lowered strength, since the material still has a very low utilization ratio in the ULS. GFRP should be considered as it is a much cheaper material, although a bit more elastic and not as strong as carbon fibers. As of today, GFRP is more common than CFRP as a construction material for bridges in shorter spans than that considered in this master's thesis.

Pultrusion is an interesting method, which yields a decently cheap unit price for the material when manufactured in large volumes. However, mass production of an entire cross-section is not efficient since there is a moderate need for each shape. Especially since the use of CFRP bridges should be limited to very specific occasions. If pultrusion was carried out, the bridge design would have to be made up of standard sections, like typical beams. It would also be hard to optimize the design along the cross section.

Taking inspiration from the truss bridges in the comparison may be an option. A truss solution saves a lot of height as the structural system can be placed next to the pedestrians – not underneath them. The height of the CFRP bridges is one characteristic that has not been accounted for in the comparison chapter. A truss would also allow for optimization by choosing different skin thicknesses depending on the force in the particular web. Good use would be taken from the longitudinal strength and stiffness of unidirectional CFRP. However, gluing the chords and webs together might be time consuming. The possibility of evaluating more designs and manufacturing techniques is discussed in Section 12.

As can be seen in Tables 7.11 and 7.12, the bridges are designed to have a decent margin to the maximum deflection; that is, a moderate utilization ratio. The reason, which is briefly discussed in Section 7.3, is the awareness that the hand calculations will give a slightly different stiffness than the FE model. This is due to the assump-

tion of full interaction in the cross-section and the simplification made in not taking the orthotropic material properties into consideration to a full extent.

### 10.3 Dynamic Response

In the dynamic analyses, each of the bridge designs is evaluated three times depending on the amount of pedestrian mass added to their modal masses. The extra mass from the pedestrians have a big influence on the bridges' eigenfrequencies, especially when lightweight footbridges are considered. For example, when footbridge alternative CFRP1 has a mass addition from a crowd density of  $0.5 \text{ pedestrians}/\text{m}^2$  (that is, CFRP<sub>1,0.5</sub>), the system's modal mass is increased by one third, compared with an empty bridge (CFRP<sub>1,0</sub>). As the pedestrians add a mass but do not add any stiffness, the eigenfrequencies go down, as remembered from Equation 4.2.

CFRP<sub>1,0</sub> passes the dynamic test, without any further investigation, as the eigenfrequencies are high enough, according to Eurocode (see Section 4.6.1). The first eigenmode is torsional/horizontal, hence a limit value of  $2.5 \text{ Hz}$  according to the Eurocode. The second eigenmode is a vertical mode, for which the Eurocode states a limit value of  $5.0 \text{ Hz}$ , see Section 4.6.1. The same values are suggested in the Sétra code, see Figure 4.13.

CFRP<sub>1,0.5</sub> also matches the requirements. Since the first vertical eigenfrequency is lower than  $5.0 \text{ Hz}$ , an acceleration analysis is carried out. From this, a maximum acceleration is determined as  $0.436 \text{ m}/\text{s}^2$ ; significantly below the limit stated in the Eurocode –  $0.7 \text{ m}/\text{s}^2$ . Since  $0.5 \text{ pedestrians}/\text{m}^2$  is by far the most common design pedestrian density within Swedish bridge engineering, design alternative CFRP1 should be considered as a – dynamically – decent design.

The reason why CFRP<sub>1,0.5</sub> fulfills dynamic vibration requirements while CFRP<sub>1,0.8</sub> does not, is primarily the higher eigenfrequency; and secondly the greater density of the crowd that imposes the dynamic load. Since the maximum accelerations are proportional to the crowd density as well as the  $\psi$  factor, see Table 4.6, it is easy to prove that the eigenfrequency has a much greater significance than the pedestrian density imposing the dynamic load, for the maximum accelerations of this particular footbridge.

The bridge in consideration, CFRP<sub>1,0.5</sub>, has an eigenfrequency influenced by the mass of  $0.5 \text{ pedestrians}/\text{m}^2$ . The top acceleration of  $0.436 \text{ m}/\text{s}^2$ , previously mentioned, appears when the bridge is exposed to a dynamic load from the same pedestrian density. However, if CFRP<sub>1,0.5</sub> would instead be exposed to a dynamic load imposed by  $0.8 \text{ pedestrians}/\text{m}^2$ , the accelerations at resonance would be multiplied by a factor of  $8/5$ , giving an acceleration of  $0.698 \text{ m}/\text{s}^2$ , which is still acceptable.

When it comes to the influence of the eigenfrequencies of CFRP<sub>1,0.5</sub> and CFRP<sub>1,0.8</sub>, on the accelerations, the difference becomes more significant. The first vertical

eigenfrequency of CFRP1<sub>0.5</sub>, that is, 4.8568 *Hz*, yields a reduction factor of 0.179 according to Table 4.10 and Figure 4.13. CFRP1<sub>0.8</sub> has a slightly lower eigenfrequency, namely 4.5249 *Hz*. That yields a reduction factor  $\psi$  of 0.594, and when exposed to a dynamic load imposed by 0.8 *pedestrians/m<sup>2</sup>*, the maximum acceleration becomes 1.588 *m/s<sup>2</sup>*, which is not even close to acceptable. If the dynamic load CFRP1<sub>0.8</sub> would instead be dynamically loaded by 0.5 *pedestrians/m<sup>2</sup>*, the accelerations would be multiplied by factor 0.5/0.8, making the top acceleration 0.993 *m/s<sup>2</sup>*, which is not still acceptable.

It can be concluded from these simple calculations, that the crowd density's biggest influence on the accelerations of the particular bridge design is associated with its influence on the eigenfrequency and, thereby, on the reduction factor. Putting it in other words: A slight change in crowd density might yield a big change in  $\psi$ , see Table 4.6.

This conclusion is valid when the system, like those investigated, has a first vertical eigenfrequency around 4.2–5.0 *Hz*. As can be read out the steep slope of the graph in Figure 4.10 for the particular eigenfrequency range, an eigenfrequency difference of 0.8 *Hz* can be the difference between a big dynamic load and no dynamic load at all.

Following is a brief investigation of the critical value for the eigenfrequency at which CFRP1<sub>0.5</sub> barely passes the acceleration requirement for crowd class III. The limit value for acceptable vertical acceleration, that is, 0.7 *m/s<sup>2</sup>*, is obtained at a  $\psi$  value according to Equation 10.1.

$$\psi = \frac{a_{max}(\phi)}{a(1)} = \frac{0.7}{0.436/0.179} = 0.2874 \quad (10.1)$$

This reduction factor is given at an eigenfrequency of 4.4296 *Hz*, which is a decrease of 0.4272 *Hz* from the actual value.

In Table 9.10, maximum accelerations are summarized for all combinations; bridge alternatives and load classes. As can be seen, CFRP2 does not pass any acceleration test. In contrast to the eigenfrequencies of CFRP1, CFRP2<sub>0</sub>'s first eigenfrequency is vertical. It gives a reduction factor  $\psi$  of 0.546; however, that does not reduce the load enough to yield acceptable accelerations. CFRP2<sub>0.5</sub> and CFRP2<sub>0.8</sub> both have higher masses, and their eigenfrequencies give them  $\psi$  factors that are equal to 1.0. Hence, accelerations that are way too big.

It can be proven that a high crowd density is good for the bridge in eigenfrequency ranges that yield a reduction factor equal to 1.0. Assume that the reduction factor of CFRP2<sub>0</sub> is set to 1.0. The accelerations for a dynamic load from 0.5 *pedestrians/m<sup>2</sup>* would be increased from 1.077 *m/s<sup>2</sup>* to 1.9725 *m/s<sup>2</sup>*. This increased acceleration would have been higher than the maximum acceleration obtained for CFRP2<sub>0.5</sub> at the same dynamic load, 1.64 *m/s<sup>2</sup>*. However, since the accelerations are not acceptable in either case, an added mass cannot solely solve the vibration problem for lightweight bridges like the ones modeled, but it has to be combined with additional

actions. For instance, mechanical dampers can be installed in specific spots, prepared during the construction phase, as mentioned in Section 4.4.1.2.

For both CFRP1 and CFRP2, the crowd masses' damping contribution do not compensate for the increase in  $\psi$  factors they cause. That is, for footbridges like the ones considered, keeping the self-weight as low as possible is recommended, to keep the eigenfrequencies decently close to (or above)  $5.0\text{ Hz}$ . Optimizing the design will do good with this aspect in mind. This conclusion is supported by the fact that the slender, lightweight, design gets acceptable accelerations for moderate crowd densities, while the accelerations of the more heavy, bulky design are too big in either case.

Among all the mass and load combinations treated, it shall still be borne in mind that in reality, the pedestrian mass, the eigenfrequency, the dynamic load, and the accelerations are all somewhere between the calculated values. It can also be discussed whether the eigenfrequencies of the bridges are realistic values for the step frequencies. Sétra states that normal step frequencies are in a range up to  $2.4\text{ Hz}$ , that is, about half of the eigenfrequency. However, at a design stage, the eigenfrequencies should be used since they represent worst case scenario.

## 10.4 Buckling

The risk for normal buckling in the webs is very significant, especially for the slender cross-section. Here are a few suggestions on how to stabilize the structure against normal buckling:

- More vertical stiffeners; the current CTC distance being  $6.4\text{ m}$ .
- Inserting horizontal web stiffeners. Such stiffeners should run along the whole bridge span and, for aesthetic reasons, be placed on the inside of each web. They should be placed somewhere in the compressed zone, which also simplifies the installation of the stiffeners, that is, the factory workers do not have to reach very deep into the box girder for this procedure. However, it should be considered that there will be a conflict between the horizontal and the vertical stiffeners that has to be accounted for.
- The webs can always be made thicker, which also allows for lower webs; however, that would increase the self-weight and decrease the eigenfrequency, while as the discussion in Section 10.3 hints that a lowered eigenfrequency is a bad thing in this case, as it increases the  $\psi$  factor.
- One popular solution to buckling issues is splitting the webs into two skins with a few set of PVC foam between them. This would also increase the self-weight, but the solution is worth considering.

# 11

## Conclusion

A CFRP footbridge in the location studied in this master's thesis would not be a reasonable alternative to a steel truss footbridge, since the concept of truss bridges has been optimized over a long time, making truss bridges a very competitive solution, especially with regards to economics. However, that does not conclude that CFRP would never be a reasonable construction material for a footbridge in spans greater than 30 *m*. It is uncertain how much the design can be optimized, although 50 % should not be seen as unrealistic. If the material savings are combined with a well-considered application, the concept might prove to be economically advantageous.

More research is needed. For instance, thorough life cycle cost (LCC) analyses, are suggested for any application where a CFRP bridge is considered. Effort must be spent on pointing out the special cases, where a CFRP would have full use of its beneficial characteristics. Cases must be found, where the conditions are too difficult for a truss bridge to beat the whole span. Such conditions would be a span so long that truss bridges cannot span them without an intermediate support, the construction of which would cause expensive traffic disruptions. Truss bridges tend to have vibration problems in long spans; in which a CFRP bridge might take advantage from its low self-weight and, thereby, high eigenfrequency.

Since the material of CFRP is expensive and the manufacturing process is time-consuming, a lot of effort must be put on the design concept, to create a design that is material-efficient and allows for a decently quick production. Money can be saved by establishing the footbridge on a weak ground, which would not withstand a structure of a conventional self-weight.

If one of the design principles tried in this thesis would be developed further, it should be the slender version, called CFRP1. The bulky CFRP2 is too expensive, too heavy to have a sufficient eigenfrequency, and too lightweight to have a sufficient damping. Given the limitations of this thesis, CFRP1 fits the dynamic requirements that are normally applied in Sweden. It does so thanks to its relatively high eigenfrequency. However, considering its low self-weight, dynamic issues might still be present in practice. The master's thesis group is not convinced that fulfilled dynamic requirements actually yield a completely satisfying comfort. As dynamic requirements on footbridges are defined as of today, the dynamic load on footbridges with eigenfrequencies greater than 5.0 *Hz* is defined as zero. That is, there is no consideration of the low self-weight of such bridges, although a lightweight structure

generally has a relatively big tendency to vibrate.

Strictly following the load model given in Sétra, it turns out that the dynamic loads are so significant for a lightweight bridge like the CFRP ones considered (with a first vertical eigenfrequency of roughly 4–5  $Hz$ , that a very low reduction factor ( $\psi$ ) must be obtained. Thus, the eigenfrequency is very important for the bridge to match the requirements. Increased crowd densities influence the dynamic loading more by lowering the eigenfrequency than by altering the density of the pedestrian traffic does.

Furthermore, the additional crowd masses influence the eigenfrequency negatively more than they influence the damping positively. That is, if the eigenfrequency is decreased by a mass addition, that mass addition will not compensate for the lowered eigenfrequency. In conclusion, for footbridges like the ones considered, keeping the self-weight as low as possible is recommended, to keep the eigenfrequencies close to (or above) 5.0  $Hz$ . Optimizing the bridge design, hence a lowered self-weight, will do good in this matter.

# 12

## Further Studies

There are obviously several aspects not accounted for in this master's thesis. As suggested in the conclusions, Chapter 11, a lot of effort should be spent on optimizing the design in order to save time and material. Optimizing the design can mean either varying the plate thicknesses and fiber directions along the span length. It could also include a survey aiming to determine what manufacturing methods and what material qualities yield the most cost-efficient design. Alternatives to high strength and standard modulus fibers should be considered. One of them could be GFRP. Most certainly, elaborating with different structural systems can also be worth the effort. A truss system, as mentioned in Section 10.2, is one suggestion.

Further analyses of the costs of the bridge concepts are suggested. For instance, LCC analyses of potentially suitable applications would give a clarified view of the costs over time.

Dynamic response for lightweight footbridges, especially for CFRP footbridges, is a interesting topic that should be researched more. Some topics within dynamic response that could be studied are:

- The dynamic analyses made in Brigade/Plus by the master's thesis group can be made experimentally, in a smaller scale, to verify the conclusions made.
- The HSI effect on lightweight footbridges in CFRP. One way could be verifying the calculation model published by Zäll (2018) using an FE model.
- Investigate how the configuration of the matrix in CFRP can influence material's contribution to the damping behavior. The master's thesis group has made decent research on the topic. Based on the lack of information available at CFRP manufacturing companies as of today, the group does not evaluate this as a way to control the damping. This phenomenon may be studied experimentally.





# 13

## References

Ahlgren, P. & Edwijn, J. (2017) *Flexural Strengthening of Concrete Structures with Prestressed FRP Composite*. Master's thesis, Chalmers University of Technology, Departement of Civil and Environmental Engineering. <http://publications.lib.chalmers.se/records/fulltext/252925/252925.pdf> (2018-03-11).

Al-Emrani, M., Engström, B., Johansson, M. & Johansson, P. (2013) *Bärande konstruktioner, Del 1*. Gothenburg: Chalmers University of Technology, Departement of Civil and Environmental Engineering.

American Chemical Society (2018) *High Performance Carbon Fibers: National Historic Chemical Landmark*. <https://www.acs.org/content/acs/en/education/whatischemistry/landmarks/carbonfibers.html> (2018-03-02).

Armstrong, T. (2013) *An Overview of Global Cement Sector Trends: Insights from the Global Cement Report 10<sup>th</sup> Edition*. [Powerpoint presentation]. XXX Technical Congress, 2013-09-02, Lima, Peru. [http://www.ficem.org/boletines/ct-2013/presentaciones2013/1-EXPERTOS/2\\_THOMAS-ARMSTRONG/ICR-FICEM-Presentation-Handout-30Aug13.pdf](http://www.ficem.org/boletines/ct-2013/presentaciones2013/1-EXPERTOS/2_THOMAS-ARMSTRONG/ICR-FICEM-Presentation-Handout-30Aug13.pdf) (2018-03-05).

Bank, L.C. (2006) *Composites for Construction: Structural Design With FRP Materials*. Hoboken, NJ, USA: John Wiley & Sons, Inc. [https://books.google.se/books?hl=sv&lr=&id=1B2mTpDtUoAC&oi=fnd&pg=PR13&dq=Composites+for+construction:+Structural+design+with+FRP+materials&ots=71HAtPwhFK&sig=agvKlT2pWk53xj17UbMHPbVtx4Y&redir\\_esc=y#v=onepage&q&f=false](https://books.google.se/books?hl=sv&lr=&id=1B2mTpDtUoAC&oi=fnd&pg=PR13&dq=Composites+for+construction:+Structural+design+with+FRP+materials&ots=71HAtPwhFK&sig=agvKlT2pWk53xj17UbMHPbVtx4Y&redir_esc=y#v=onepage&q&f=false) (2018-02-12).

Blevins, R.D. (1979) *Formulas for Natural Frequency and Mode Shape*. New York, NY: Van Nostrand Reinhold Co.

Carlsson, P. (2018) *Fiberkompositbroar i Malmö (Fiber Composite Bridges in Malmö)* [Powerpoint presentation]. Brobyggardagen (Bridge Day), 2018-01-29.

Clarke, J. L. (1996) *Structural Design of Polymer Composites: Eurocomp Design Code and Background Document*. New York, NY, USA: CRC Press.  
[https://books.google.se/books?hl=sv&lr=&id=z-Vr90utc2oC&oi=fnd&pg=PP1&dq=Structural+Design+of+Polymer+Composites:+Eurocomp+Design+Code+and+Background+Document.&ots=rojryY78G\\_R&sig=7712NxYw4Tk4Z-\\_EJuSAwNHhy9I&redir\\_esc=y#v=onepage&q=Structural%20Design%20of%20Polymer%20Composites%3A%20Eurocomp%20Design%20Code%20and%20Background%20Document.&f=false](https://books.google.se/books?hl=sv&lr=&id=z-Vr90utc2oC&oi=fnd&pg=PP1&dq=Structural+Design+of+Polymer+Composites:+Eurocomp+Design+Code+and+Background+Document.&ots=rojryY78G_R&sig=7712NxYw4Tk4Z-_EJuSAwNHhy9I&redir_esc=y#v=onepage&q=Structural%20Design%20of%20Polymer%20Composites%3A%20Eurocomp%20Design%20Code%20and%20Background%20Document.&f=false) (2018-02-12).

Dallard, P., Fitzpatrick, T., Flint, A., Low, A., Rodsill Smith, R., Willford, M. & Roche, M. (2001) *London Millennium Bridge: Pedestrian-induced Lateral Vibrations*. Journal of Bridge Engineering, vol. 6, issue 6. <https://ascelibrary-org.proxy.lib.chalmers.se/doi/pdf/10.1061/%28ASCE%291084-0702%282001%296%3A6%28412%29> (2018-04-01).

Eriksson, P. & Pagander Tysnes, H. (2013) *Vibration Response of Lightweight Pedestrian Bridges*. Master's thesis, Chalmers University of Technology, Department of Civil and Environmental Engineering. <http://publications.lib.chalmers.se/records/fulltext/186575/186575.pdf> (2018-02-19).

Falk, A. (2014) Materialkombinationer kräver nya visioner (Material Combinations Require New Visions). *Husbyggaren (The House Builder)*, number 5, 2014. [https://issuu.com/husbyggaren/docs/14-1724\\_hb\\_nr5-2014](https://issuu.com/husbyggaren/docs/14-1724_hb_nr5-2014) (2018-05-08).

Fiberline (2013) <https://fiberline.com/how-we-install-bridges-we-fly-them> (2018-05-14).

Fiberline (2014) <https://fiberline.dk/thornaby-station-gangbro> (2018-05-16).

Fiberline (2018) [https://fiberline.com/thornaby-station-footbridge?utm\\_source=eMarketeer.com&utm\\_medium=email&utm\\_content=EN%2BBroer%2Bstring%2B%25232&utm\\_campaign=Copy%2Bof%2BBroer%2BAutomation%2Bstring&EMTID=ItsBFh6x3za75Cq0n3gg](https://fiberline.com/thornaby-station-footbridge?utm_source=eMarketeer.com&utm_medium=email&utm_content=EN%2BBroer%2Bstring%2B%25232&utm_campaign=Copy%2Bof%2BBroer%2BAutomation%2Bstring&EMTID=ItsBFh6x3za75Cq0n3gg) (2018-05-13).

Fireco (2018) *Basculé FRP Composite Footbridge – Fredrikstad*. <http://www.fireco.no/?news=bascule-frp-composite-footbridge-fredrikstad> (2018-03-09).

Google Maps (2018) [maps.google.com](https://maps.google.com) (2018-05-14)

Gurit (2018a) *Guide to Composites*. Newport, Isle of Wight, United Kingdom: Gurit. <http://www.gurit.com/-/media/Gurit/Datasheets/guide-to-composites.ashx> (2018-03-09).

- Gurit (2018b) *Mechanical Properties Prepregs*. Newport, Isle of Wight, United Kingdom: Gurit.
- Gurit (2018c). *Gurit® PVC: Structural Foam Core*. Newport, Isle of Wight, United Kingdom: Gurit. <http://www.gurit.com/Our-Business/Composite-Materials/Structural-Core-Materials/Gurit-PVC> (2018-04-04).
- Haghani, R., Ascione, L., Caron, J.F., Correia, J.R., de Corte, W., Godonou, P., Knipper, J., Moussiaux, E., Mottram, T., Oppe, M., Silvestre, N., Thorning, P. & Tromp, L. (2007) *Prospect for New Guidance in the Design of FRP Structures*.
- Haghani, R.; Yang, J. (2016) *Application of FRP Materials for Construction of Culvert Road Bridges*. Gothenburg, Sweden: Chalmers University of Technology. <http://publications.lib.chalmers.se/records/fulltext/233171/233171.pdf> (2018-05-30).
- Hagmans (2005) *Säkerhetsdatablad – Acrydur S*. <http://www.hagmans.se/produktinformation/varuinfo/Acrydur%20S.pdf> (2018-03-05).
- Hjelm, M.; Karlsson, N. (2014) *En jämförande studie om kostnadseffektiviteten hos fiberarmerade kompositbroar (A Comparative Study on the Cost-efficiency of Fiber Reinforced Composite Bridges)*. Bachelor's thesis, Chalmers University of Technology, Department of Civil and Environmental Engineering. <http://publications.lib.chalmers.se/records/fulltext/202369/202369.pdf> (2018-05-08).
- Holmes, M. (2014) *Global Carbon Fibre Market Remains on Upward Trend*. Reinforced Plastics, vol. 58, issue 6, p. 39. doi: 10.1016/S0034-3617(14)70251-6.
- Jain, R. & Lee, L. (2012) *Fiber Reinforced Polymer (FRP) Composites for Infrastructure Applications: Focusing on Innovation, Technology Implementation and Sustainability*. New York, NY, USA: Springer. <https://link-springer-com.proxy.lib.chalmers.se/book/10.1007%2F978-94-007-2357-3#about> (2018-02-12).
- Jarkiewicz, A. (2012) *Vision Älvstaden*. [http://alvstaden.goteborg.se/wp-content/uploads/2015/05/vision\\_alvstaden\\_sv\\_web.pdf](http://alvstaden.goteborg.se/wp-content/uploads/2015/05/vision_alvstaden_sv_web.pdf) (2018-02-06).
- Kolstein, M.H. (2008) *Fibre Reinforced Polymer (FRP) Structures*. Delft University of Technology, Faculty of Civil Engineering and Geosciences.
- Kraker, B. de. (2013) *A Numerical – Experimental Approach in Structural Dynamics*. Maastricht, Netherlands: Shaker Publishing BV.
- Leander, J. & Karoumi, R. (2013) *Dynamics of thick bridge beams and its influence on fatigue life predictions*. Journal of Constructional Steel Research, vol. 89, pp. 262-271. <https://doi.org/10.1016/j.jcsr.2013.07.012> (2018-05-17).

- Mara, V. (2014) *Fibre Reinforced Polymer Bridge Decks: Sustainability and a Novel Panel-level Connection*. Licentiate thesis, Chalmers University of Technology, Department of Civil and Environmental Engineering. <http://publications.lib.chalmers.se/records/fulltext/222054/222054.pdf> (2018-02-06).
- Mara, V. (2015) *Numerical Modelling of Composite Materials with Abaqus – Guidelines*. Chalmers University of Technology, Department of Civil and Environmental Engineering.
- OECD (2010) *Perspectives on Steel by Steel-using Industries*. [Powerpoint presentation]. 68<sup>th</sup> Steel Committee Meeting, Paris, France, May 6<sup>th</sup>–7<sup>th</sup>. <https://www.oecd.org/sti/ind/45145459.pdf> (2018-04-04).
- Pedersen, L. (2012): Damping Effect of Humans. *Topics on the Dynamics of Civil Structures*, vol. 1. New York, NY, USA: Springer. [https://link-springer-com.proxy.lib.chalmers.se/content/pdf/10.1007%2F978-1-4614-2413-0\\_1.pdf](https://link-springer-com.proxy.lib.chalmers.se/content/pdf/10.1007%2F978-1-4614-2413-0_1.pdf) (2018-04-27).
- Peeters, J. (2011) *Resistance to UV-light*. Rotterdam, Netherlands: Fibercore Europe.
- Porter, T. (2004) *Wood Identification and Use*. Lewes, United Kingdom: Guild of Master Craftsman Publications Ltd.
- Potyrala, P.B. (2011) *Use of Fibre Reinforced Polymeromposites in Bridge Construction. State of the Art in Hybrid and All-composite Structures*. [Master thesis] Polytechnical University of Catalonia, Department of Construction Engineering. <http://hdl.handle.net/2099.1/12353> (2018-02-06).
- Reeve, S. (2018) World's First Composite Bridge Turns 25. *Composite Advantage*. <https://www.compositeadvantage.com/blog/worlds-first-composite-bridge-turns-25> (2018-05-17).
- Reynolds, N. (2002) *Millennium Bridge Reopens – and Now it's Wobble-free: Thousands Walk Over the Thames After 'Heroic Failure' is Steadied by £5M*. The Telegraph. <https://www.telegraph.co.uk/news/> (2018-04-04).
- Rupakhety, R. & Sigbjörnsson, R. (2017) *Computational Mechanics 1: Lecture Notes*. Reykjavik, Iceland: University of Iceland.

Rutgersson, B. (2014) Krav på inspektion av byggnadsverk (Requirements on Inspections of Structures). *Trafikverket (Swedish Traffic Administration)*. [https://batman.trafikverket.se/batinfo/Batman/BiblioteketPDF/01\\_Dokument%20Batman/Krav%20Insp%20Byggnadsverk%20inkl%20Beslut.pdf](https://batman.trafikverket.se/batinfo/Batman/BiblioteketPDF/01_Dokument%20Batman/Krav%20Insp%20Byggnadsverk%20inkl%20Beslut.pdf) (2018-05-18).

Saba, N.; Jawaid, M.; Allothman, O.Y.; Paridah, M.T. (2015) A Review on Dynamic Mechanical Properties of Natural Fibre Reinforced Polymer Composites. *Construction and Building Materials*, vol. 106. [https://ac-els-cdn-com.proxy.lib.chalmers.se/S0950061815307479/1-s2.0-S0950061815307479-main.pdf?\\_tid=1fe52e59-45e1-449d-acb7-911abb15043f&acdnat=1524830169\\_549c61b921aa3af44e3107614f5949b4](https://ac-els-cdn-com.proxy.lib.chalmers.se/S0950061815307479/1-s2.0-S0950061815307479-main.pdf?_tid=1fe52e59-45e1-449d-acb7-911abb15043f&acdnat=1524830169_549c61b921aa3af44e3107614f5949b4) (2018-04-27).

Sétra (2006) *Footbridges: Assessment of Vibrational Behaviour of Footbridges Under Pedestrian Loading*. Bagneux, France: Service d'Études Techniques des Routes et Autoroutes (Service of Technical Studies of Streets and Highways). <http://www.projektering.nu/files/Footbridges.pdf> (2018-04-01).

Shahabpoor, E.; Pavić, A. (2012): Comparative Evaluation of Current Pedestrian Traffic Models on Structures. *Topics on the Dynamics of Civil Structures*, vol. 1. New York, NY, USA: Springer. <https://link-springer-com.proxy.lib.chalmers.se/content/pdf/10.1007%2F978-1-4614-2413-0.pdf> (2018-04-27).

SIS (1990) *Eurocode: Basis of Structural Design*.

SIS (1991) *Eurocode 1: Actions on Structures*.

SIS (1995) *Eurocode 5: Design of Timber Structures*.

Thorsson, P.; Dynefors, B.; Kihlman, T.; Kropp, W.; & Svensson, P. (2008) *Materie- och Vågteori (Theory of Matter and Waves)*. Gothenburg, Sweden: Chalmers University of Technology.

Trafikverket (2016) *Krav Brobyggande*. Borlänge, Sweden: TDOK 2016:0204.

Trafikverket (2018a) *Villkor*. <https://www.trafikverket.se/for-dig-i-branschen/vag/Transportdispens/Villkor/> (2018-05-09).

Trafikverket (2018b) *Bilaga Kalkylvärden ASEK 6.1 (Appendix Calculation Values ASEK 6.1)*. [Spreadsheet] [https://www.google.se/url?sa=t&rct=j&q=&esrc=s&source=web&cd=2&cad=rja&uact=8&ved=0ahUKEwiAr-rP7P3aAhUDCSwKHcKNCRIQFggrMAE&url=https%3A%2F%2Fwww.trafikverket.se%2Fcontentassets%2F4b1c1005597d47bda386d81dd3444b24%2Fasek-6.1%2Fbilaga\\_kalkylvarden\\_asek\\_6\\_1.xlsx&usg=A0vVaw3EBjKIJ-LqoQDXfZi2u8Po](https://www.google.se/url?sa=t&rct=j&q=&esrc=s&source=web&cd=2&cad=rja&uact=8&ved=0ahUKEwiAr-rP7P3aAhUDCSwKHcKNCRIQFggrMAE&url=https%3A%2F%2Fwww.trafikverket.se%2Fcontentassets%2F4b1c1005597d47bda386d81dd3444b24%2Fasek-6.1%2Fbilaga_kalkylvarden_asek_6_1.xlsx&usg=A0vVaw3EBjKIJ-LqoQDXfZi2u8Po) (2018-05-11).

Trafikverket (2018c) *GC-bro över SJ å Kroktorpsvägen i Åby, Norrköpings kommun. (Footbridge Crossing Railway and Kroktorp Road in Åby, Norrköping Municipality.)* <https://batman.trafikverket.se/BatmanVyBilderPublik/b/ba548b8d-87c3-4ea7-a85b-26341219b303.jpg> (2018-05-14).

Tuakta, C. (2005) *Use of Fiber Reinforced Polymer Composite in Bridge Structures*. Ph.D. thesis, Massachusetts Institute of Technology, Department of Civil and Environmental Engineering. <http://hdl.handle.net/1721.1/31126> (2018-02-12).

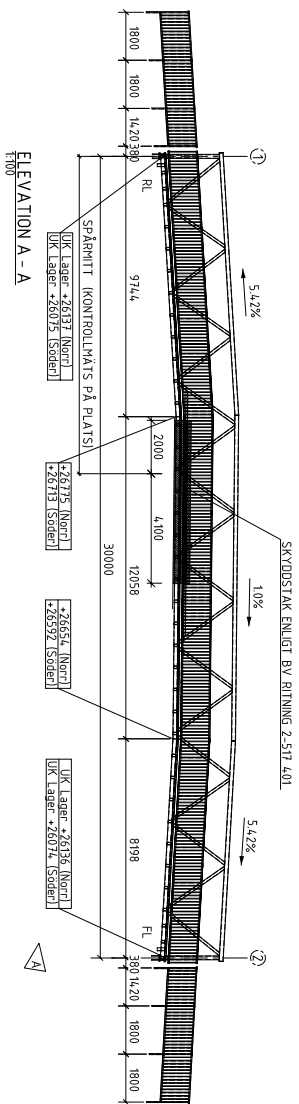
Täljsten, B. (2011) *Handbok för dimensionering och utförande i samband med förstärkning av betongkonstruktioner med pålimmade fiberkompositer. (Handbook for Sizing and Execution for Strengthening of Concrete Structures Using Glued-on Fiber Composites)*. Luleå, Sweden: Luleå University of Technology.

Wang, D.; Gao, S.; Kasperski, M.; Liu, H.; Jin, L. (2011) The Dynamic Characteristics of A Couple System by Pedestrian Bridge and Walking Persons. *Applied Mechanics and Materials*, vol. 71–78. <https://search-proquest-com.proxy.lib.chalmers.se/docview/1443877549?pq-origsite=summon> (2018-04-27).

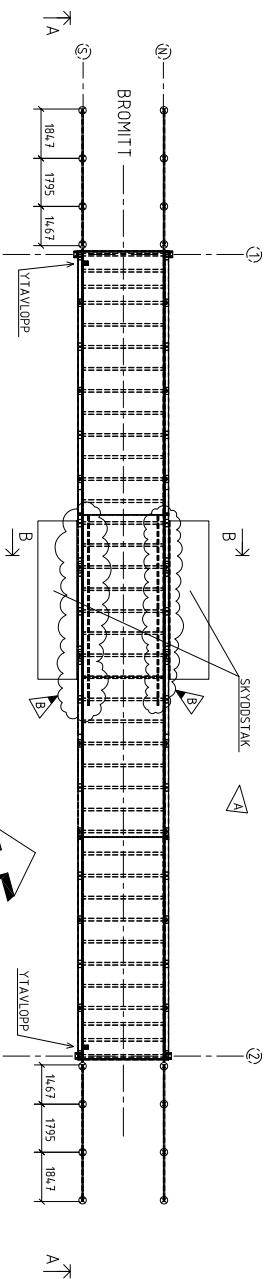
Zäll, E. (2018) *Footbridge Dynamics: Human–Structure Interaction* Licentiate thesis, Royal University of Technology, School of Architecture and the Built Environment.

# A

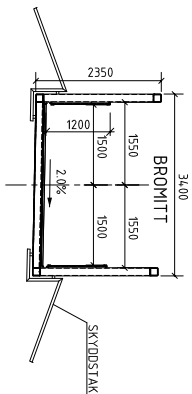
## Appendix: Bridge 581-909-1 Drawings



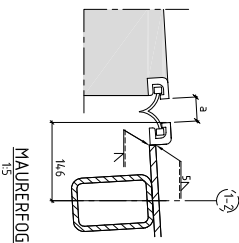
ELEVATION A-A



PLAN

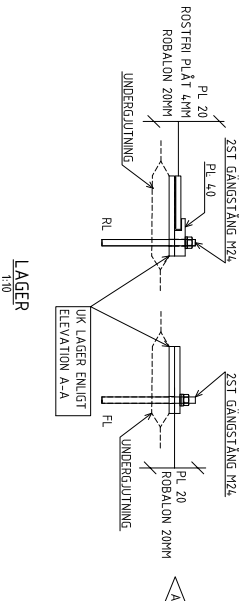


B-B



MAURERFÖG

TEMPERATURRÖRELSER		
TRIL	-34	68
TRIL	75	45
TRIL	34	11
2FL	+34/-34	35



LAGER

LAGERINSTÄLLNING

TEMPERATURRÖRELSER		
TEMPERATUR T <sub>c</sub>	a-mm	-20
-34	-20	-12
-20	-12	-11
-15	-11	-6
0	-6	0
15	0	6
20	6	10
34	10	

## STÅL

STÅLQUALITET: MATERIAL ENL. NADIS/S35-EN 10 025-41 OCH S5-EN 10 13, OM EJ ANNAT ANGES.

UTFÖRANDEKLASS: GB

SKÅRKLASS: SK2

SVETSKLASS: V8 DÄR INTE ANNAT ANGES I RESPEKTIVE FIGUR.

KORROSIVITETSKLASS: C5-M enl BSK 99 Tabell 8.72e, system S709.

VERKSTÅDS- OCH

MONTAGESVETSNÄR: SVETSNING FÅR ENDAST UTFÖRAS AV SVETSNÄR

SOM AVLAGT GODKÄNT PROV ENLIGT SS-EN 287-1 ALT. SS 06 52 01 OCH

SKALL UTFÖRAS ENLIGT AV BESTÄLLAREN GODTAGEN

SVETSPÅN UPPRÄTTAD AV ENTREPRENÖREN

SÄMLIGA KONTAKTYTOR TÅTSVETSNÄS

KÄLSVETSNÄR MED A-MÅTT 5mm OM EJ ANNAT ANGES.

SVETSELEKTRODER MED  $\phi_{ele} > 500\mu\text{m}$  ENLIGT SS-EN 499-E.2.2 B

(SEGHETSKLASS E) OM INTE ANNAT ANGES PÅ RITNING. KOPPLÄTAR

SVETSNÄS TILL VVR.

FRI KANT: UTFÖRS ENLIGT BRO 2004, 513c.

MONTÄRNING: MONTÄRPLAN SKALL UPPRÄTTAS AV ENTREPRENÖREN OCH ÖVERSÄNDAS TILL

BESTÄLLAREN FÖR GODTAGANDE.

ROSTSKYDD: BSK 99 Tabell 8.72e SYSTEM S709

TÄCKFÄRGENS YTTRE SKITT UTFÖRS MED KOLOR RAL 7016.

FÄRDIGPÅLNING SKA UTFÖRAS I VERKSTAD.

SKRIVFÖRBÄNDRINGSKLASS: S27 OM INGET ANNAT ANGES I RESPEKTIVE FIGUR. S27-FÖRBAND SAMBÖRNAS

ALLTID.

AVVÄGNINGSMARKERINGAR: BRON SKALL FÖRSES MED

AVVÄGNINGSMARKERINGAR ENLIGT BRO 2004, 511 OCH I ÖRFÄTTNING ENLIGT 4.114.2.

AVVÄGNINGSMARKERINGAR: BRON SKALL FÖRSES MED

AVVÄGNINGSMARKERINGAR ENLIGT BRO 2004, 511 OCH I ÖRFÄTTNING ENLIGT 4.114.2.

AVVÄGNINGSMARKERINGAR: BRON SKALL FÖRSES MED

AVVÄGNINGSMARKERINGAR ENLIGT BRO 2004, 511 OCH I ÖRFÄTTNING ENLIGT 4.114.2.

AVVÄGNINGSMARKERINGAR: BRON SKALL FÖRSES MED

AVVÄGNINGSMARKERINGAR ENLIGT BRO 2004, 511 OCH I ÖRFÄTTNING ENLIGT 4.114.2.

AVVÄGNINGSMARKERINGAR: BRON SKALL FÖRSES MED

AVVÄGNINGSMARKERINGAR ENLIGT BRO 2004, 511 OCH I ÖRFÄTTNING ENLIGT 4.114.2.

AVVÄGNINGSMARKERINGAR: BRON SKALL FÖRSES MED

AVVÄGNINGSMARKERINGAR ENLIGT BRO 2004, 511 OCH I ÖRFÄTTNING ENLIGT 4.114.2.

AVVÄGNINGSMARKERINGAR: BRON SKALL FÖRSES MED

AVVÄGNINGSMARKERINGAR ENLIGT BRO 2004, 511 OCH I ÖRFÄTTNING ENLIGT 4.114.2.

AVVÄGNINGSMARKERINGAR: BRON SKALL FÖRSES MED

Mark	Size	No. Top of Steel	Weight
Total for	0	assemblies	0.0

TVÄRSNITTSAREN: FÖR STÅLDETLARER FÅR INNEHÅLLA EN MINUSAVVIKELSE AV HÖGST 6%.

PLANÄTT PÅ RITNING AR

TEORETISKA "KANT I KANT" MÅTT.

HANSYN ÄR EJ TAGEN TILL FÖRBEREDNING

VERKSTADEN VÄLJER SJÄLV SVETSPÅL OCH SVETSNÄSA SAMT ÖVERMÅTT FÖR SVETSKRYNNING.

HÅLTÄNSNING OCH SVETSNING: UTÖVER VAD SOM ANGES PÅ RITNING, FÅR EJ SKA ULTAN KONTAKT MED KONSTRUKTÖREN.

TILLÄGGSKONTROLL: SKA UTFÖRAS ENLIGT BESTÄLLAREN GODTAGEN

TILLÄGGSKONTROLLPLAN STÅL.

UPPRÄTTAD AV FB ENGINEERING AB

TÄTHETSPROVNING: FACKVERKEN

SAMT PROBENSTÖMEN UTFÖRS

SOM SUTNA PROFILER ENLIGT BRO 2004, 512D.

ÖVERHÖJNING: BRON ÄR RITAD MED 20MM ÖVERHÖJNING FÖR ATT

KOMPENSERA NEDBÖJNING AV EGENVIKT.

BRO DETALJER

BELÄGGNING GÅNGBANA: BRON SKA FÖRSES MED 30MM GUTTSÄFALT.

LOKALT FALL TILL YTAVLOPPEN

MEH HANSYN TILL BRONS LUTNING.

SKYDDSANORDNING: RÄCKET

GÄLVAS ENLIGT BESTÄLLARENS ANVISNINGAR.

INFÄSTNING AV RÄCKE PÅ BRON

SKALL KLARA SÄTTNING PÅ 19mm I VERTIKALLED. BULTSKRUV I

RÄCKETS ÖVERKANT SKALL VARA FÖRSÄKNITA.

JÖRNING AV BRON SKALL

UTFÖRAS ENLIGT BVS 510 UTGÅVA 5. GÅNGAD DEL AV

JÖRANSLUTNING SKYDDAS VID YTBENHÄNDLING.

AVVÄGNINGSMARKERINGAR: BRON SKALL FÖRSES MED

AVVÄGNINGSMARKERINGAR ENLIGT BRO 2004, 511 OCH I ÖRFÄTTNING ENLIGT 4.114.2.

AVVÄGNINGSMARKERINGAR: BRON SKALL FÖRSES MED

AVVÄGNINGSMARKERINGAR ENLIGT BRO 2004, 511 OCH I ÖRFÄTTNING ENLIGT 4.114.2.

AVVÄGNINGSMARKERINGAR: BRON SKALL FÖRSES MED

AVVÄGNINGSMARKERINGAR ENLIGT BRO 2004, 511 OCH I ÖRFÄTTNING ENLIGT 4.114.2.

AVVÄGNINGSMARKERINGAR: BRON SKALL FÖRSES MED

AVVÄGNINGSMARKERINGAR ENLIGT BRO 2004, 511 OCH I ÖRFÄTTNING ENLIGT 4.114.2.

AVVÄGNINGSMARKERINGAR: BRON SKALL FÖRSES MED

AVVÄGNINGSMARKERINGAR ENLIGT BRO 2004, 511 OCH I ÖRFÄTTNING ENLIGT 4.114.2.

AVVÄGNINGSMARKERINGAR: BRON SKALL FÖRSES MED

AVVÄGNINGSMARKERINGAR ENLIGT BRO 2004, 511 OCH I ÖRFÄTTNING ENLIGT 4.114.2.

AVVÄGNINGSMARKERINGAR: BRON SKALL FÖRSES MED

AVVÄGNINGSMARKERINGAR ENLIGT BRO 2004, 511 OCH I ÖRFÄTTNING ENLIGT 4.114.2.

Fästställe enligt skrivelse daterad 2003-04-07

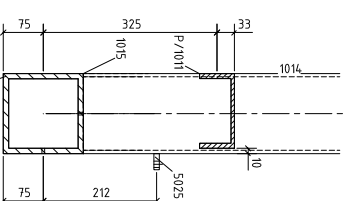
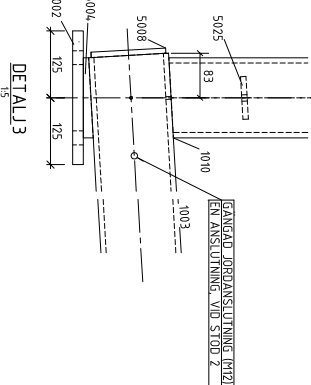
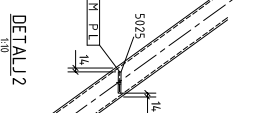
SKALA 1:100 1:10 01

1:100 1:10 01



[illegible]

## SPÅRMITT



BET	ANT	JÄRNINGEN ANSVAR	DATUM	SIGN
3	1	MATERIALISTA	03-04-03	MVA
4	6	411: ARS: ENA, JORDNIN	03-04-01	MVA

**FB**  
FLYGEÄLTSTRYK

**FB Engineering AB**  
BOX 12076 402 41 GÖTEBORG

TEL: 010-850 0000  
FAX: 010-850 0000

UPPDRAIC NR	RITAD/KONSTR AV	HANDLÖGARE
161893	M/V/H-1	M/H

DATUM	ANSVARIG
2009-02-20	TASHEM

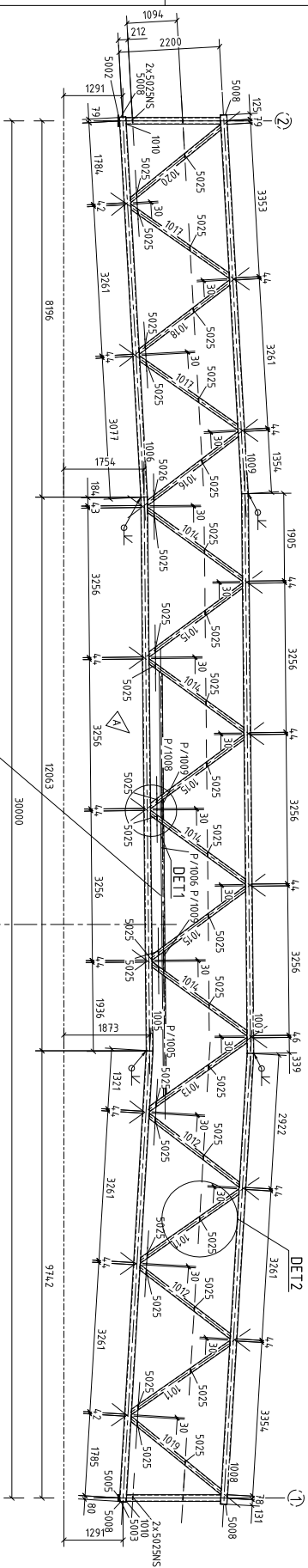
Himmelsårsmåttet Åhr

GC-Bro över järnvägen Järna-Åby

SKALA	NUMMER	BET
Fackverk Söder		

1:50	1:10	02	B
1:20	1:5		

## 1:50

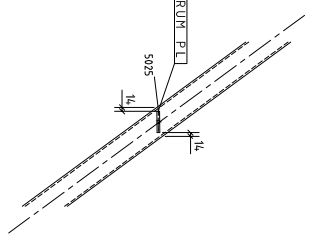



ANKARSKENA FÖR INFÄSTNING AV SKYDDSTAK

## SPÅRMITT

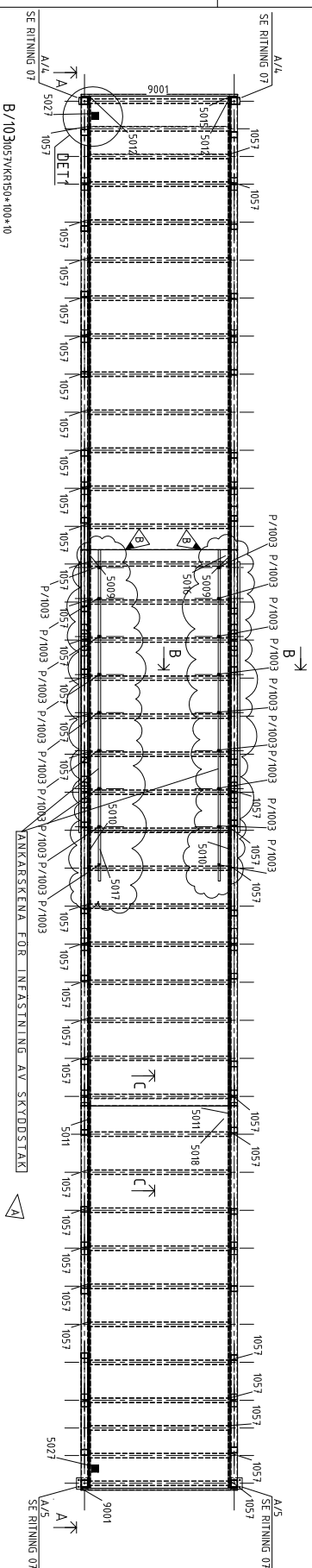
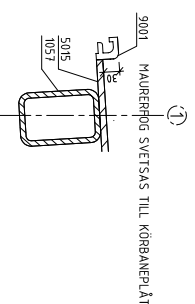
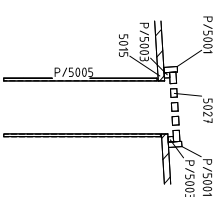
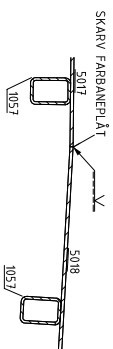
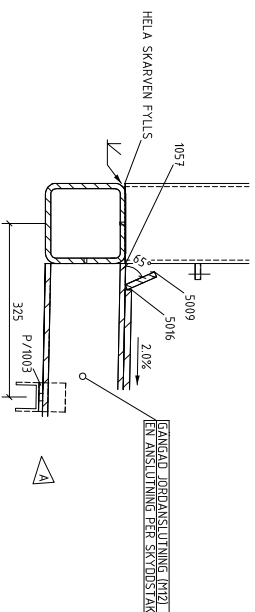


MÅTT PÅ ELEVATION TAGET TILL CENTRUM PL



Fastisbild enligt skrivelse daterad 2009-04-07									
3	1	MATELLUSTA	07-01-03	P.A.					
3	1	STH	07-01-03	P.A.					
1	1	AMT	07-01-03	P.A.					
1	1	AMT	AMERICAN ASER		DATA		SON		
ARBETSPÄTTNING									
LECOR									
									
<b>FB Engineering AB</b> Box 919, 421 01 Stockholm Uppdrags nr: 2009-01-07 Datum: 2009-01-07									
SBT/KONSERV AV 100% avskrivning 2009-01-07									
Humpelgårdssom ädel, Åby GC-Bro över järnvägsgräns Järna-Åby S-Bro över									
SKALA	1:20	1:50	1:100	1:200	1:500	1:1000	1:2000	1:5000	1:10000
NUMMER	03								B
1	2	3	4	5	6	7	8	9	10

The diagram illustrates a cross-section of a wall with two different opening types. The top opening is labeled 'P/5002' and features a circular hole with horizontal internal reinforcement. The bottom opening is labeled 'P/5004' and shows a rectangular hole with vertical internal reinforcement. Dimensions are provided for both: a height of 370 mm from the top edge to the center of the opening, and a width of 150 mm for the opening itself. A total width of 230 mm is indicated at the base. Arrows labeled 'E' point upwards, indicating the direction of external pressure or wind load.



Fastslått enligt skrivelse daterad 2009-04-07									
3	2	101	ABSCC 14	19-01-01	11	14	14	14	14
4	3	101	ABSCC 14	19-01-01	11	14	14	14	14
5	4	101	ABSCC 14	19-01-01	11	14	14	14	14
6	5	101	ABSCC 14	19-01-01	11	14	14	14	14
7	6	101	ABSCC 14	19-01-01	11	14	14	14	14
8	7	101	ABSCC 14	19-01-01	11	14	14	14	14
9	8	101	ABSCC 14	19-01-01	11	14	14	14	14
10	9	101	ABSCC 14	19-01-01	11	14	14	14	14
11	10	101	ABSCC 14	19-01-01	11	14	14	14	14
12	11	101	ABSCC 14	19-01-01	11	14	14	14	14
13	12	101	ABSCC 14	19-01-01	11	14	14	14	14
14	13	101	ABSCC 14	19-01-01	11	14	14	14	14
15	14	101	ABSCC 14	19-01-01	11	14	14	14	14
16	15	101	ABSCC 14	19-01-01	11	14	14	14	14
17	16	101	ABSCC 14	19-01-01	11	14	14	14	14
18	17	101	ABSCC 14	19-01-01	11	14	14	14	14
19	18	101	ABSCC 14	19-01-01	11	14	14	14	14
20	19	101	ABSCC 14	19-01-01	11	14	14	14	14
21	20	101	ABSCC 14	19-01-01	11	14	14	14	14
22	21	101	ABSCC 14	19-01-01	11	14	14	14	14
23	22	101	ABSCC 14	19-01-01	11	14	14	14	14
24	23	101	ABSCC 14	19-01-01	11	14	14	14	14
25	24	101	ABSCC 14	19-01-01	11	14	14	14	14
26	25	101	ABSCC 14	19-01-01	11	14	14	14	14
27	26	101	ABSCC 14	19-01-01	11	14	14	14	14
28	27	101	ABSCC 14	19-01-01	11	14	14	14	14
29	28	101	ABSCC 14	19-01-01	11	14	14	14	14
30	29	101	ABSCC 14	19-01-01	11	14	14	14	14
31	30	101	ABSCC 14	19-01-01	11	14	14	14	14
32	31	101	ABSCC 14	19-01-01	11	14	14	14	14
33	32	101	ABSCC 14	19-01-01	11	14	14	14	14
34	33	101	ABSCC 14	19-01-01	11	14	14	14	14
35	34	101	ABSCC 14	19-01-01	11	14	14	14	14
36	35	101	ABSCC 14	19-01-01	11	14	14	14	14
37	36	101	ABSCC 14	19-01-01	11	14	14	14	14
38	37	101	ABSCC 14	19-01-01	11	14	14	14	14
39	38	101	ABSCC 14	19-01-01	11	14	14	14	14
40	39	101	ABSCC 14	19-01-01	11	14	14	14	14
41	40	101	ABSCC 14	19-01-01	11	14	14	14	14
42	41	101	ABSCC 14	19-01-01	11	14	14	14	14
43	42	101	ABSCC 14	19-01-01	11	14	14	14	14
44	43	101	ABSCC 14	19-01-01	11	14	14	14	14
45	44	101	ABSCC 14	19-01-01	11	14	14	14	14
46	45	101	ABSCC 14	19-01-01	11	14	14	14	14
47	46	101	ABSCC 14	19-01-01	11	14	14	14	14
48	47	101	ABSCC 14	19-01-01	11	14	14	14	14
49	48	101	ABSCC 14	19-01-01	11	14	14	14	14
50	49	101	ABSCC 14	19-01-01	11	14	14	14	14
51	50	101	ABSCC 14	19-01-01	11	14	14	14	14
52	51	101	ABSCC 14	19-01-01	11	14	14	14	14
53	52	101	ABSCC 14	19-01-01	11	14	14	14	14
54	53	101	ABSCC 14	19-01-01	11	14	14	14	14
55	54	101	ABSCC 14	19-01-01	11	14	14	14	14
56	55	101	ABSCC 14	19-01-01	11	14	14	14	14
57	56	101	ABSCC 14	19-01-01	11	14	14	14	14
58	57	101	ABSCC 14	19-01-01	11	14	14	14	14
59	58	101	ABSCC 14	19-01-01	11	14	14	14	14
60	59	101	ABSCC 14	19-01-01	11	14	14	14	14
61	60	101	ABSCC 14	19-01-01	11	14	14	14	14
62	61	101	ABSCC 14	19-01-01	11	14	14	14	14
63	62	101	ABSCC 14	19-01-01	11	14	14	14	14
64	63	101	ABSCC 14	19-01-01	11	14	14	14	14
65	64	101	ABSCC 14	19-01-01	11	14	14	14	14
66	65	101	ABSCC 14	19-01-01	11	14	14	14	14
67	66	101	ABSCC 14	19-01-01	11	14	14	14	14
68	67	101	ABSCC 14	19-01-01	11	14	14	14	14
69	68	101	ABSCC 14	19-01-01	11	14	14	14	14
70	69	101	ABSCC 14	19-01-01	11	14	14	14	14
71	70	101	ABSCC 14	19-01-01	11	14	14	14	14
72	71	101	ABSCC 14	19-01-01	11	14	14	14	14
73	72	101	ABSCC 14	19-01-01	11	14	14	14	14
74	73	101	ABSCC 14	19-01-01	11	14	14	14	14
75	74	101	ABSCC 14	19-01-01	11	14	14	14	14
76	75	101	ABSCC 14	19-01-01	11	14	14	14	14
77	76	101	ABSCC 14	19-01-01	11	14	14	14	14
78	77	101	ABSCC 14	19-01-01	11	14	14	14	14
79	78	101	ABSCC 14	19-01-01	11	14	14	14	14
80	79	101	ABSCC 14	19-01-01	11	14	14	14	14
81	80	101	ABSCC 14	19-01-01	11	14	14	14	14
82	81	101	ABSCC 14	19-01-01	11	14	14	14	14
83	82	101	ABSCC 14	19-01-01	11	14	14	14	14
84	83	101	ABSCC 14	19-01-01	11	14	14	14	14
85	84	101	ABSCC 14	19-01-01	11	14	14	14	14
86	85	101	ABSCC 14	19-01-01	11	14	14	14	14
87	86	101	ABSCC 14	19-01-01	11	14	14	14	14
88	87	101	ABSCC 14	19-01-01	11	14	14	14	14
89	88	101	ABSCC 14	19-01-01	11	14	14	14	14
90	89	101	ABSCC 14	19-01-01	11	14	14	14	14
91	90	101	ABSCC 14	19-01-01	11	14	14	14	14
92	91	101	ABSCC 14	19-01-01	11	14	14	14	14
93	92	101	ABSCC 14	19-01-01	11	14	14	14	14
94	93	101	ABSCC 14	19-01-01	11	14	14	14	14
95	94	101	ABSCC 14	19-01-01	11	14	14	14	14
96	95	101	ABSCC 14	19-01-01	11	14	14	14	14
97	96	101	ABSCC 14	19-01-01	11	14	14	14	14
98	97	101	ABSCC 14	19-01-01	11	14	14	14	14
99	98	101	ABSCC 14	19-01-01	11	14	14	14	14
100	99	101	ABSCC 14	19-01-01	11	14	14	14	14